NOAA Technical Memorandum
NWS TDL 81

The NEXRAD Severe Weather Potential Algorithm

David H. Kitzmiller, Wayne E. McGovern, and Robert E. Saffle

Techniques Development Laboratory
Silver Spring, MD
February 1992

UNITED STATES
DEPARTMENT OF COMMERCE / National Oceanic and
Atmospheric Administration / National Weather Service

NOAA TECHNICAL MEMORANDUMS

National Weather Service, Techniques Development Laboratory Series

The primary purpose of the Techniques Development Laboratory of the Office of Systems Development is to translate increases of basic knowledge in meteorology and allied disciplines into improved operating techniques and procedures. To achieve this goal, the Laboratory conducts applied research and development aimed at the improvement of diagnostic and prognostic methods for producing weather information. The Laboratory performs studies both for the general improvement of prediction methodology used in the National Weather Service and for the more effective utilization of weather forecasts by the ultimate user.

NOAA Technical Memorandums in the National Weather Service Techniques Development Laboratory series facilitate rapid distribution of material that may be preliminary in nature and which may be published formally elsewhere at a later date. Publications 1 through 5 are in the former series Weather Bureau Technical Notes (TN), Techniques Development Laboratory (TDL) Reports; publications 6 through 36 are in the former series ESSA Technical Memorandums, Weather Bureau Technical Memorandum, (WBTM). Beginning with TDL 37, publications are now part of the series NOAA Technical Memorandums, National Weather Service (NWS).

Publications listed below are available from the National Technical Information Service, U.S. Department of Commerce, Sills Bldg., 5285 Port Royal Road, Springfield, VA 22161. Prices on request. Order by accession number (given in parentheses).

ESSA Technical Memorandums

WBTM TDL 20 — A Comparison of Two Methods of Reducing Truncation Error. Robert J. Bermowitz, May 1969, 7 pp. (PB-184-741)

WBTM TDL 21 — Automatic Decoding of Hourly Weather Reports. George W. Hollenbaugh, Harry R. Glahn, and Dale A. Lowry, July 1969, 27 pp. (PB-185-806)

WBTM TDL 22 — An Operationally Oriented Objective Analysis Program. Harry R. Glahn, George W. Hollenbaugh, and Dale A. Lowry, July 1969, 20 pp. (PB-186-129)

WBTM TDL 23 — An Operational Subsynoptic Advection Model. Harry R. Glahn, Dale A. Lowry, and George W. Hollenbaugh, July 1969, 26 pp. (PB-186-389)

WBTM TDL 24 — A Lake Erie Storm Surge Forecasting Technique. William S. Richardson and N. Arthur Pore, August 1969, 23 pp. (PB-185-778)

WBTM TDL 25 — Charts Giving Station Precipitation in the Plateau States From 850- and 500-Millibar Lows During Winter. August F. Korte, Donald L. Jorgensen, and William H. Klein, September 1969, 9 pp. plus appendixes A and B. (PB-187-476)

WBTM TDL 26 — Computer Forecasts of Maximum and Minimum Surface Temperatures. William H. Klein, Frank Lewis, and George P. Casely, October 1969, 27 pp. plus appendix. (PB-189-105)

WBTM TDL 27 — An Operational Method for Objectively Forecasting Probability of Precipitation. Harry R. Glahn and Dale A. Lowry, October 1969, 24 pp. (PB-188-660)

WBTM TDL 28 — Techniques for Forecasting Low Water Occurrence at Baltimore and Norfolk. James M. McClelland, March 1970, 34 pp. (PB-191-744)

WBTM TDL 29 — A Method for Predicting Surface Winds. Harry R. Glahn, March 1970, 18 pp. (PB-191-745)

WBTM TDL 30 — Summary of Selected Reference Material on the Oceanographic Phenomena of Tides, Storm Surges, Waves, and Breakers. N. Arthur Pore, May 1970, 103 pp. (PB-193-449)

WBTM TDL 31 — Persistence of Precipitation at 108 Cities in the Conterminous United States. Donald L. Jorgensen and William H. Klein, May 1970, 84 pp. (PB-193-599)

WBTM TDL 32 — Computer-Produced Worded Forecasts. Harry R. Glahn, June 1970, 8 pp. (PB-194-262)

WBTM TDL 33 — Calculation of Precipitable Water. L. P. Harrison, June 1970, 61 pp. (PB-193-600)

WBTM TDL 34 — An Objective Method for Forecasting Winds Over Lake Erie and Lake Ontario. Celso S. Barrientos. August 1970, 20 pp. (PB-194-586)

WBTM TDL 35 — Probabilistic Prediction in Meteorology; a Bibliography. Allan H. Murphy and Roger A. Allen, June 1970, 60 pp. (PB-194-415)

WBTM TDL 36 — Current High Altitude Observations--Investigation and Possible Improvement. M. A. Alaka and R. C. Elvander, July 1970, 24 pp. (COM-71-00003)

NWS TDL 37 — Prediction of Surface Dew Point Temperatures. R. C. Elvander, February 1971, 40 pp. (COM-71-00253)

NWS TDL 38 — Objectively Computed Surface Diagnostic Fields. Robert J. Bermowitz, February 1971, 23 pp. (COM-71-0301)

NWS TDL 39 — Computer Prediction of Precipitation Probability for 108 Cities in the United States. William H. Klein, February 1971, 32 pp. (COM-71-00249)

NWS TDL 40 — Wave Climatology for the Great Lakes. N. A. Pore, J. M. McClelland, C. S. Barrientos, and W. E. Kennedy, February 1971, 61 pp. (COM-71-00368)

NWS TDL 41 — Twice-Daily Mean Heights in the Troposphere Over North America and Vicinity. August F. Korte, June 1971, 31 pp. (COM-71-0286)

NWS TDL 42 — Some Experiments With a Fine-Mesh 500-Millibar Barotropic Model. Robert J. Bermowitz, August 1971, 20 pp. (COM-71-00958)

NWS TDL 43 — Air-Sea Energy Exchange in Lagrangian Temperature and Dew Point Forecasts. Ronald M. Reap, October 1971, 23 pp. (COM-71-01112)

NWS TDL 44 — Use of Surface Observations in Boundary-Layer Analysis. H. Michael Mogil and William D. Bonner, March 1972, 16 pp. (COM-72-10641)

NWS TDL 45 — The Use of Model Output Statistics (MOS) To Estimate Daily Maximum Temperatures. John R. Annett, Harry R. Glahn, and Dale A. Lowry, March 1972, 14 pp. (COM-72-10753)

(Continued on inside back cover)

NOAA Technical Memorandum
NWS TDL 81

The NEXRAD Severe Weather Potential Algorithm

David H. Kitzmiller, Wayne E. McGovern, and Robert E. Saffle

Techniques Development Laboratory
Silver Spring, MD
February 1992

UNITED STATES DEPARTMENT OF COMMERCE
Barbara Hackman Franklin
Secretary

National Oceanic and Atmospheric Administration
Under Secretary
John A. Knauss

National Weather Service
Elbert W. Friday, Jr.
Assistant Administrator

Table of Contents

THE NEXRAD SEVERE WEATHER POTENTIAL ALGORITHM

David H. Kitzmiller, Wayne E. McGovern,
and Robert E. Saffle

ABSTRACT

The NEXRAD Severe Weather Potential (SWP) algorithm is an automated procedure for the detection of severe local storms. The algorithm identifies individual thunderstorm cells within radar imagery, and, for each cell, yields an index proportional to the probability that the cell will shortly produce damaging surface winds, large hail, or tornadoes. This index is a statistically-derived function of the storm's maximum Vertically-Integrated Liquid (VIL) and horizontal areal extent. The correlation between these storm characteristics and severe weather occurrence was first noted in the 1970's. Several National Weather Service field offices in the Central Plains and Northeast regions of the United States have successfully used VIL as a discriminator between severe and nonsevere thunderstorms.

This memorandum describes the observational data and statistical methodology employed in the development of the SWP Algorithm, and regional and seasonal variations in the VIL/severe weather relationship. The expected operational performance of the algorithm, in terms of probability of detection and false alarm ratio, is also documented.

1. INTRODUCTION

The next-generation Weather Surveillance Radar (WSR-88D) system, often referred to as NEXRAD, provides large amounts of observational data, including reflectivity and Doppler-derived wind velocity. A set of "base products" is produced directly from these data for presentation to forecasters. The system also features a variety of specialized "derived" products designed to alert forecasters to the potential for specific weather phenomena, such as mesocyclones, hail, turbulence, and heavy rainfall.

One of these automated interpretation aids is the Severe Weather Potential (SWP) algorithm, which identifies convective cells and displays a numerical index proportional to the probability that a specific cell is currently producing, or will shortly produce, severe local storm phenomena (large hail, damaging surface winds, or tornadoes). The algorithm that produces the SWP was derived objectively, through the examination of archived radar reflectivity observations and severe storm reports. Earlier versions of the SWP algorithm have been in use at selected National Weather Service radar sites since the late 1970's.

The SWP algorithm is designed primarily to assist forecasters in the task of issuing severe local storm warnings. It is particularly useful in monitoring the strength of multiple thunderstorms. As will be shown, the algorithm is capable of indicating which storms are relatively innocuous in terms of severe

weather, which ones warrant closer examination by either radar or surface spotters, and which are very likely to be severe. An objectively-derived expert system, SWP can also aid forecasters who are new to a field office and unfamiliar with local thunderstorm characteristics.

This note describes the methods used to identify and track thunderstorms in the archived radar data, and determine which tracked storms were severe. We also describe our logic in determining the optimal form of the SWP algorithm, and ways to interpret the algorithm's output in real time, over several different regions of the United States.

2. VERTICALLY-INTEGRATED LIQUID AND SEVERE WEATHER

The basis for the SWP algorithm is the correlation between radar estimates of Vertically-Integrated Liquid (VIL) and severe storm occurrence, first noted in the 1970's (Greene and Clark, 1972; Elvander, 1977). The VIL is defined as the mass of precipitation suspended above a unit area of cloud base. It is estimated from reflectivity integrated over the depth of the storm volume through an empirical relationship (based upon the Marshall-Palmer hypothesis) between reflectivity and the concentration of precipitation particles within the cloud. Thus, radar-estimated VIL is a function of both updraft speed and cloud depth.

The value of VIL rarely exceeds 10 kg m^{-2} in stratiform rainclouds. (Note that 1 kg m^{-2} is equivalent to a 1 mm layer of water if the liquid were to be completely precipitated.) Within organized convective systems, VIL usually exceeds 10 kg m^{-2} in and near active updraft regions. Typical peak values of VIL within summer storms range from 50 over Florida, to 30 over the Great Plains, and 20 over the Northeast. In each of these regions, the probability that a storm cell produces severe weather increases as the peak VIL, and/or the horizontal area covered by VIL > 10 kg m^{-2}, increases.

Operational use has already been made of both VIL and an early version of the SWP algorithm, at some earlier-generation radar (WSR-57 and WSR-74S) sites (McGovern et al., 1984; Winston and Ruthi, 1986). Twelve such sites were specially equipped with Radar Data Processor II (RADAP II) minicomputers, which provide capabilities for automated volumetric scanning and digital reflectivity processing. In order to develop and document the optimum form of the SWP algorithm, it was necessary to determine statistical correlations between VIL and severe weather occurrence near most of these RADAP II sites.

3. HISTORICAL RADAR OBSERVATIONS AND SEVERE STORM REPORTS

Volumetric radar observations in digital form have been archived at most RADAP II sites since the mid-1980's. The RADAP II controls the radar during volumetric scanning operations, ingests and processes digitized reflectivity data, provides product display functions, and archives the reflectivity data on magnetic disk for later use. During volumetric scanning, the radar antenna is stepped upward from base elevation at two-degree intervals, until no reflectivity above noise level is detected. The maximum elevation is 22 degrees. The scan sequence is generally completed in less than 5 minutes.

The RADAP II archive consists of reflectivity digitized to 16 categories, with echo location defined by azimuth, range, and elevation angle. Each reflectivity datum represents a portion of the radar beam 2 degrees wide and

1 nautical mile (1.9 km) in depth. The archive's coverage extends to approximately 230 km from the radar site. For the most complete observation sequences, new volumetric scans are available every 10 or 12 minutes, though considerable time gaps occur during some convective episodes at all sites. The location of the 12 RADAP II sites is shown in Fig. 1; a list of site names and geographic locations appears in Table 1. A complete description of the archive content and format has been prepared by McDonald and Saffle (1989).

The RADAP II WSR-57 volumetric data differ in two important respects from the reflectivity data that will be available from the WSR-88D. First, the WSR-57 beamwidth is 2.2 degrees versus 0.95 degrees for the WSR-88D. With the greater resolution, the WSR-88D will tend to measure higher peak reflectivities than those measured by the WSR-57 for storms at a similar range. Second, and perhaps more significantly, the precipitation mode volumetric scanning patterns of the WSR-88D do not comprise contiguous elevation angles. The constraints of a narrrow beamwidth and operational requirements for frequent volumetric data updates (every 5 or 6 minutes) combine to necessitate scanning strategies that "sample" the vertical structure of storms at discrete elevation angles. One of these scanning strategies uses only nine elevation angles to sample 20 degrees of vertical extent. The WSR-88D algorithms that are volume-based interpolate values for the "missing" vertical slices. Saffle et al. (1986) have estimated the impact of the WSR-88D scanning strategies on the calculations of VIL. While these data differences are potentially significant, we believe that SWP relationships developed from WSR-57 data will be operationally valid for the majority of storms even when used with WSR-88D data. SWP relationships will be developed from WSR-88D data when sufficient data are archived.

Reports of severe local storm phenomena (surface hail $\geq$ 2 cm diameter, surface wind gusts $\geq$ 50 kt, or tornadoes reaching the surface over land or fresh water) were supplied by the National Severe Storms Forecast Center (NSSFC). Along with other information, these reports provide the event location to the nearest minute in latitude and longitude, and to the nearest minute in time. The reports were systematically compared to radar echoes in order to determine which thunderstorms were severe.

4. DETERMINATION OF STORM CELL LIFE HISTORIES AND IDENTIFICATION OF SEVERE CELLS

The SWP product is based upon a spatial objective analysis of the VIL field; each datum in the analysis represents an estimate of the mean VIL over a 4 x 4 km square box, within a grid covering the entire radar umbrella to a distance of approximately 230 km (125 nautical miles) from the center. A storm "cell" is taken to be a region seven grid boxes square (28 km on a side), centered on a local maximum in the VIL field; this logic follows the initial WSR-88D SWP processing convention. Within average-sized thunderstorms, only a portion of the cell region is covered by VIL greater than 10 kg m^{-2}. In order to limit consideration to the more active cells, only those which featured at least two grid boxes (32 km^2) with VIL of 10 kg m^{-2} or more were formally identified and tracked.

To determine the VIL characteristics of individual thunderstorms, it was first necessary to define the life history of all cells for which adequate radar documentation was available. An automated cell-tracking procedure was applied to all sequences of VIL images less than 30 minutes apart. During the

tracking process, each defined cell was assigned an index number, and its position and VIL properties stored for later use. These properties included maximum VIL, average VIL, and the fraction of the cell area covered by VIL greater than various threshold values. The index number assignments were later corrected, as necessary, when manual examination of the radar imagery indicated that a cell existing in two consecutive images had been misidentified. The images were also cleared of anomalous propagation (AP) echoes and ground clutter through subjective comparison to archived Manually-Digitized Radar (MDR) data.

Cells were defined as severe according to their proximity to surface reports. Severe weather events were subjectively assigned to individual storms during the period between 20 minutes before and 10 minutes after the time of the event. Each event was assigned to only one cell. When an event was reported equally close to two or more neighboring cells, it was assigned to the most intense one.

On occasion, severe storm events (particularly high winds) were reported for which there was no VIL cell within a reasonable distance. While it is certainly possible for storms featuring low VIL to produce severe weather, these events could also include instances of incorrect times on the reports and cases of high winds not associated with convective storms. Since these events cannot be nowcasted with VIL predictors, we did not attempt to include them in our statistical sample.

When carried out over several years' observations, this cell identification and tracking process yielded information on 600 to 5000 individual storms in each radar umbrella; from 300 to 2000 of these were later used in the algorithm development. Our research has been concentrated on storms occurring during the April-September period; at most sites, insufficient radar data were collected during the autumn and winter to make reliable inferences on the nature of the VIL/severe weather relationship during those seasons. Such observations should soon be available from WSR-88D archiving operations.

5. STATISTICAL PREDICTORS OF SEVERE WEATHER

For each identified cell in each radar image, a number of VIL properties were recorded (Table 2). These properties were found to be useful as statistical predictors of severe weather probability. The predictors include maximum VIL within the cell (MAXVIL), and the number of 4 x 4 km grid blocks within the cell region covered by VIL above certain threshold values (NSIZE, SVG10, etc.). The SUMVIL, defined as the sum of the VIL values within individual grid blocks, is directly proportional to the total precipitation mass within the cell. Other predictors were included in the study, but for the present we will describe only those that enter into the SWP algorithm, or which may be easily inferred from the VIL display produced by the WSR-88D system.

The output of the SWP algorithm is defined by:

$$P = A + B\text{xVILWGT} + C\text{xSVG10} + D\text{xSVG15} + E\text{xSVG20} + F\text{xSVG25} \quad (1)$$

where the equation coefficients A-F are determined by forward-selection linear screening regression. Within the equation development sample, the severe weather predictand P was zero for a nonsevere cell and unity for a severe one.

Thus, P is a regression estimate of severe weather probability, valid for the dependent data sample. We generally refer to P as severe weather potential, however, since the dependent sample may consist of observations from several radar sites. Under these circumstances, P may not represent a reliable probability for some of the individual sites, though it should be correlated to severe weather at all of them.

These five predictors, used in the SWP equation that Elvander (1977) derived from Oklahoma data, are the only ones calculated for use in the initial WSR-88D SWP algorithm. However, the equation coefficients A-F are adaptation data that may be varied from site to site. The algorithm in its present form includes no other reflectivity information, or any Doppler-derived information. Our goal, then, was to derive a severe weather detection algorithm that makes optimum use of these predictors within as many geographic regions and synoptic situations as possible.

To create the predictor/predictand dataset needed in regression analysis, it was necessary to choose one point in each cell's life history to describe that cell. For cells not associated with a severe weather report, that point was the one at which it reached its greatest overall development. The SUMVIL index provides a measure of storm development in that it is directly proportional to total precipitation mass. Therefore, we used cell properties at the time SUMVIL was greatest in developing the SWP equation. In a similar manner, cells associated with severe reports were described according to their peak development between 20 minutes before and 10 minutes after they produced severe weather. For cells featuring multiple severe events, the overall peak development was considered.

6. GEOGRAPHICAL SCREENING OF THE DEVELOPMENT DATA SAMPLE

The problems inherent in verifying rare events such as severe storms are well known. Most reports in the NSSFC log are from the general public, and the likelihood of verifying any storm as severe is largely dependent upon whether that storm affects a populated area. Over central Florida, for example, severe storm reports from 1973 to 1988 were strikingly concentrated near metropolitan areas (e.g., Tampa-St. Petersburg, Orlando), and along the more heavily developed portions of coastline (see Fig. 2). Some large sections of the sparsely-inhabited interior of the peninsula, such as the counties near Lake Okeechobee, yielded no severe reports at all during this 16-year period. While the distribution of severe events might be influenced by local climatology (e.g., sea-breeze convergence regions), or by chance, it appears that population density is the strongest influence.

Similar spatial patterns in reports appeared within all RADAP II umbrellas. We therefore believe that our sample of storm cell observations, if taken as a whole, would seriously underrepresent the true fraction of the cells that were severe. To avoid incorporating this bias toward nonsevere cells in the SWP algorithm, we considered only those cells which traversed regions of each umbrella that had historically provided the most reports. At most sites, this subsample was one fourth to one third of the whole. This screening procedure yielded what we believe to be the closest possible estimate of the actual percentage of severe cells.

7. STATISTICAL RELATIONSHIPS BETWEEN VIL AND SEVERE WEATHER OCCURRENCE OVER DIFFERENT REGIONS AND SEASONS

The relationship between VIL and severe weather near three selected radar sites is illustrated in Figs. 3-5. These figures represent data from the warm season, April to September, from three climatically different regions. It can be seen that the fraction of cells producing severe phenomena increases with VIL and with cell size at all sites, though the relationship is most striking at Amarillo, Texas (AMA) and Binghamton, New York (BGM). Note that the overall percentage of severe cells, and the distribution of VIL and cell size, varies markedly from site to site, as well.

Near AMA, in the Texas Panhandle region, VIL and severe weather are very well correlated. The Amarillo area, like most of the central Plains, is subject to strong thunderstorms associated with synoptic-scale systems during the spring months, and with mesoscale or local influences, such as surface heating, during the summer. About 12% of all cells in this sample were severe. Less than 2% of the cells with maximum VIL less than 30 kg m^{-2} were severe, while over 40% of those with VIL $\geq$ 50 were severe (Fig. 3a). Likewise, the horizontal extent of the convective cell is a significant indicator of storm severity. As mentioned earlier, VIL in excess of 10 kg m^{-2} is associated with thunderstorms; of all cells with 26 analysis grid blocks or more with VIL > 10, 40% were severe, while those cells with less than 11 such grid blocks had less than a 3% chance of being severe (Fig. 3b). A linear regression relationship between the severe weather probability and SWP VIL predictors at this site is:

$$P = 1.83 + 0.041\ \text{VILWGT} - 0.83\ \text{SVG10} \qquad (2)$$

where P is the probability in percent. The multiple correlation coefficient for this equation is 0.42 (the predictor combination explains $.42^2$, or 18%, of the variance in the severe weather predictand). While it might seem counterintuitive that the SVG10 coefficient is negative, it must be recalled that the sign of this coefficient depends upon the partial correlation between SVG10 and P with VILWGT held constant. Given the high correlation between SVG10 and VILWGT, this partial correlation is negative, and thus for a particular value of VILWGT, an increase of SVG10 actually corresponds to a lower severe weather probability.

The SWP predictors not appearing in (2) contributed only small additional amounts to the multiple correlation. In this and the remaining derivations, an F-test, adjusted to account for a pool of five predictors (see Draper and Smith, 1981), was employed to terminate predictor selection. Experimentation showed that forcing all five predictors into the regression equation resulted in a deterioration in verification scores when the equation was tested on independent data.

Of all the sites studied, the BGM umbrella, which covers New York and northern Pennsylvania, had the highest percentage of storm cells with severe weather (32% over population centers, Fig. 4). Though storms were much less frequent than over the Plains or Florida, most were associated with synoptic-scale disturbances. The presence of favorable upper-air conditions, such as strong vertical shear and high wind speeds, caused many high wind events. Virtually all identified cells had at least a 15% chance of being severe, and a majority of cells exceeding a VIL of 30 kg m^{-2} were severe. Though these

results are based on a limited data sample, they agree with the findings of forecasters at BGM. Linear screening regression based upon BGM's data yielded the local SWP equation:

$$P = 18.5 + 0.040 \text{ VILWGT}. \quad (3)$$

The linear correlation between P and VILWGT in the BGM umbrella is 0.46.

In the subtropical environment of Tampa Bay, Florida (TBW), where widespread thunderstorms are an almost daily occurrence during the summer, only a small fraction (5%) of the cells were severe (Fig. 5). For TBW, cells were identified and tracked only if radar indicated a VIL of 20 or greater. This local constraint greatly reduced the total number of cells, while eliminating almost none of the severe ones. The VIL-SWP relationship here is weak compared to those observed near AMA and BGM; though severe events such as wind gusts and small tornadoes are common during the Florida warm season, they are produced by only a small fraction of the numerous large thunderstorms. The presence of abundant moisture and warm air causes many storms to build to considerable depth and horizontal extent, and VIL and SVG10 are large. However, the typical storm environment during the summer, with weak upper-level winds and only moderate instability, is not conducive to widespread severe weather outbreaks. The single-site SWP equation based upon all available data at TBW is:

$$P = 1.10 + 0.005 \text{ VILWGT}. \quad (4)$$

The VILWGT/severe weather linear correlation is very low, only 0.09, reflecting the small number of severe cells in the data sample and the low degree of severe/nonsevere discrimination given by the VIL predictors. Still, our results show that even in this subtropical environment, severe weather is most frequent within the largest, deepest storms.

Similar documentation of VIL-severe weather relationships for the other RADAP II sites with sufficient observational data appears in the Appendix.

As is apparent in Figs. 3-5, the fraction of storm cells that produce severe weather varies markedly with geographic location. There is, therefore, no one manner to interpret VIL over the entire United States. For this reason, the coefficents A-F in (1) have been made site-adaptable within the WSR-88D processing system, enabling the SWP algorithm to reflect varying climatology (Jendrowski, 1988).

While Figs. 3-5 demonstrate regional differences in the VIL-SWP relationship, we are confident that the radar characteristics of severe storms over neighboring umbrellas should be similar. The relationships between severe weather and maximum VIL near Amarillo and near Wichita, Kansas, (ICT, Fig. 6), are strikingly similar. It is probably fortuitous that the two histograms are so alike in all VIL categories, but this result suggests that climatology, rather than chance or variations in radar calibration, caused the marked differences among the TBW, AMA, and BGM results.

Given the significant effect of geographical location on the VIL-severe weather relationship, it is not surprising that time of year has an effect on the relationship over a given region, as well. To demonstrate this effect, the AMA and ICT data samples were divided into spring (April-May) and summer

(June-August) subgroups. As shown in Fig. 7, derived from AMA data, for most MAXVIL classes up to 60 kg m^{-2}, spring cells are more than twice as likely to feature severe weather as are summer cells. The spring storms develop in relatively cold but more unstable conditions; thus they are generally shallower than the summertime cells but more likely to feature intense convective circulation, with resulting hail and high winds. Also, the vertical wind shear favoring hail and tornado development is more common in the spring. This seasonal effect on the VIL/severe weather relationship was documented for Oklahoma by Beasley (1986), and has been often noted by field forecasters.

8. EFFECTS OF RANGE UPON VIL ESTIMATES

Radar estimates of VIL are necessarily less accurate at long ranges. Because of the curvature of the earth, the lower portions of distant storms, where reflectivity is typically largest, are overshot by the radar beam. Furthermore, high-reflectivity areas within distant storms cannot be fully resolved because of beam spreading. Thus, VIL estimates tend to be lower at longer distance ranges.

As shown in Fig. 8a, VIL estimates within the AMA umbrella tend to be lower for cells beyond 150 km (about 80 nautical miles) than for cells closer to the site. A significantly smaller percentage of the distant cells feature VIL's above 40 kg m^{-2} than do the nearer cells. This effect might be less apparent with the WSR-88D, which has a beam width half that of the WSR-57.

Range also has some effect upon the relationship between estimated VIL and severe weather potential (Fig. 8b). Though a somewhat higher percentage of the distant cells were severe overall (12% compared to 10%), it appears that range itself causes the severe weather threat to be greater for most VIL values, particularly above 30.

Because the percentage of cells with severe reports tended to vary significantly with range at most sites (this variation being due to chance), we have not attempted to quantify range effects more fully. It should be noted, however, that even the WSR-88D will probably underestimate VIL, and thus SWP, for distant storms. Recent work within TDL suggests that the partial VIL above 15,000 feet has nearly the same information with regard to severe weather that total VIL does, and this quantity might later be utilized in providing SWP estimates at longer ranges.

9. DERIVATION OF EQUATIONS FOR THE SWP ALGORITHM

The SWP algorithm was developed on the basis of the statistical sample described above, which contains data on a considerable number of cells (approximately 6500) from many of the RADAP II sites. There are a number of logical courses of action to take in developing classical statistical forecasting equations such as the SWP algorithm. We investigated four such options.

The first option was the creation of single-site (SS) equations, derived from each radar umbrella's data and designed to be applied only within a region near that radar. Sample SWP equations (2)-(4) were derived in this manner. The chief advantage of this approach is that the SS equations are automatically calibrated to local climatology, and the equation results represent actual probabilities. The second option, considered in order to

overcome the lack of sufficient data at some sites, was the creation of regional equations, based upon observations from several neighboring sites. The regional equations should still be fairly well calibrated to local climatology.

The third and fourth options involve combining the data from all sites, an approach which has the advantage of a large sample size. The pure generalized operator (GENOP) approach would provide one equation to be applied at all sites. It would then be necessary to present guidance on interpreting the algorithm output at individual sites. Finally, the GENOP method may be modified to account for local climatology, by determining a different constant (coefficient A in (1)) for each site's equation, such that the mean SWP value is equal to the percentage of severe cells actually observed at that site. The other coefficients, which multiply VIL terms, would be the same at all sites.

In practice, more than one of these methods would probably be needed to supply all regions of the United States with SWP algorithm coefficients, since there are no RADAP II sites over the northern Plains, the upper Midwest, or anywhere west of the Continental Divide. While some regions could use a local equation, others could use a general operator or regional one.

Our final choice was based upon the availability of archived data at individual RADAP II sites and upon the skill level of the algorithm output when it was used to produce categorical (yes/no) severe weather nowcasts for a test sample of independent data. The reduction of probabilistic forecasts to categorical ones follows current forecasting practice, in which official warnings are issued for only a fraction of all thunderstorms. While categorical forecasts issued under conditions of uncertainty contain less information than probabilistic statements, there are formidable logistical problems involved in providing updates on the location and intensity of multiple storms every few minutes. Thus, the current practice of warning for selected storms, that have at least some minimum potential for severe weather, will likely have to be continued for some time.

Given a large and fully representative sample of observations at all sites, it would have been advantageous to develop SWP equations for the locality of each site. For many RADAP II sites, however, this attractive option could not be exercised due to a lack of data. For any site, the number of cell observations depended upon local climate, the length of the archiving period, and sometimes upon long-term mechanical problems with the RADAP II unit itself. For most sites, we had at least 500 cells that passed over population centers. At Tampa Bay, there were nearly 1100, and Amarillo and Wichita had over 1600. However, Binghamton and Jackson, Kentucky, (JKL) had less than 300 each. Such small samples might yield statistically unreliable probability equations when applied to independent data. It might be possible to develop reliable equations from data at several neighboring sites, but some regions (particularly the Northeast) had sites with few or no observations, making the regional equation approach difficult to implement in practice.

Finally, and perhaps most important, we found that single-station or regionalized SWP equations yielded virtually no advantage over a general operator equation when the SWP value was reduced to a severe/nonsevere forecast. The probabilistic-to-categorical forecast conversion is done by selecting a threshhold SWP value and forecasting all cells to be severe or

nonsevere based solely upon the threshold. The selection of an optimum threshold takes into account both the local skill of the SWP equation, and the relationship between SWP and actual severe weather probability. As will be shown, the skill levels of the categorical forecasts were very similar regardless of whether they were derived from SS, regional, or GENOP probabilistic equations.

The experimental process by which we reached this conclusion was as follows. First, a single-station SWP equation was derived with a randomly-selected portion of the data available for that site. The remaining portion, taken from one third of the calendar days on which any storm cell observations existed, was withheld and later used as an independent sample. Second, a general operator equation was derived. The development sample consisted of the same data employed in the SS development, plus all data from all of the other radar sites. Finally, the SS and GENOP equations were compared by verifying their forecasts against the observations in the independent data.

It was not logical to compare the actual SWP values from the two equations, since the general operator was usually biased with respect to the single-station data sample. However, it was useful to compare the two sets of probabilistic forecasts in terms of the categorical forecasts they would yield. Test categorical forecasts for each storm cell in the independent sample were generated from a range of SWP threshold values, and forecast scores were compared.

Verification results for severe/nonsevere storm forecasts may be summarized in a 2 x 2 contingency table as shown in Fig. 9. Here, x represents the number of severe cells forecasted to be severe ("hits"), y represents the number of severe cells <u>not</u> forecasted to be severe ("misses"), and z is the number of nonsevere cells forecasted to be severe ("false alarms").

Several useful forecasts scores can be derived from this contingency table. The probability of detection (POD), defined by x/(x+y), is the fraction of severe cells correctly identified. The false alarm ratio (FAR), given by x/(x+z), is the fraction of all severe forecasts that are false alarms. Note that if the threshold SWP value is set very high, not enough severe storms would be detected, while if the threshold is set too low, too many false alarms would be issued. The critical success index (CSI) or threat score, given by x/(x+y+z), is the fraction of "hit" forecasts among all those in which severe weather either was forecasted or ocurred. The CSI (Donaldson et al., 1975) may be considered to represent a measure of the balance between too high an FAR and too low a POD.

The single-station and general operator equations for AMA were compared as follows. The equations derived by forward-selection screening regression are, respectively:

$$P_{SS} = 1.033 + .042\text{xVILWGT} - .836\text{xSVG10}, \text{ and} \quad (5)$$

$$P_{GEN} = 6.038 + .046\text{xVILWGT} - .975\text{xSVG10} - .609\text{xSVG20}. \quad (6)$$

Note that (5) differs from (2) because only about two thirds of the AMA data was employed in the derivation of (5). The selection procedure yielded three terms in (6) and only two in (5) because the selection cutoff depends in part upon the size of the development sample, which was larger for (6). Scores for

categorical forecasts based upon both of these equations appear in Fig. 10. These scores are based upon a verification sample of 573 cells withheld from the development of the equations. Both POD and FAR decrease monotonically as the threshold SWP value is raised, while the CSI peaks at one value, which may be interpreted as the peak skill. Note that the GENOP and SS equations yield the same maximum CSI value (0.34).

Very similar results were obtained when this comparison was repeated with BGM and TBW observations (see Figs. 11 and 12). Both the maximum CSI, and the threshold that yields it, vary significantly from site to site, but at none of the three did the single-station equation yield a marked improvement over the general operator approach. Regional equations, and a general operator equation adjusted to local climatology, were also derived for the AMA and BGM umbrellas; again, they were not appreciably better than the GENOP equation.

This finding appears to be due to the fact that the VILWGT predictor alone accounts for most of the reduction of variance in both the SS and GENOP equations. The linear correlation between any two of the five available predictors is generally 0.80 or even higher; thus none of the predictors yield much information independent of the others. The inclusion of the predictors other than VILWGT only slightly increases the correlation between P and severe weather occurrence, and has little influence on the skill level of categorical forecasts based on the SWP algorithm's output. Therefore, the categorical forecast skill in terms of POD, FAR, and CSI is nearly the same for SS and GENOP equations, once the yes/no thresholds are adjusted to account for climatic differences.

However, the optimum probabilistic-categorical conversion threshold, and the skill level of the categorical forecasts, vary markedly from site to site. An evaluation of the GENOP SWP threshold that yields a POD of 0.8 for nine RADAP II sites is shown in Fig. 13. The numbers in parentheses represent the CSI at this threshold. The thresholds are for the entire warm season, except at OKC, AMA, and ICT, where they are for the spring season. In general, the threshold is largest (10 and above) in regions characterized by the highest VIL values. The skill of the SWP algorithm as indicated by the CSI is largest over areas with the highest percentage of cells that are severe (the Plains and New York).

In summary, it is apparent that the SWP output must be interpreted differently at different sites, regardless of whether SS or GENOP equations are used, in order to correct for variations in regional storm climatology and the fact that VIL yields more information on severe weather potential in some regions than in others. Furthermore, single-station or regional equations based upon the limited predictor set currently available yield little additional information when compared with the general operator equation. Finally, we presently possess little or no archived observational data for much of the United States, and thus cannot develop reliable single-station equations for many localities. For these reasons, we believe that the best approach to implementing the SWP algorithm lies in a general operator equation, with information on local interpretation of the algorithm being made available to forecasters.

10. RECOMMENDED SWP ALGORITHM

On the basis of these findings, we have recommended to the NEXRAD Operational Support Facility (OSF) that all WSR-88D sites be initially supplied with the equation coefficients for a single, general operator equation. The equation was derived from all available data at seven RADAP II sites (AMA, BGM, BNA, GCK, ICT, LIC, and UMN), and a limited amount of data from OKC. This development sample contains 6529 cells, of which 909 (14%) were severe. The relationship is:

$$P = 5.820 + 0.046 \times VILWGT - 0.964 \times SVG10 - 0.576 \times SVG20. \quad (7)$$

Tests have shown that incorporating the remaining two predictors yields no higher correlation to the severe weather predictand when verified upon independent data.

The Appendix of this note contains documentation on adapting the interpretation of this equation to as many local sites as possible, including tables giving actual severe weather probability as a function of the P value and of the cell maximum VIL, and local categorical forecast scores for a range of SWP thresholds. Where sufficient data were available, these findings were further stratified by season.

11. PLANNED REFINEMENTS TO THE SWP ALGORITHM

It is very important to note that our choice of a single equation for the initial SWP algorithm was largely due to the constraint of a very limited predictor set. The selection of predictors by Elvander (1977) was based only upon observations from Oklahoma during the 1972 spring season. Additional predictors, especially some based upon vertical storm structure, such as echo height and reflectivity aloft, might yield independent information on storm severity at many of the sites. Given more predictors that are less strongly correlated to the original five, it will likely be possible to develop single-station equations that are superior to the general operator we now recommend. Experiments involving the incorporation of such predictors are now underway.

We have also shown that the interpretation of VIL depends upon conditions within the thunderstorm environment. It would be highly useful to develop a version of the SWP algorithm that explicitly accounts for the effect of the storm environment on the VIL-severe weather relationship, as we have implicitly tried to do in deriving single-site and seasonal SWP equations. We are currently experimenting with the inclusion of environmental predictors, such as upper-air winds, temperature, and stability, in the SWP relationship. Such an algorithm could be implemented most easily within the Advanced Weather Interactive Processing System (AWIPS), which will feature the capability of combining observations from multiple observing platforms.

Of course, Doppler velocity and spectral observations could prove to be the most important indicators of severe weather. We plan to investigate these data when a sufficient quantity is archived.

Perhaps the most basic refinements of all can be made when WSR-88D archives are available from areas such as the Southeast, the lower Mississippi Valley, the northern Plains, and the desert Southwest. Though all of these regions experience significant severe weather, no systematic archive of volumetric

radar observations exists for their thunderstorms. We hope to present information on the severe weather interpretation of reflectivity and Doppler data over these areas in the future.

ACKNOWLEDGEMENTS

The development of the SWP algorithm was possible only with the cooperation of the National Weather Service field office personnel who archived the raw reflectivity data and forwarded it to TDL for final processing and interpretation.

We are also indebted to Melvina McDonald for her organization and monitoring of the RADAP II archive, and to the many cooperative education students who carried out the tedious work of transferring the raw radar data from diskette to magnetic tape at TDL.

Much of the computer code used in interpreting the reflectivity data was developed by Paul Jendrowski, currently employed by UNISYS. A PC-based program for editing storm cell location data, which greatly facilitated this entire effort, was developed by Michael Young and Thomas Renkevens. The majority of the subjective severe storm identification process was carried out by Jay Breidenbach, Jeffrey Peters, and Thomas Renkevens.

For much of the statistical analysis involved in the algorithm development, we are indebted to Dr. Robert G. Miller, now retired from TDL.

REFERENCES

Beasley, R. A., 1986: An analysis of operational RADAP II parameters, corresponding synoptic variables, and concurrent severe weather events in Oklahoma. M. S. Thesis, Univ. of Oklahoma, 223 pp.

Draper, N. R., and H. Smith, 1981: Applied Regression Analysis. New York, John Wiley and Sons, 709 pp.

Donalson, R. J. Jr., R. M. Dyer, and J. J. Kraus, 1975: An objective evaluator of techniques for predicting severe weather events. Preprints Ninth Conference on Severe Local Storms, Norman, Amer. Meteor. Soc., , 321-326.

Elvander, R. C., 1977: Relationships between radar parameters observed with objectively-defined echoes and reported severe weather occurrences. Preprints Tenth Conference on Severe Local Storms, Omaha, Amer. Meteor. Soc., 73-76.

Greene, D. R., and R. A. Clark, 1972: Vertically-integrated liquid--a new analysis tool. Mon. Wea. Rev., 100, 548-552.

McDonald, M., and R. E. Saffle, 1989: RADAP II archive data user's guide. TDL Office Note 89-2, National Weather Service, NOAA, U.S. Department of Commerce, 16 pp. [Available from Techniques Development Laboratory, W/OSD2, National Weather Service, 1325 East West Highway, Silver Spring, Md. 20910].

McGovern, W. E., R. E. Saffle, and K. C. Crawford, 1984: Verification results from 1982-84 operational radar reflectivity experiment. Preprints 22nd Conference on Radar Meteorology, Zurich, Amer. Meteor. Soc., 188-191.

Saffle, R. E., W. E. McGovern, and M. McDonald, 1986: Use of RADAP II data to estimate the impact of NEXRAD scan strategies on calculations of vertically integrated liquid water. Preprints 23rd Conference on Radar Meteorology, Snowmass, Amer. Meteor. Soc., JP60-JP61.

Winston, H. A., and L. J. Ruthi, 1986: Evaluation of RADAP II severe-storm-detection algorithms. Bull. Amer. Meteor. Soc., 67, 145-150.

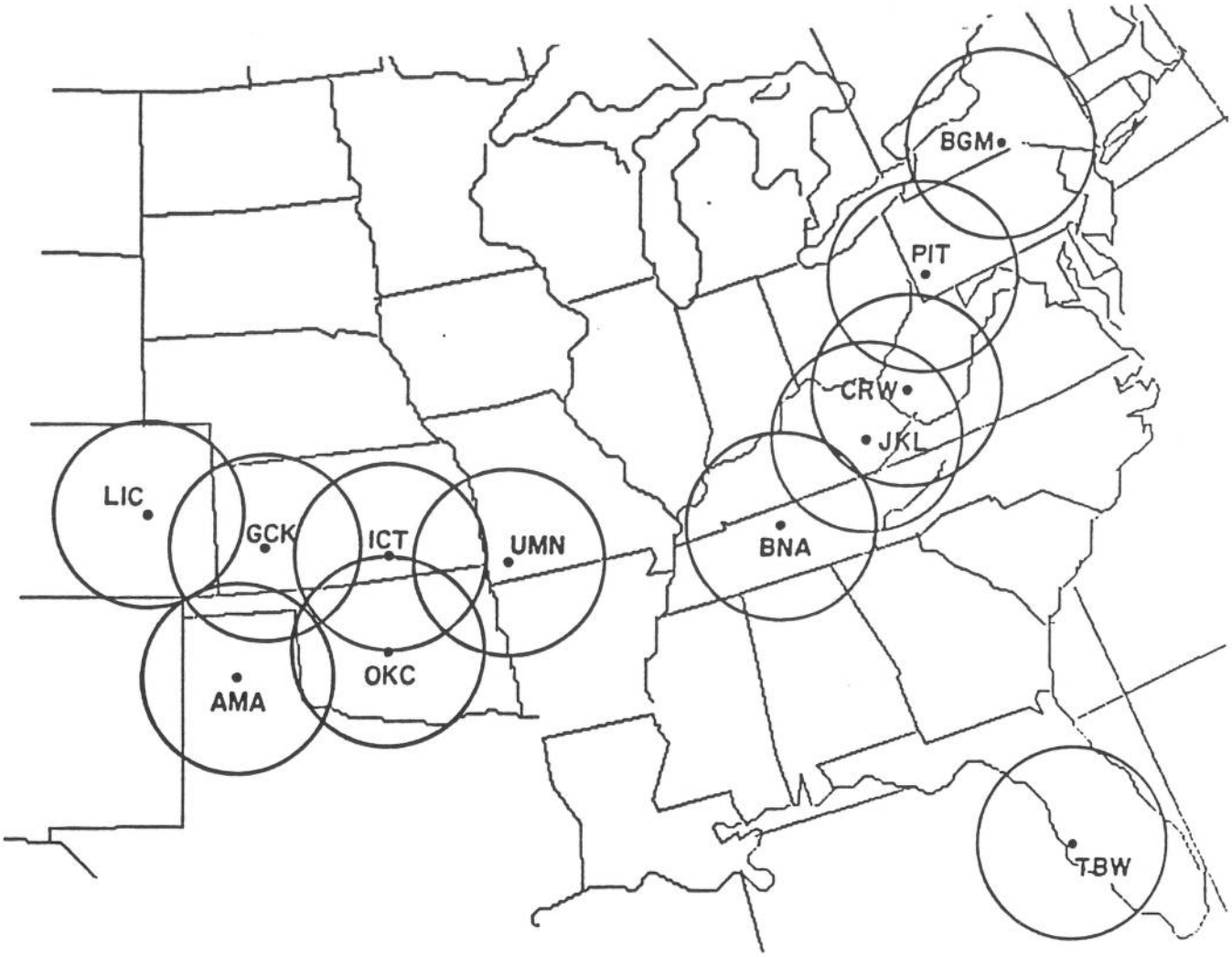

Figure 1. Locations of WSR-57 sites equipped with RADAP II. The circles about each site show the 230-km range.

Table 1. RADAP II sites.

Station	Call letters	Latitude (deg)	Latitude (min)	Longitude (deg)	Longitude (min)
Amarillo, Tex.	AMA	35	13	101	42
Binghamton, N. Y.	BGM	42	12	75	59
Charleston, W. Va.	CRW	38	23	81	36
Garden City, Kans.	GCK	37	55	100	42
Jackson, Ky.	JKL	37	35	83	18
Limon, Colo.	LIC	39	11	103	42
Monett, Mo.	UMN	36	52	93	53
Nashville, Tenn.	BNA	36	15	86	34
Oklahoma City, Okla.	OKC	35	24	97	36
Pittsburgh, Pa.	PIT	40	32	80	13
Tampa Bay, Fla.	TBW	27	42	82	24
Wichita, Kans.	ICT	37	39	97	26

Table 2. Severe weather predictors derived from VIL. The predictors denoted by VILWGT, SVG10, SVG15, SVG20, and SVG25 are those incorporated in the WSR-88D SWP algorithm.

NSIZE:	Number of 4 x 4 kilometer analysis grid boxes within the storm cell area that feature VIL $\geq$ 10 kg m^{-2}
MAXVIL:	Maximum VIL value within the storm cell (kg m^{-2})
VILWGT:	(VIL-Weight) NSIZE times MAXVIL
SUMVIL:	Sum of the VIL values within grid boxes that feature VIL $\geq$ 10 kg m^{-2} (proportional to cell's total precipitation mass)
SVG10:	Number of grid boxes with VIL > 10 kg m^{-2} (SVG10 is not identical to NSIZE)
SVG15:	Number of grid boxes with VIL > 15 kg m^{-2}
SVG20:	Number of grid boxes with VIL > 20 kg m^{-2}
SVG25:	Number of grid boxes with VIL > 25 kg m^{-2}

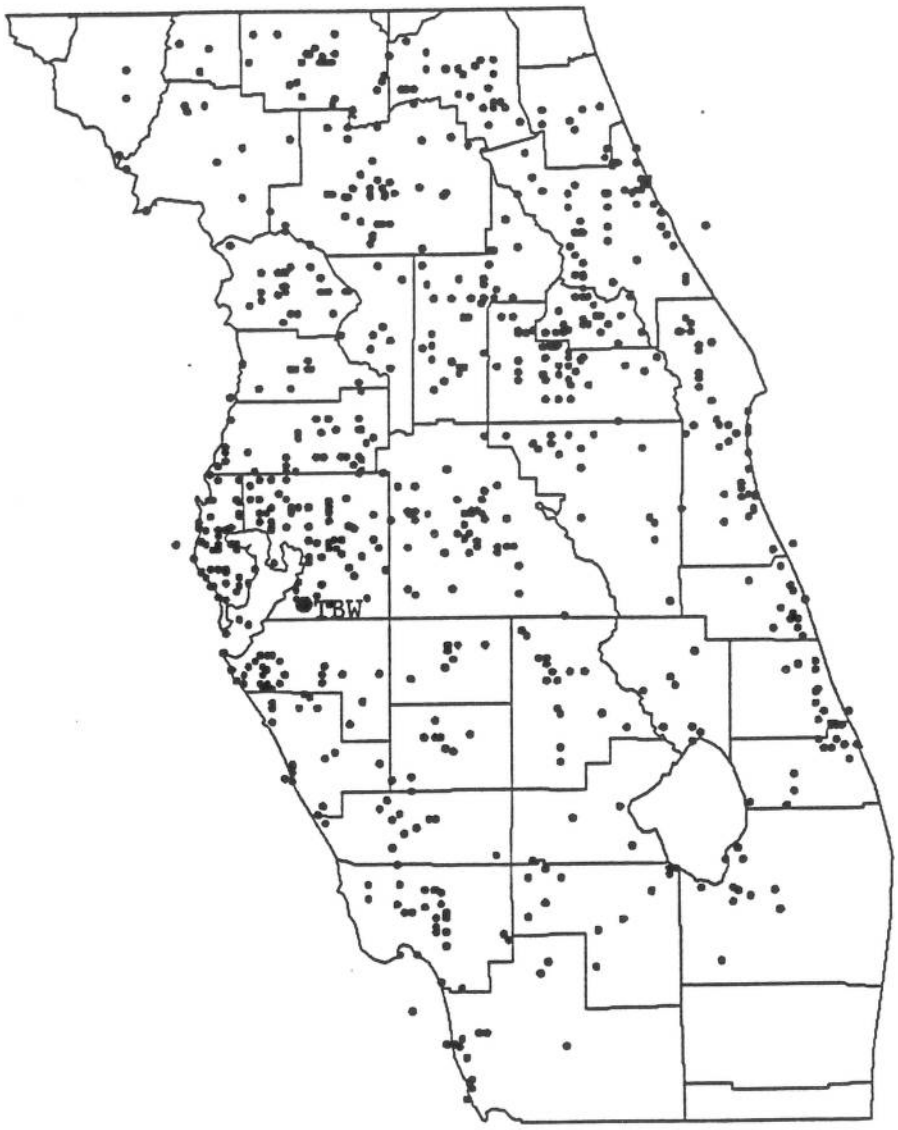

Figure 2. Distribution of severe local storm reports within 230 km of the Tampa Bay radar site (TBW). Some dots represent multiple reports. No reports beyond 230 km from TBW are included, hence the blank areas over the southernmost counties on the map.

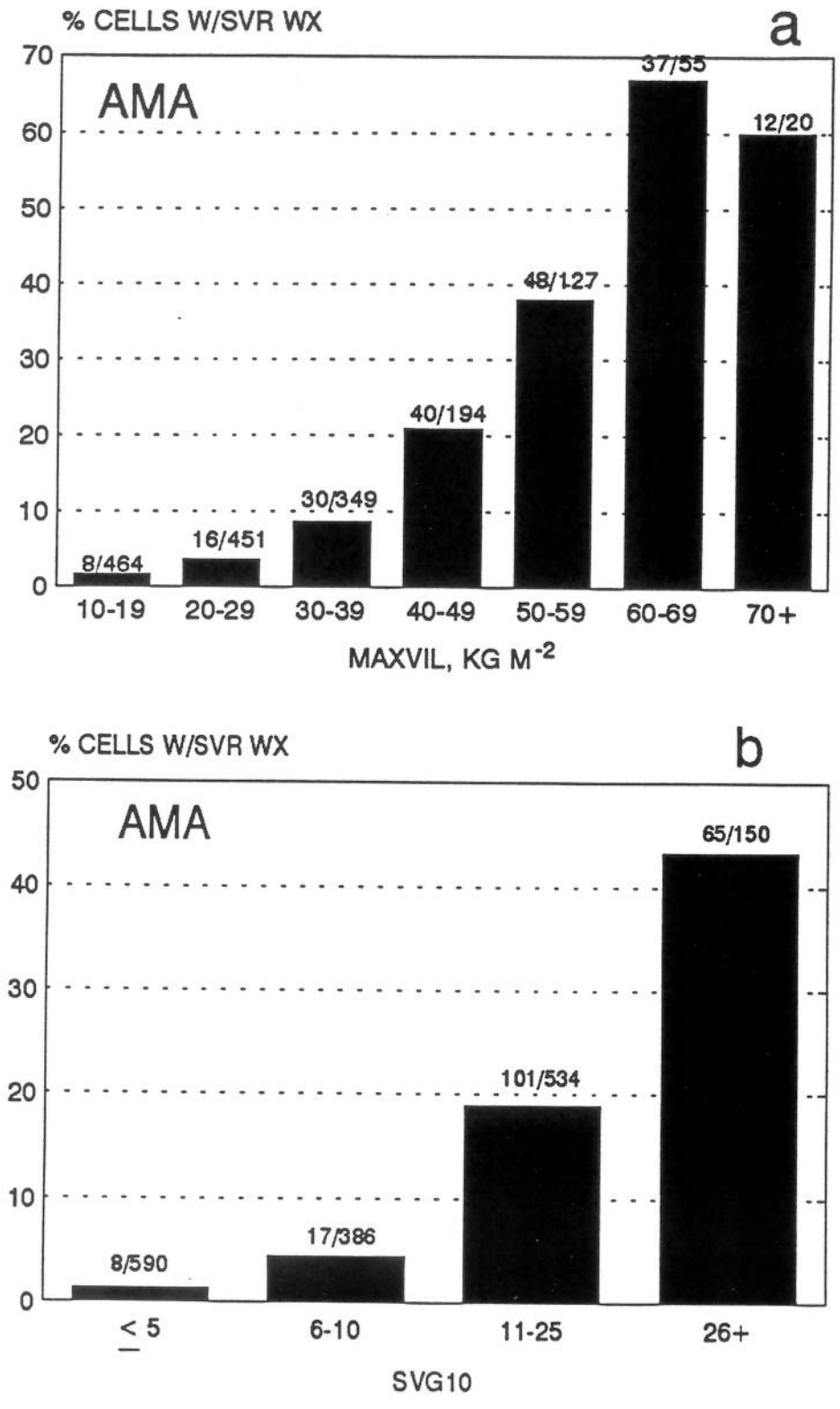

Figure 3. Percentage of severe thunderstorm cells as a function of (a) cell maximum VIL and (b) number of 4 x 4 km grid blocks with VIL $\geq$ 10 kg m^{-2}, near the Amarillo, Texas (AMA) radar site. Data are from the April-September period, 1985-1989.

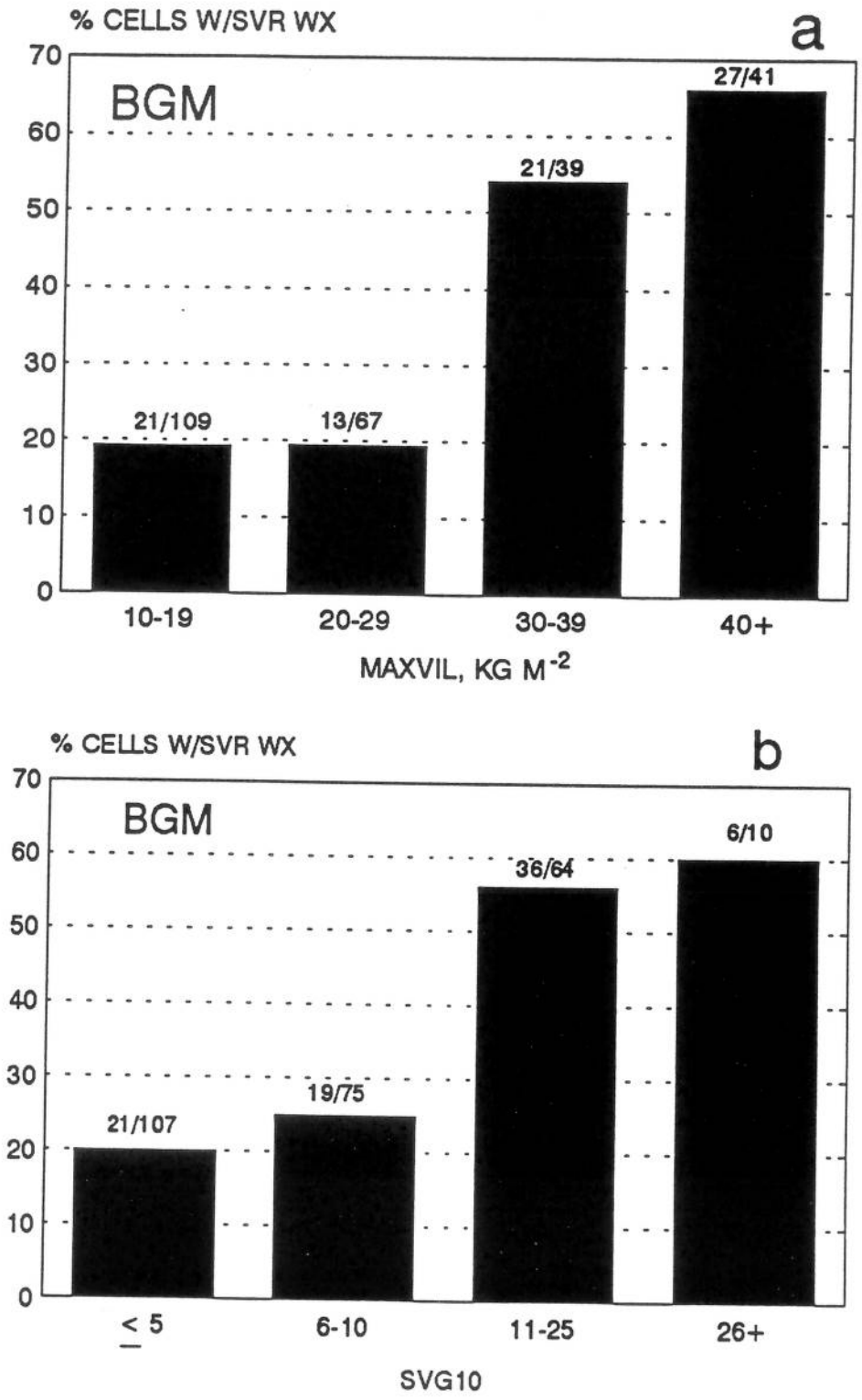

Figure 4. As in Fig. 3, except for the Binghamton, New York (BGM) radar umbrella. Data are from the April-September period, 1988-1990.

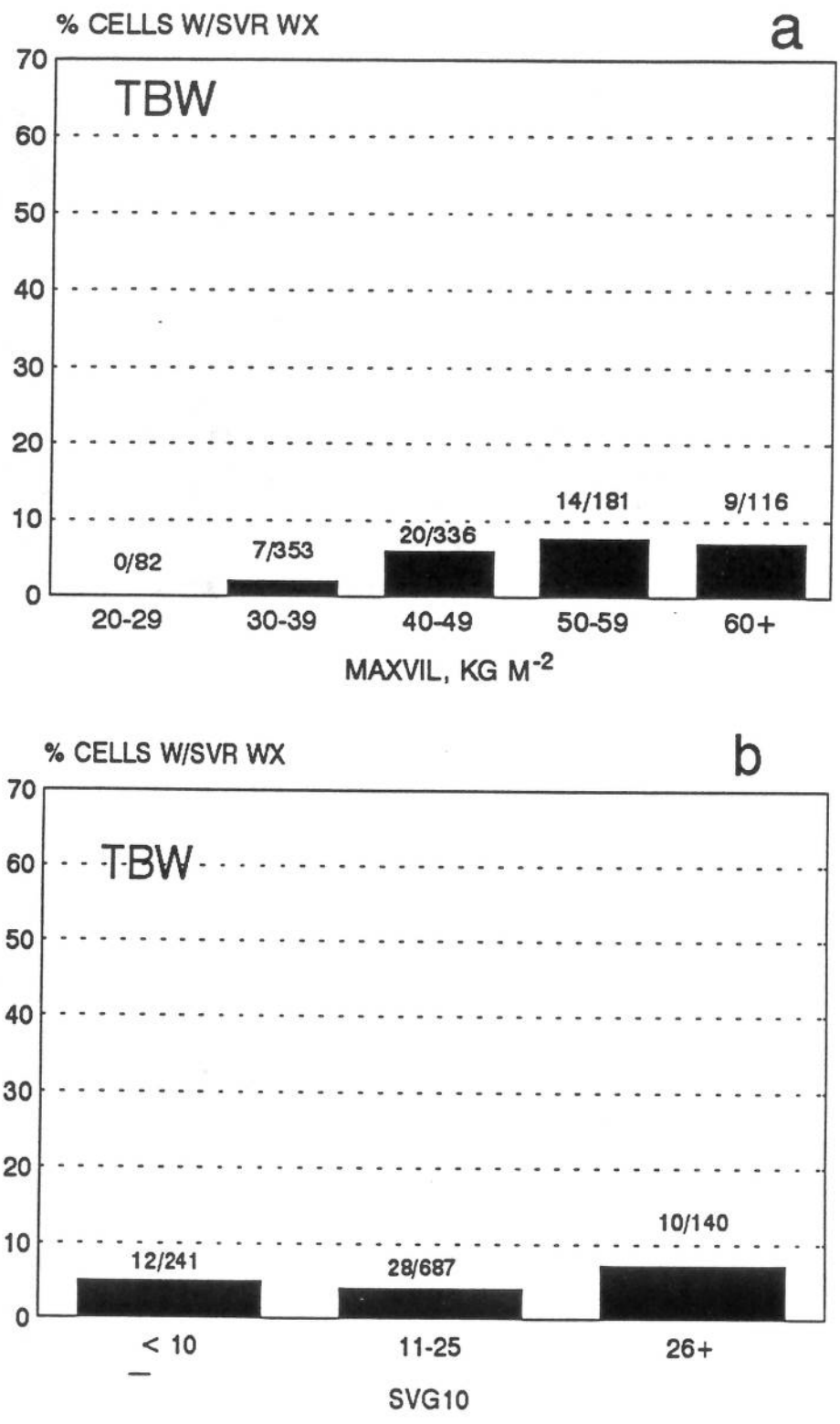

Figure 5. As in Fig. 3, except for the Tampa Bay, Florida (TBW) radar umbrella.

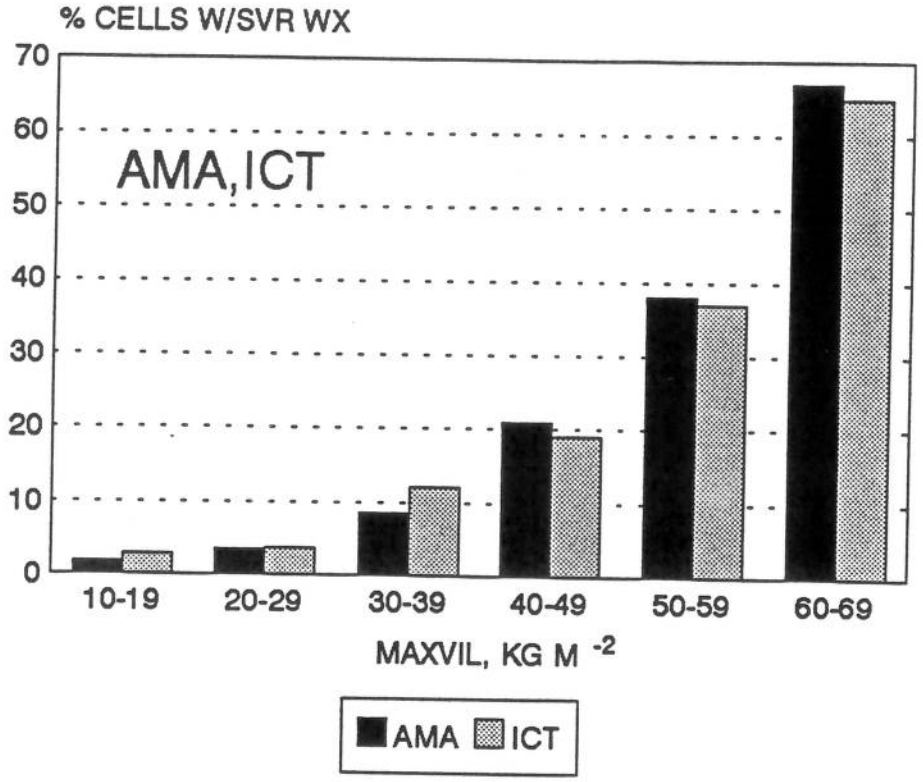

Figure 6. Percentage of storm cells with severe weather as a function of cell maximum VIL near Amarillo (AMA, black bars) and Wichita, Kansas (ICT, gray bars).

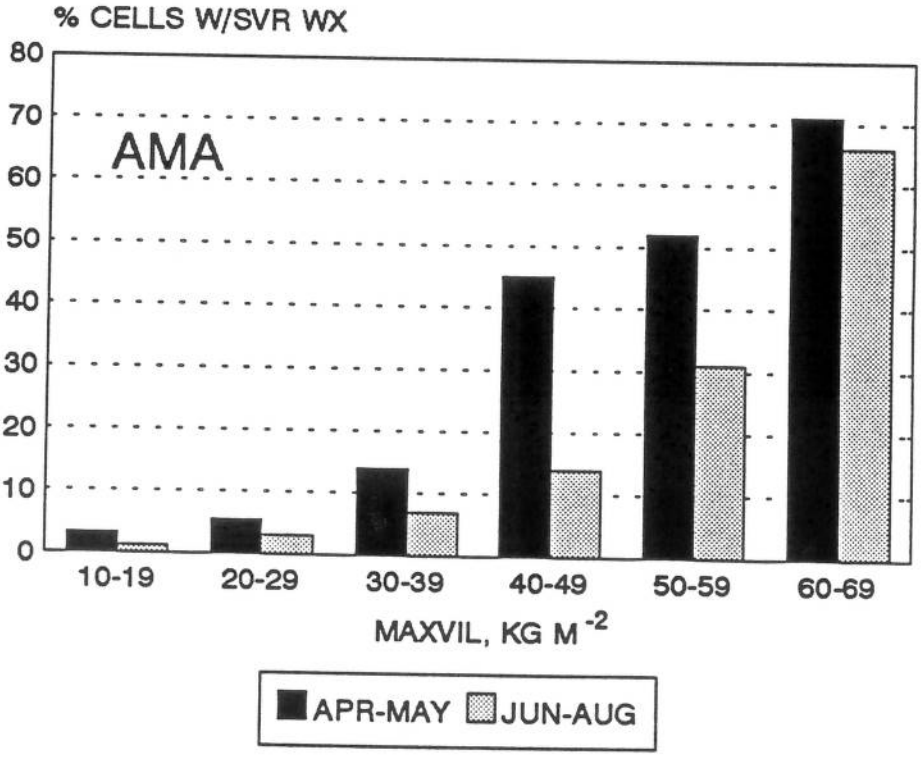

Figure 7. Percentage of severe cells as a function of maximum VIL near AMA, during spring (black bars) and summer (gray bars).

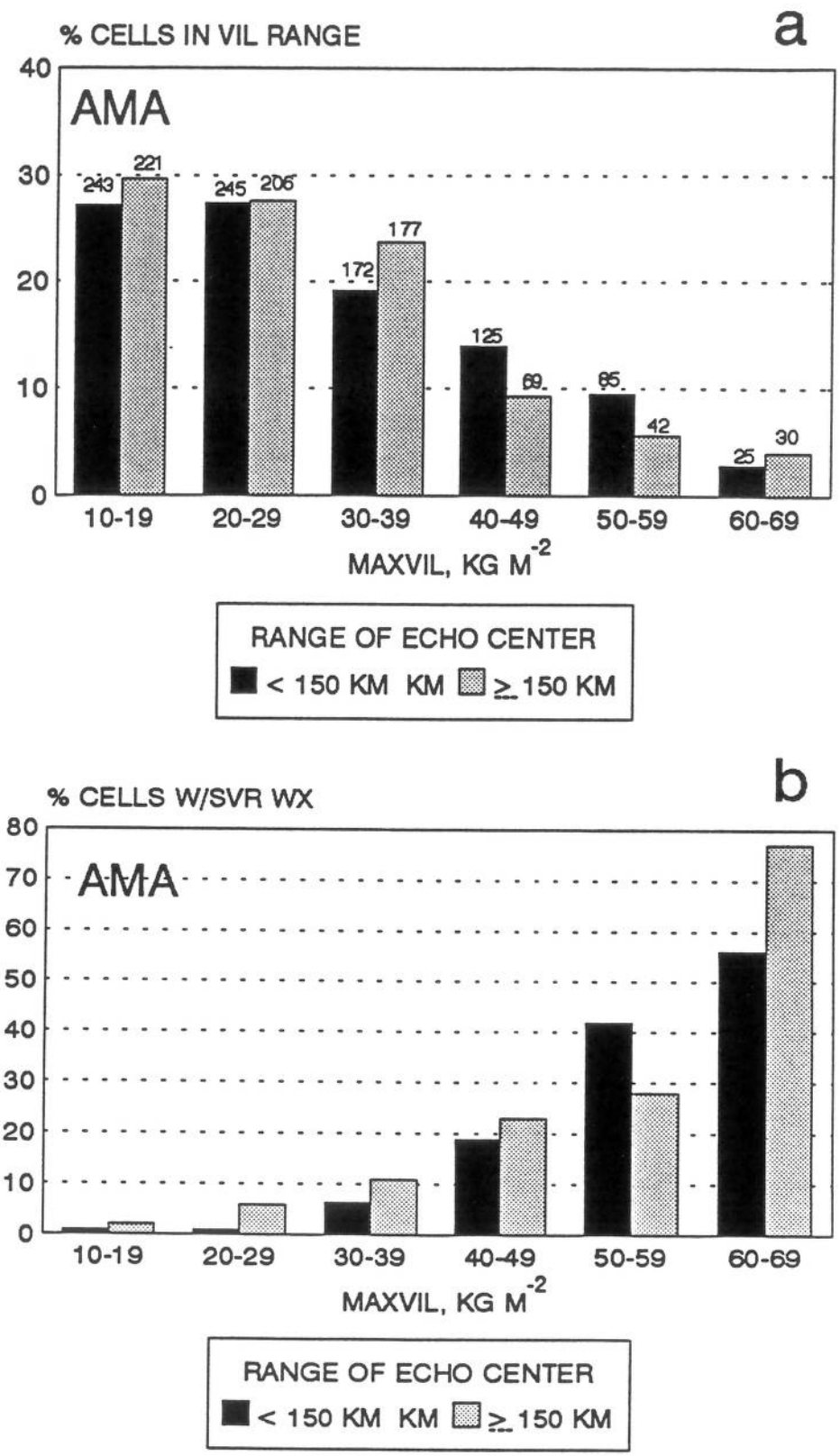

Figure 8. Effects of range upon (a) VIL estimates and (b) the apparent VIL/severe weather relationship. Observations are from the AMA umbrella. Numbers over histogram bars in (a) indicate the number of storm cells in each category.

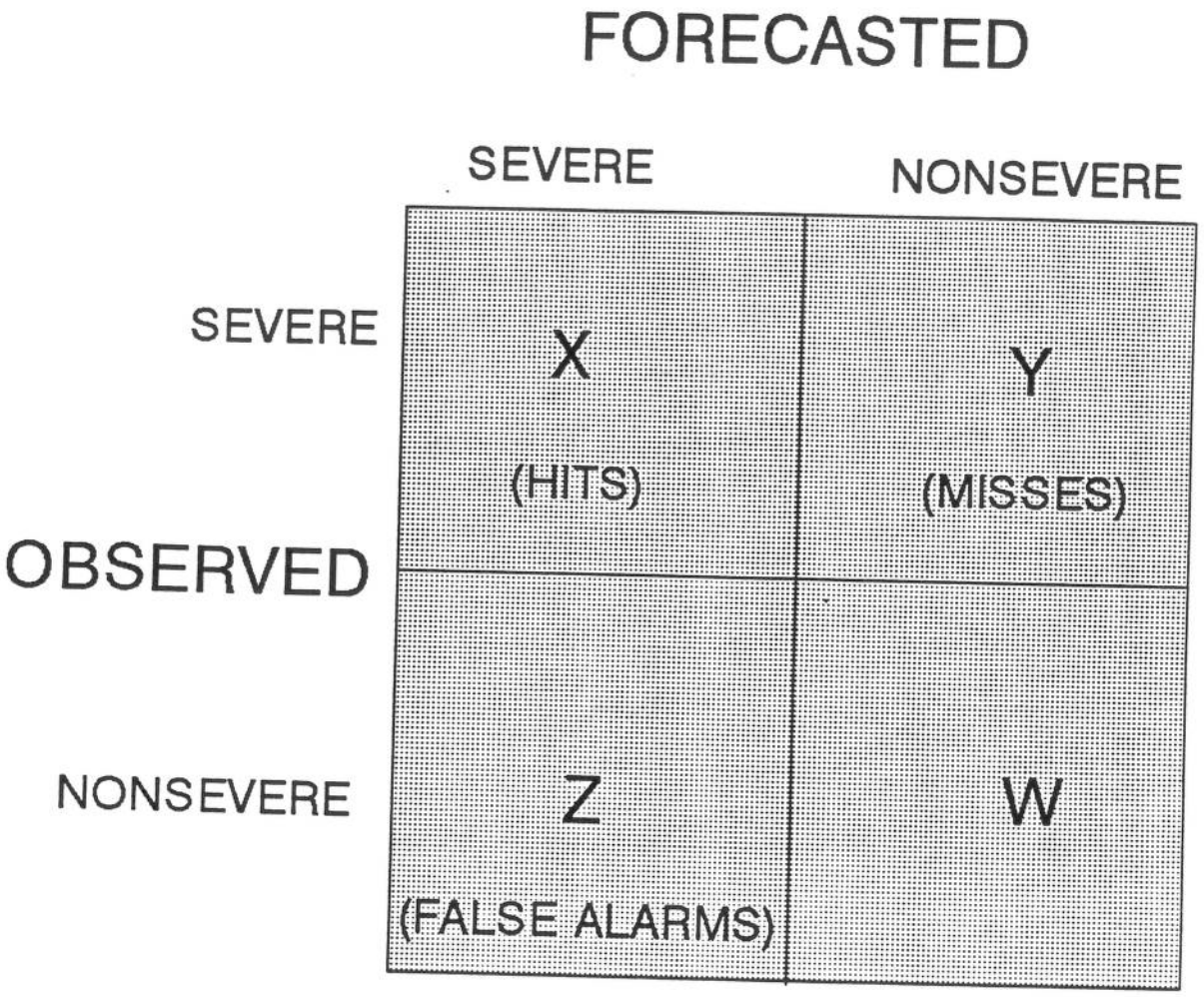

Figure 9. Contingency table for verification of categorical (severe/ nonsevere) forecasts.

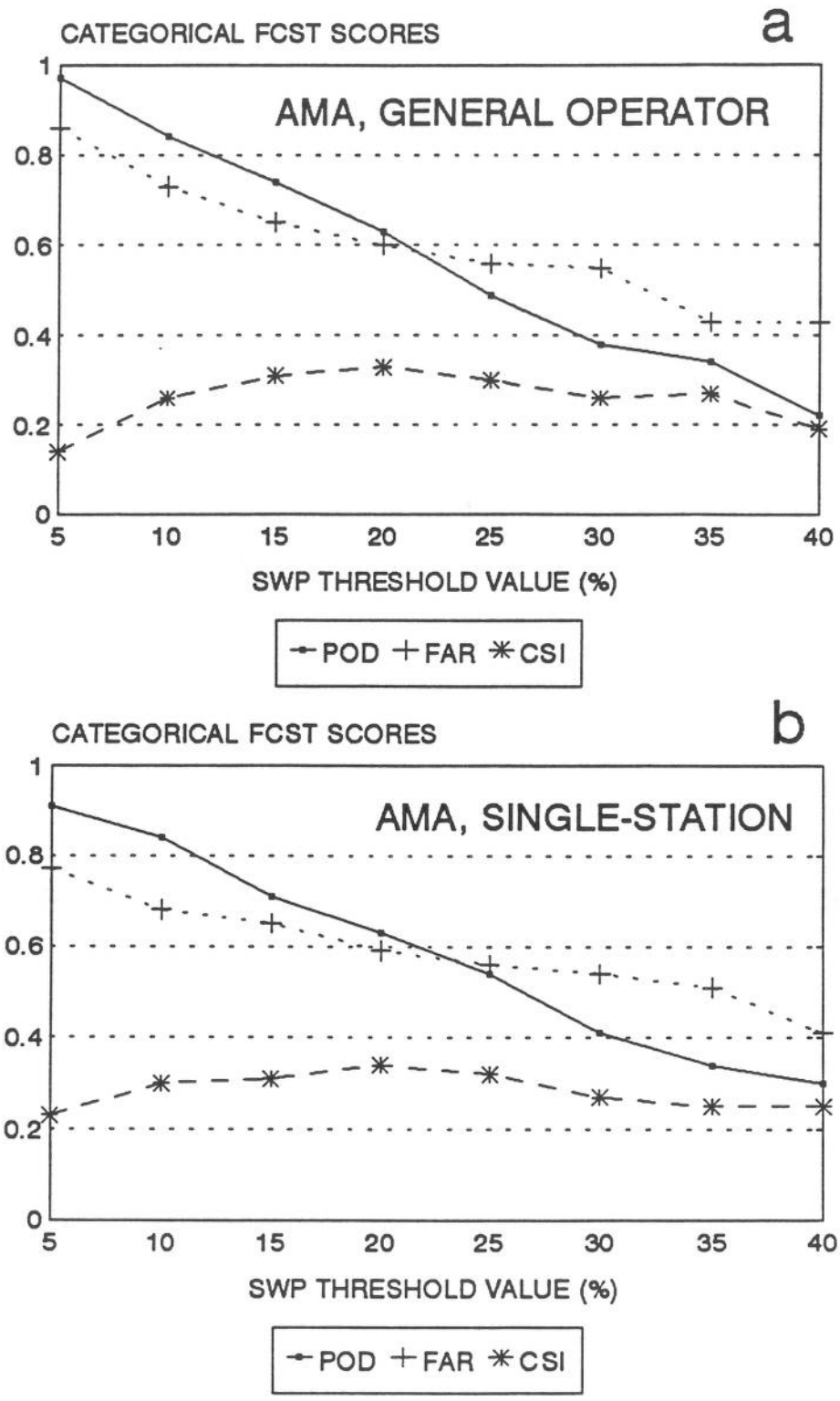

Figure 10. Categorical forecast scores as functions of threshold SWP value for the AMA umbrella, for SWP derived from (a) a general-operator probability equation and (b) a single-station equation. The scores are defined in the text.

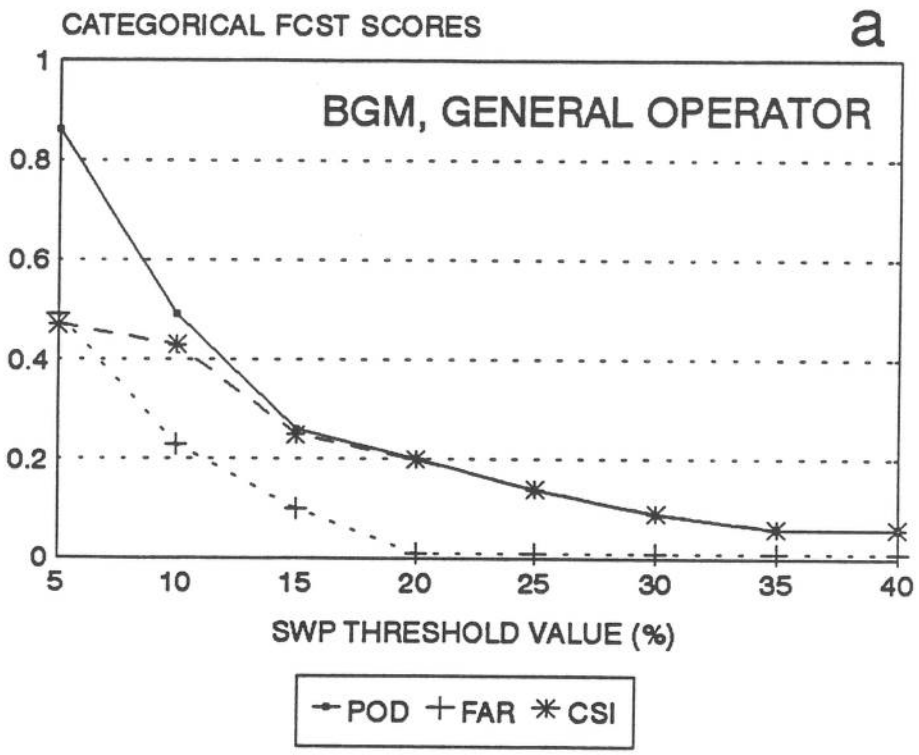

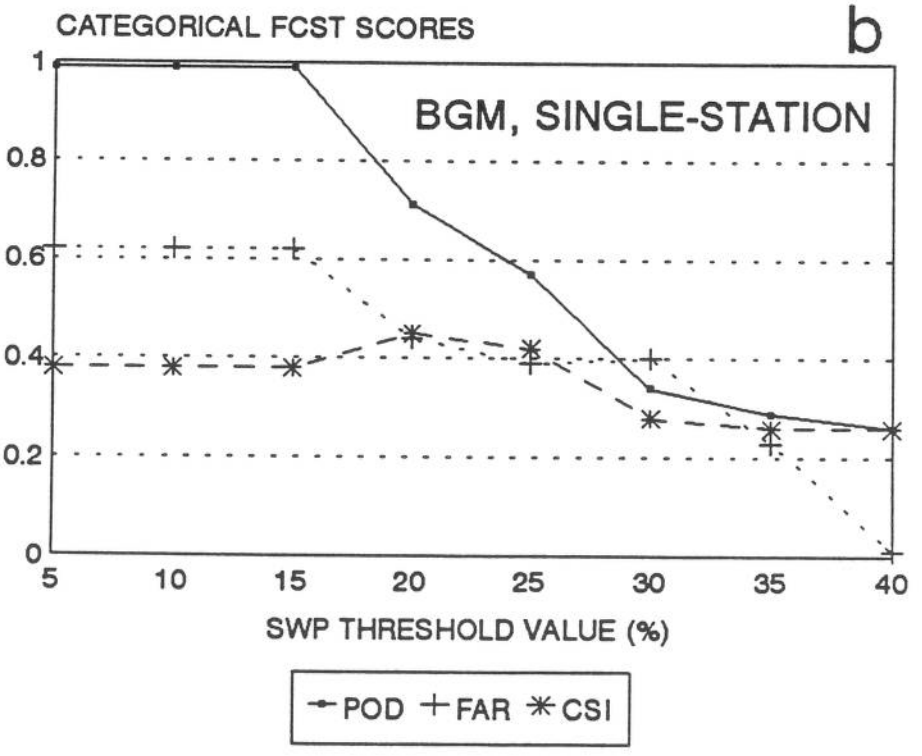

Figure 11. As in Fig. 10, except for the BGM umbrella.

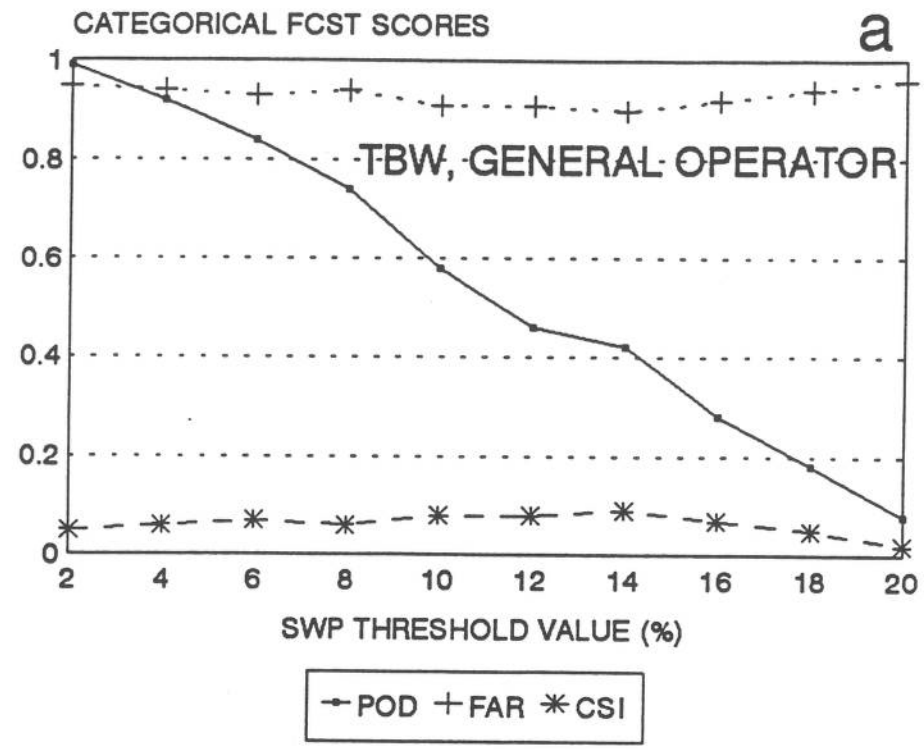

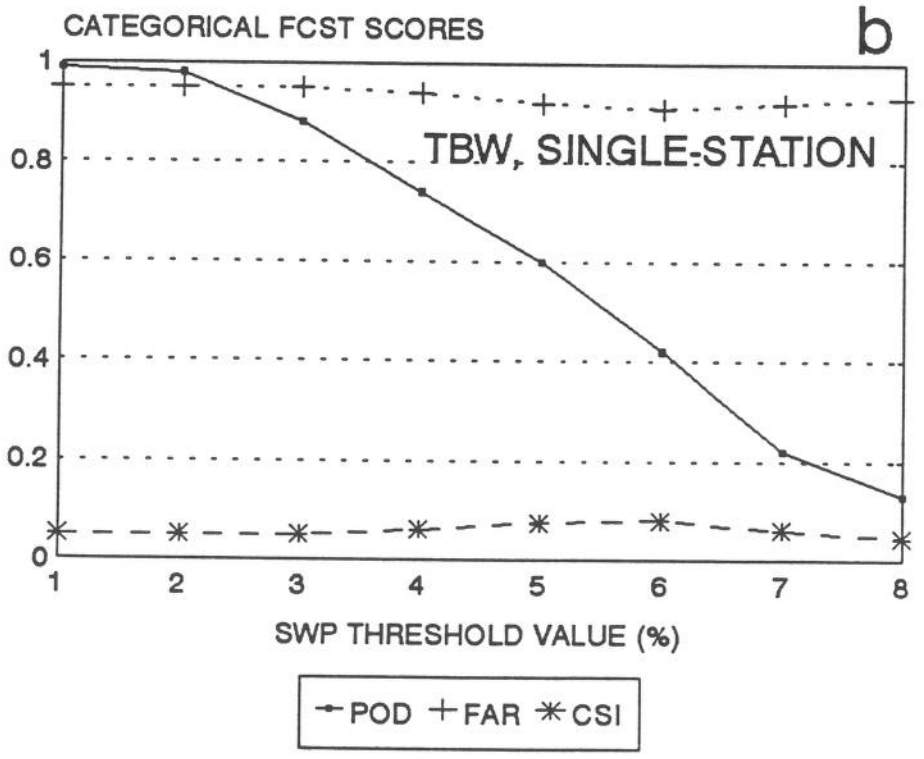

Figure 12. As in Fig. 10, except for the TBW umbrella.

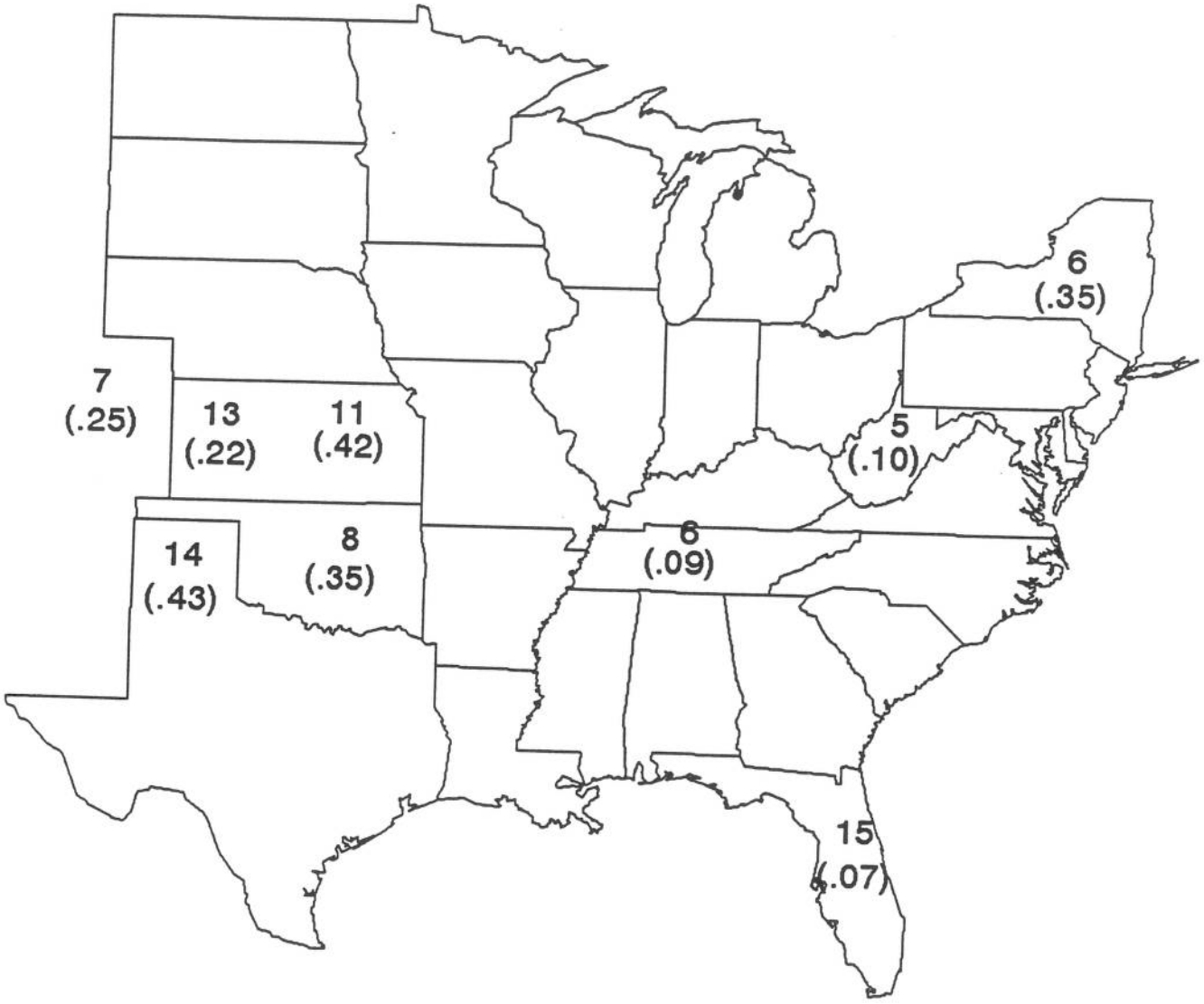

Figure 13. SWP threshold values that yield a categorical POD of 0.8, and corresponding CSI values (in parantheses). Threshold values are for an SWP general operator equation based upon all data at nine RADAP sites.

APPENDIX

CHARACTERISTICS OF THE SWP ALGORITHM OVER DIFFERENT REGIONS AND SEASONS

This appendix contains information on the radar characteristics of thunderstorms and severe local storms within individual RADAP umbrellas. As noted earlier, the relationship between VIL and severe weather probability is markedly dependent upon the thunderstorm environment. Rather shallow thunderstorms with only moderately high VIL are much more likely to produce severe weather given cold, highly unstable conditions than given warm, marginally unstable conditions.

Since the SWP algorithm in its present form cannot directly account for changes in the VIL-severe weather relationship due to environmental conditions, we have documented as fully as possible the properties of the algorithm within different geographical areas. This appendix contains information on severe storm climatology and radar characteristics near nine of the twelve RADAP II sites, including the observed relative frequency of severe cells as a function of maximum VIL and SWP value. For those sites with sufficient data, the results have been stratified by season of the year.

We also present verification scores for categorical (severe/nonsevere) nowcasts derived solely from SWP algorithm output, through the application of threshold values for the SWP. The verification scores were derived by applying the SWP algorithm given by (7) to all of the storm cells that passed over populated portions of the radar umbrella. Since the data sample used to derive (7) is considerably larger than the verification sample for any one site, the scores are probably indicative of those that would be achieved with independent data. The verification counts and scores, explained in detail in Section 9, are briefly recapitulated below:

X: number of severe cells correctly forecasted (hits);
Y: severe cells forecasted to be nonsevere (misses);
Z: nonsevere cells forecasted to be severe (false alarms);
W: nonsevere cells correctly forecasted;

POD = X/(X+Y), probability of detection;
FAR = Z/(X+Z), false alarm ratio;
CSI = X/(X+Y+Z), critical success index or threat score;
Bias = (X+Z)/(X+Y), ratio of severe forecasts to severe events.

The POD, FAR, and CSI are also presented graphically as functions of threshold SWP values.

A1. AMARILLO, TEXAS (AMA)

The storm data sample for AMA contains 1660 cells, of which 191 (12%) were severe. Data were available for the period April-September 1985-89. We were able to stratify the sample into spring (April-May) and summer (June-September) portions; the spring portion contained 363 cells with 74 (20%) severe, while the summer portion contained 1297 cells, of which 117 (9%) were severe.

Fig. A1 shows the percentage of storm cells with severe weather as a function of SWP value and cell maximum VIL, for the spring months. The fractional expression above each histogram bar represents the total number of cells and the number of severe cells falling into that predictor category. Percentage values for categories with relatively few cells must be used with caution, since such subsamples may be unrepresentative.

For the spring period, most severe weather is associated with cells having an SWP of at least 15, or VIL in excess of 40 kg m^{-2}. More than half the storms with SWP above 30 are severe.

Table A1 shows verification scores for the spring months for categorical (severe/nonsevere) nowcasts derived from the SWP algorithm through the application of a range of threshold values. The POD, FAR, and CSI scores as functions of threshold SWP value are summarized graphically in Fig. A2. As shown in the table, it should be possible to nowcast objectively for individual cells with a POD of 0.8 and an FAR of 0.5, and a bias of 1.7, applying an SWP threshold value of 13. The skill level of the algorithm when applied to purely independent data could be somewhat lower.

Table A2 and Figs. A3 and A4 present the same results from radar and storm observations during the summer (June-September) period. The overall percentage of cells with severe weather is about half that observed during the spring. The predictive value of the SWP algorithm is lower, as might be expected given the lower relative frequency of severe cells. Severe storm probability increases rapidly above an SWP of 20, or VIL of 50. As shown in Table A2, it should be possible to detect 80% of the severe cells by applying an SWP threshold of 13, but the FAR and bias in the forecasts would be considerably higher than in the spring, near 0.7 and 3, respectively.

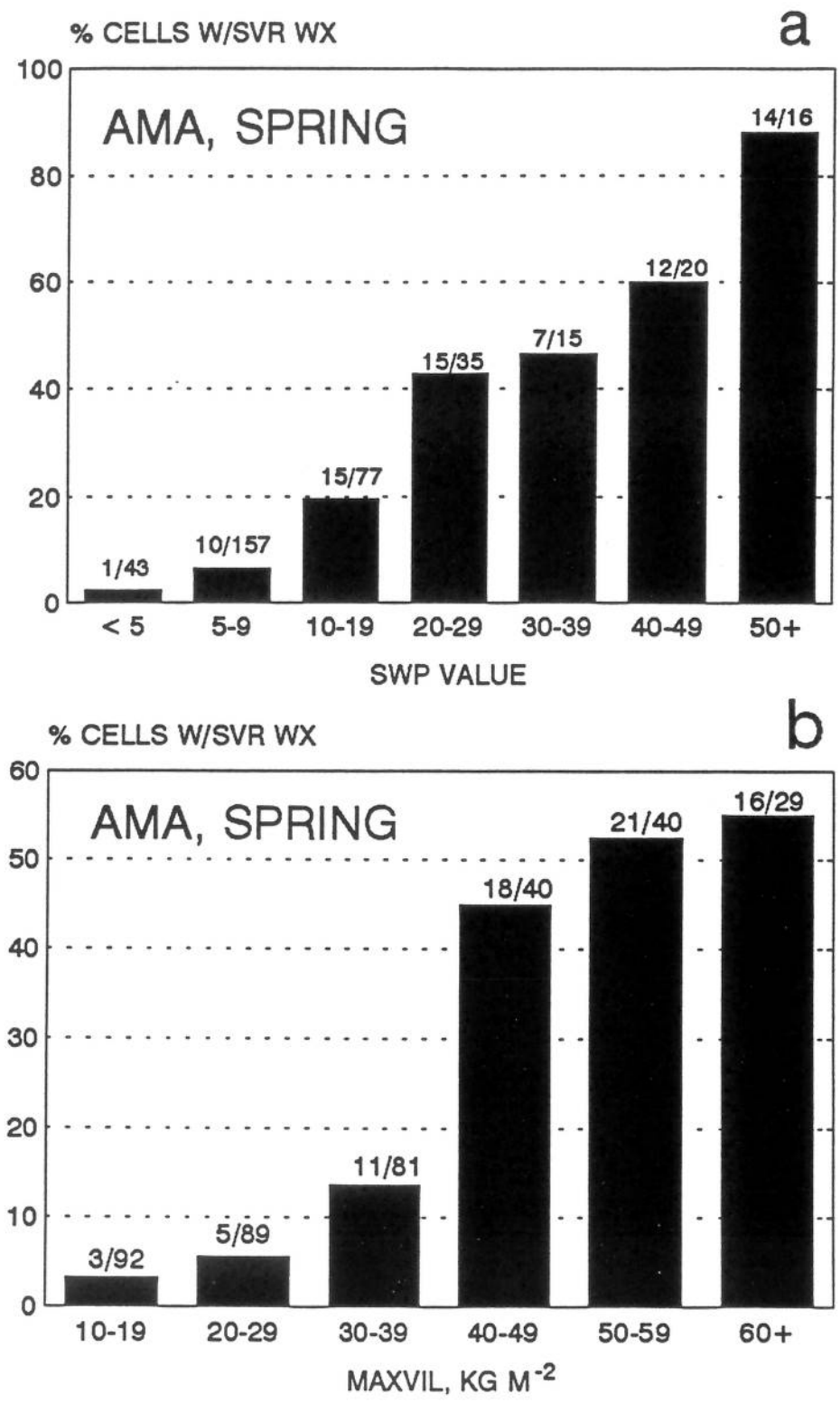

Figure A1. Percentage of thunderstorm cells with severe weather as a function of (a) SWP value and (b) maximum VIL, for AMA during the spring months. The number of severe and nonsevere cells in each category appear above each histogram box.

Table A1. Categorical forecast verification scores for AMA, April-May period. Variables are explained in the text.

SWP Threshold	POD	FAR	CSI	Bias	X	Y	Z	W
1	1.00	.80	.20	4.93	73	0	287	1
2	1.00	.80	.20	4.92	73	0	286	2
3	1.00	.79	.21	4.88	73	0	283	5
4	1.00	.79	.21	4.74	73	0	273	15
5	.99	.78	.22	4.40	72	1	249	39
6	.97	.73	.27	3.59	71	2	191	97
7	.90	.69	.30	2.90	66	7	146	142
8	.89	.65	.33	2.56	65	8	122	166
9	.88	.63	.35	2.38	64	9	110	178
10	.85	.61	.36	2.21	62	11	99	189
11	.84	.57	.40	1.93	61	12	80	208
12	.84	.54	.42	1.82	61	12	72	216
13	.81	.52	.43	1.68	59	14	64	224
14	.79	.51	.43	1.63	58	15	61	227
15	.78	.50	.44	1.56	57	16	57	231
16	.75	.48	.45	1.44	55	18	50	238
17	.71	.46	.44	1.33	52	21	45	243
18	.68	.46	.43	1.26	50	23	42	246
19	.68	.45	.44	1.25	50	23	41	247
20	.66	.44	.43	1.18	48	25	38	250
21	.60	.46	.40	1.12	44	29	38	250
22	.58	.45	.39	1.04	42	31	34	254
23	.56	.44	.39	1.00	41	32	32	256
24	.53	.44	.38	.96	39	34	31	257
25	.52	.42	.38	.89	38	35	27	261
26	.51	.40	.38	.85	37	36	25	263
27	.49	.37	.38	.78	36	37	21	267
28	.48	.36	.38	.75	35	38	20	268
29	.47	.36	.37	.73	34	39	19	269
30	.45	.35	.36	.70	33	40	18	270
31	.45	.33	.37	.67	33	40	16	272
32	.44	.32	.36	.64	32	41	15	273
33	.42	.33	.35	.63	31	42	15	273
34	.42	.30	.36	.60	31	42	13	275
35	.42	.26	.37	.58	31	42	11	277
36	.41	.27	.36	.56	30	43	11	277
37	.40	.28	.35	.55	29	44	11	277
38	.38	.26	.34	.52	28	45	10	278
39	.38	.26	.34	.52	28	45	10	278
40	.36	.28	.31	.49	26	47	10	278

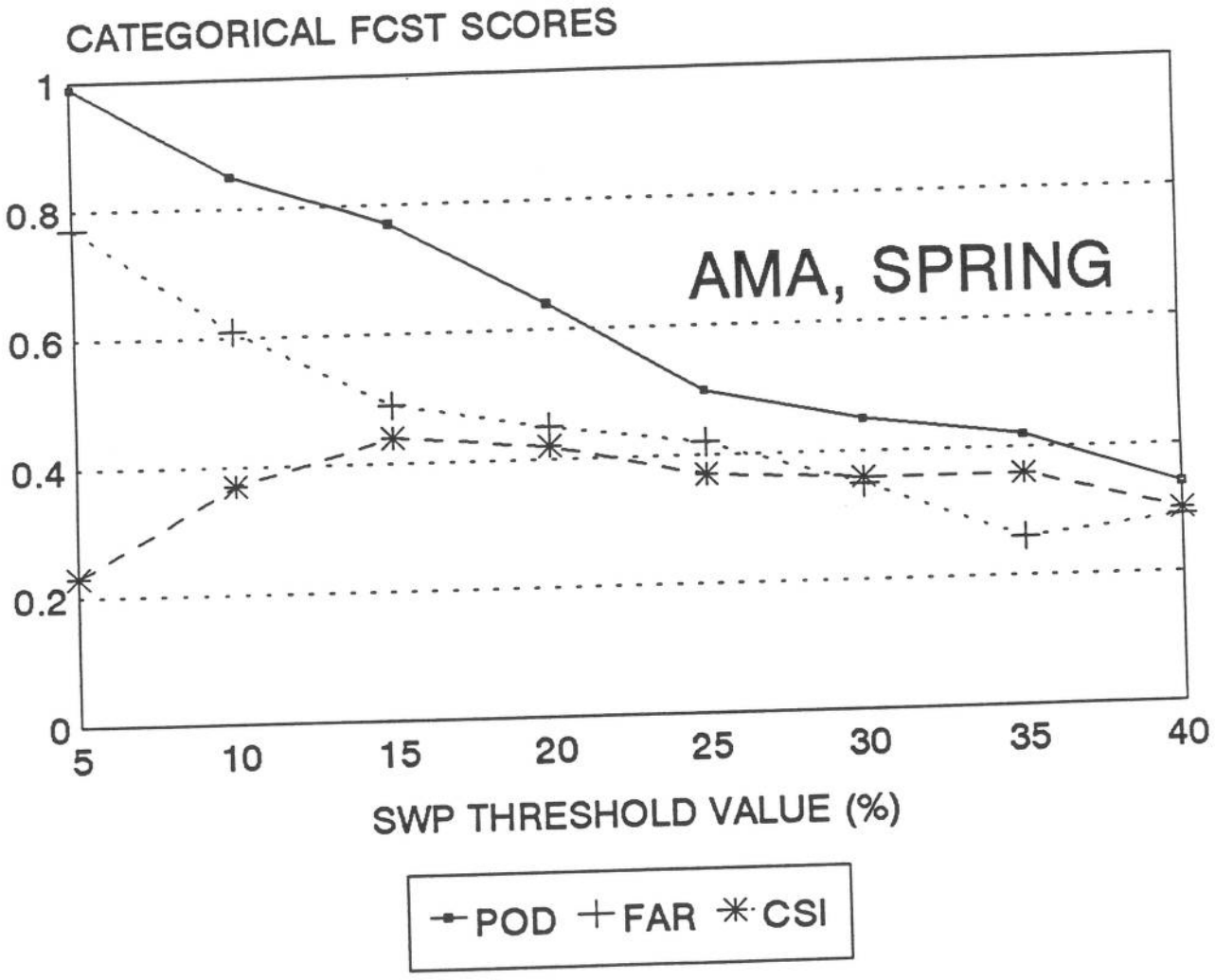

Figure A2. Categorical forecast scores as functions of threshold SWP value, for AMA during the spring months (April-May). Variables are explained in the text.

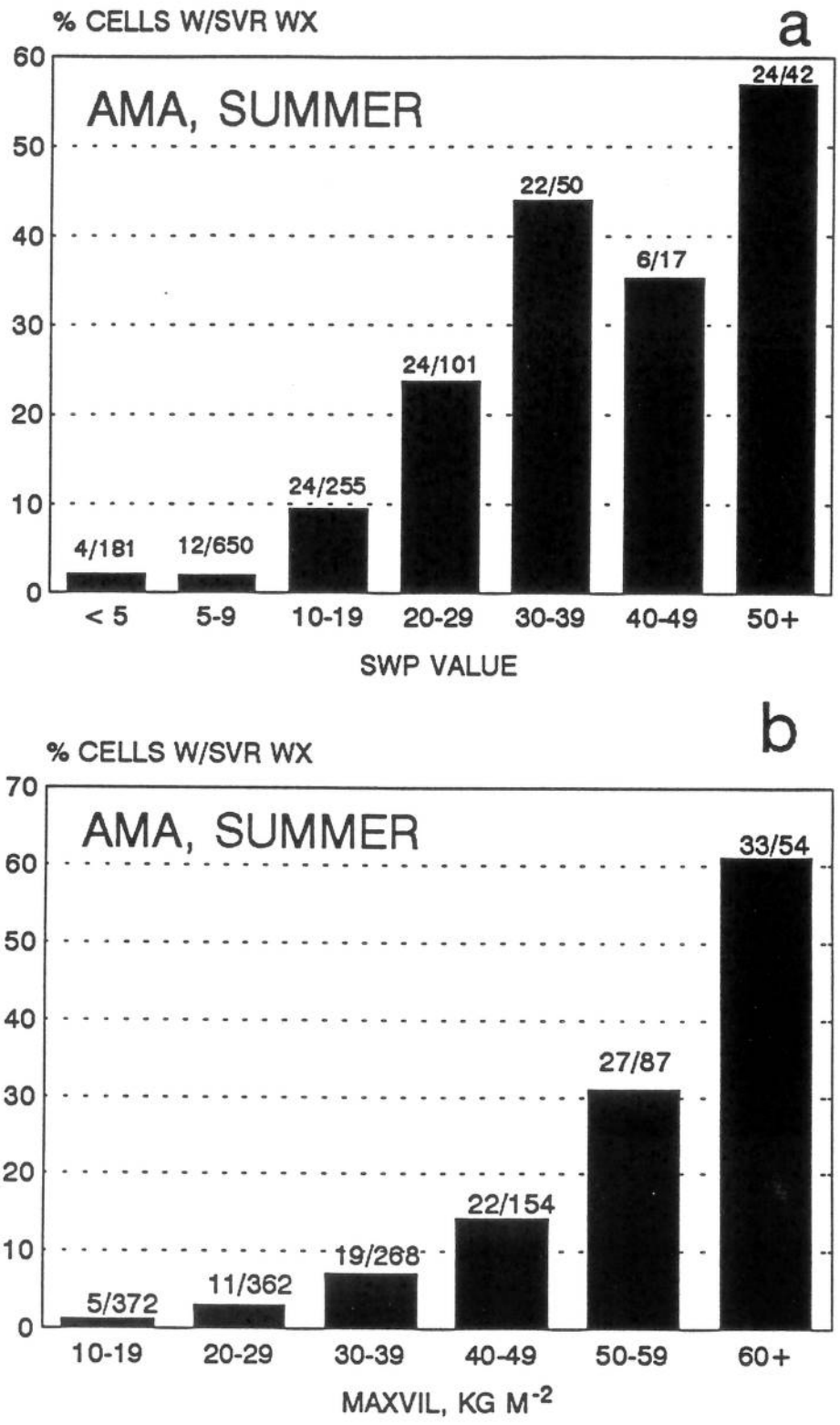

Figure A3. As in Fig. A1, except for AMA during the summer months (June-September).

Table A2. As in Table A1, except for AMA during the summer months (June-September).

SWP Threshold	POD	FAR	CSI	Bias	X	Y	Z	W
1	1.00	.91	.09	11.16	116	0	1179	0
2	1.00	.91	.09	11.15	116	0	1177	2
3	1.00	.91	.09	11.10	116	0	1172	7
4	1.00	.91	.09	10.90	116	0	1148	31
5	.97	.90	.10	9.71	112	4	1014	165
6	.93	.87	.13	7.19	108	8	726	453
7	.91	.84	.15	5.86	106	10	574	605
8	.88	.82	.17	4.94	102	14	471	708
9	.86	.80	.19	4.31	100	16	400	779
10	.85	.79	.21	3.99	99	17	364	815
11	.84	.77	.22	3.66	98	18	327	852
12	.84	.74	.24	3.28	97	19	283	896
13	.79	.73	.25	2.95	92	24	250	929
14	.74	.73	.25	2.72	86	30	229	950
15	.73	.71	.26	2.53	85	31	209	970
16	.72	.70	.27	2.38	83	33	193	986
17	.71	.68	.28	2.20	82	34	173	1006
18	.69	.66	.30	2.00	80	36	152	1027
19	.66	.65	.30	1.91	77	39	144	1035
20	.65	.64	.30	1.79	75	41	133	1046
21	.60	.64	.29	1.66	70	46	123	1056
22	.57	.62	.29	1.50	66	50	108	1071
23	.56	.60	.30	1.41	65	51	98	1081
24	.53	.59	.30	1.30	62	54	89	1090
25	.52	.58	.30	1.23	60	56	83	1096
26	.50	.57	.30	1.16	58	58	76	1103
27	.46	.56	.29	1.04	53	63	68	1111
28	.46	.54	.30	.99	53	63	62	1117
29	.45	.53	.30	.95	52	64	58	1121
30	.44	.52	.30	.92	51	65	56	1123
31	.42	.51	.29	.87	49	67	52	1127
32	.41	.51	.29	.84	48	68	49	1130
33	.40	.47	.29	.75	46	70	41	1138
34	.38	.48	.28	.72	44	72	40	1139
35	.34	.49	.26	.67	40	76	38	1141
36	.32	.49	.24	.63	37	79	36	1143
37	.29	.50	.23	.59	34	82	34	1145
38	.28	.49	.22	.56	33	83	32	1147
39	.28	.48	.22	.53	32	84	30	1149
40	.25	.49	.20	.49	29	87	28	1151

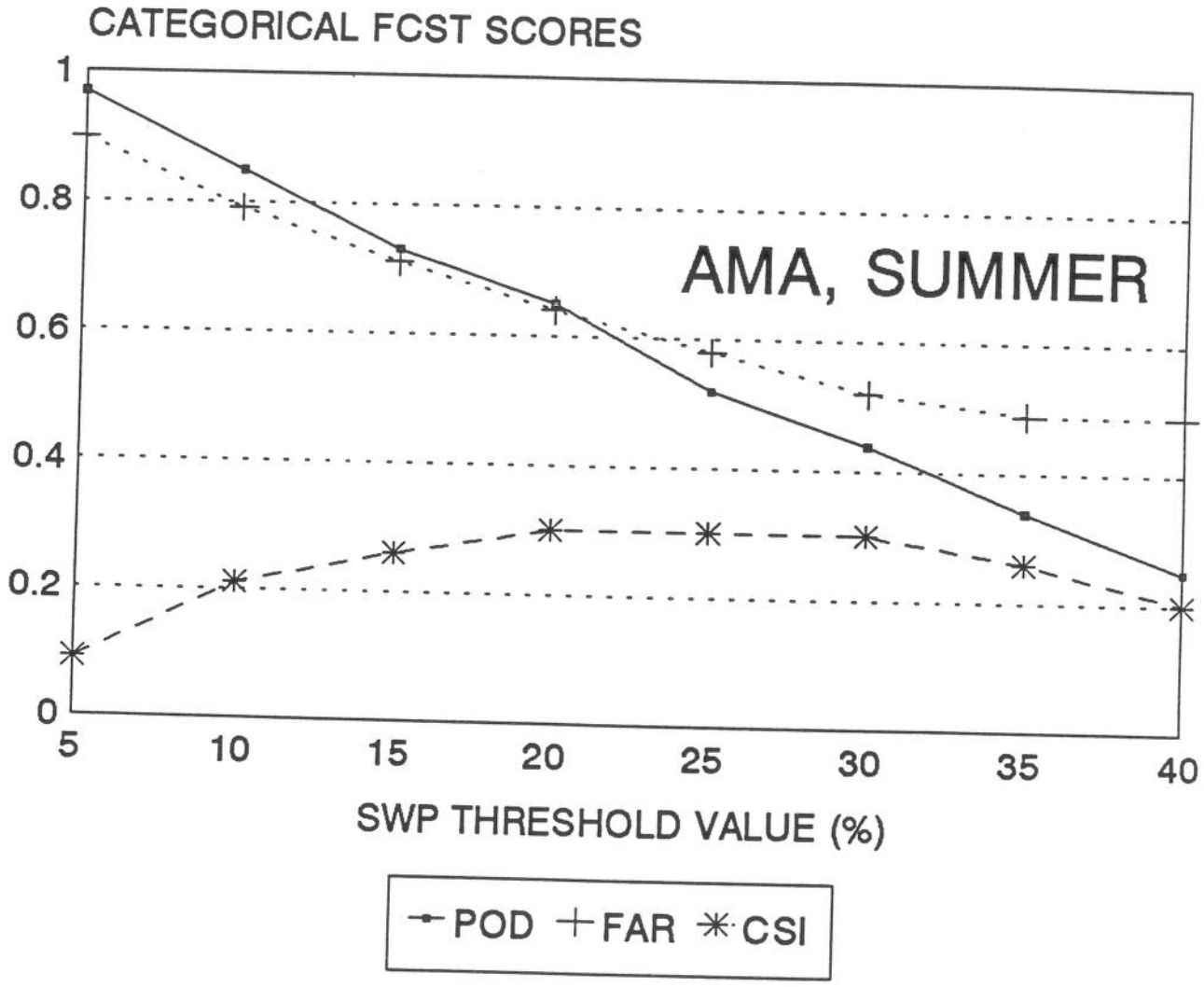

Figure A4. As in Fig. A2, except for AMA during the summer months (June-September).

A2. BINGHAMTON, NEW YORK (BGM)

The period of record for RADAP II observations at BGM begins in 1988. Our data sample from this site spans the period April-September, 1988 to 1990. Though this region experiences fewer thunderstorms than those surrounding other RADAP sites, the area has the highest percentage of severe cells of all (82 severe of 256 observed, or 34%). This intense activity might be due to the synoptic-scale support that accompanies most thunderstorm events over the northeastern United States, even during the summer months. Most of the severe weather events featured high winds. The data from this site demonstrate the value of VIL-based forecasting methods for some thunderstorm environments that are dissimilar to those of the Central Plains, where the potential for VIL was first realized.

Even the lower VIL and SWP categories for this region feature significant severe weather, and most storms with VIL values above 30 kg m^{-2} are severe (Fig. A5). Though the SWP algorithm yields a peak CSI near 0.38 for a threshold value of 10 (Table A3 and Fig. A6), the POD decreases rapidly for thresholds greater than 5, with a threshold of 6 giving a POD of 0.74 and an FAR of 0.65.

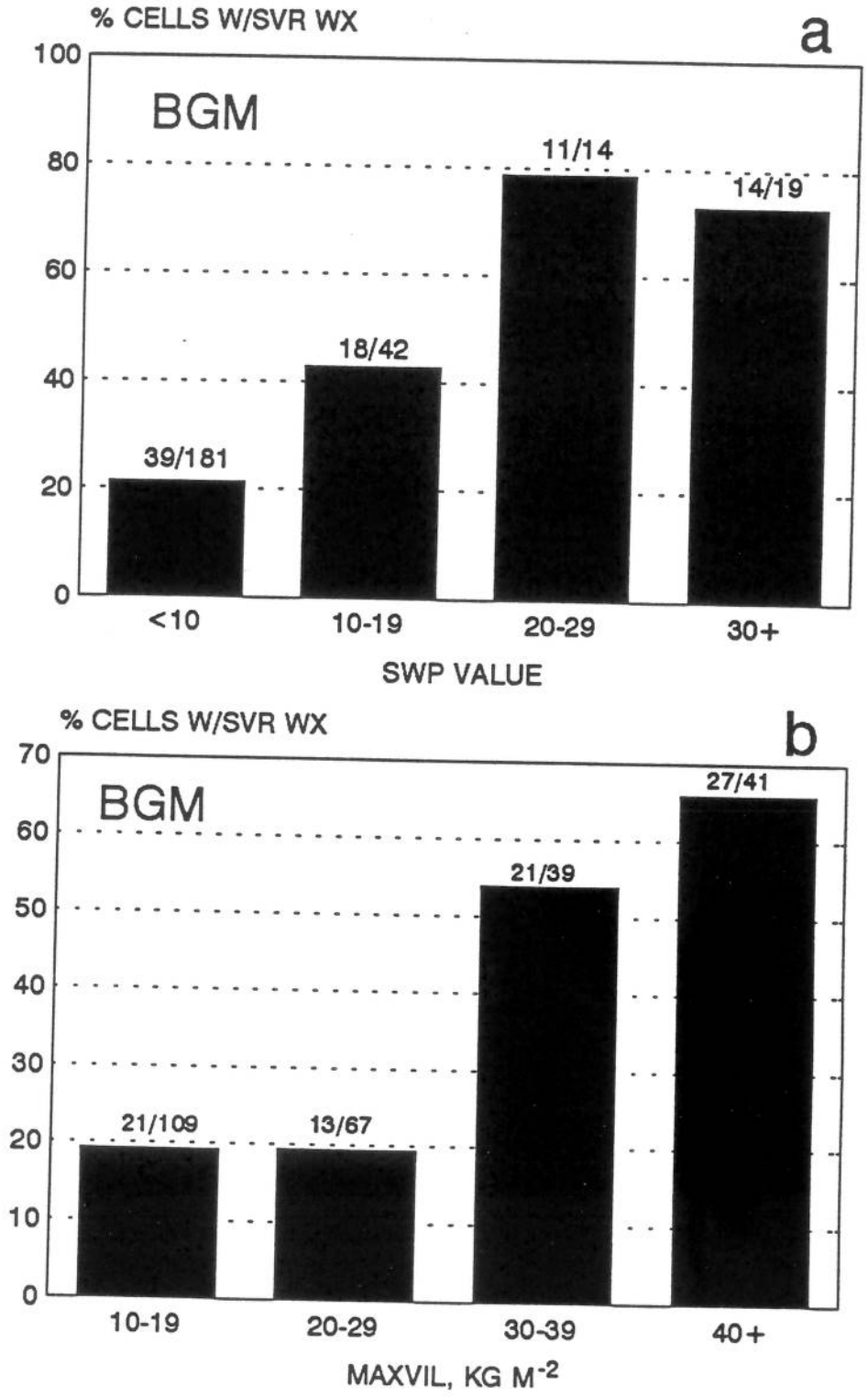

Figure A5. As in Fig. A1, except for BGM during the April-September period, 1988-90.

Table A3. As in Table A1, except for BGM, April-September period, 1988-90.

SWP Threshold	POD	FAR	CSI	Bias	X	Y	Z	W
1	1.00	.68	.32	3.12	82	0	174	0
2	1.00	.68	.32	3.12	82	0	174	0
3	1.00	.68	.32	3.10	82	0	172	2
4	.98	.67	.32	3.00	80	2	166	8
5	.90	.65	.34	2.55	74	8	135	39
6	.74	.61	.35	1.89	61	21	94	80
7	.61	.52	.36	1.28	50	32	55	119
8	.57	.48	.37	1.11	47	35	44	130
9	.54	.47	.36	1.01	44	38	39	135
10	.52	.43	.38	.91	43	39	32	142
11	.46	.41	.35	.78	38	44	26	148
12	.44	.39	.34	.72	36	46	23	151
13	.41	.35	.34	.63	34	48	18	156
14	.38	.34	.32	.57	31	51	16	158
15	.35	.29	.31	.50	29	53	12	162
16	.34	.30	.30	.49	28	54	12	162
17	.34	.28	.30	.48	28	54	11	163
18	.32	.28	.28	.44	26	56	10	164
19	.30	.24	.28	.40	25	57	8	166
20	.30	.24	.28	.40	25	57	8	166
21	.30	.24	.28	.40	25	57	8	166
22	.29	.23	.27	.38	24	58	7	167
23	.27	.24	.25	.35	22	60	7	167
24	.24	.26	.22	.33	20	62	7	167
25	.21	.23	.20	.27	17	65	5	169
26	.21	.23	.20	.27	17	65	5	169
27	.21	.23	.20	.27	17	65	5	169
28	.21	.23	.20	.27	17	65	5	169
29	.20	.24	.18	.26	16	66	5	169
30	.17	.26	.16	.23	14	68	5	169
31	.16	.24	.15	.21	13	69	4	170
32	.15	.20	.14	.18	12	70	3	171
33	.13	.21	.13	.17	11	71	3	171
34	.13	.21	.13	.17	11	71	3	171
35	.13	.21	.13	.17	11	71	3	171
36	.13	.21	.13	.17	11	71	3	171
37	.12	.23	.12	.16	10	72	3	171
38	.11	.25	.11	.15	9	73	3	171
39	.09	.22	.08	.11	7	75	2	172
40	.09	.22	.08	.11	7	75	2	172

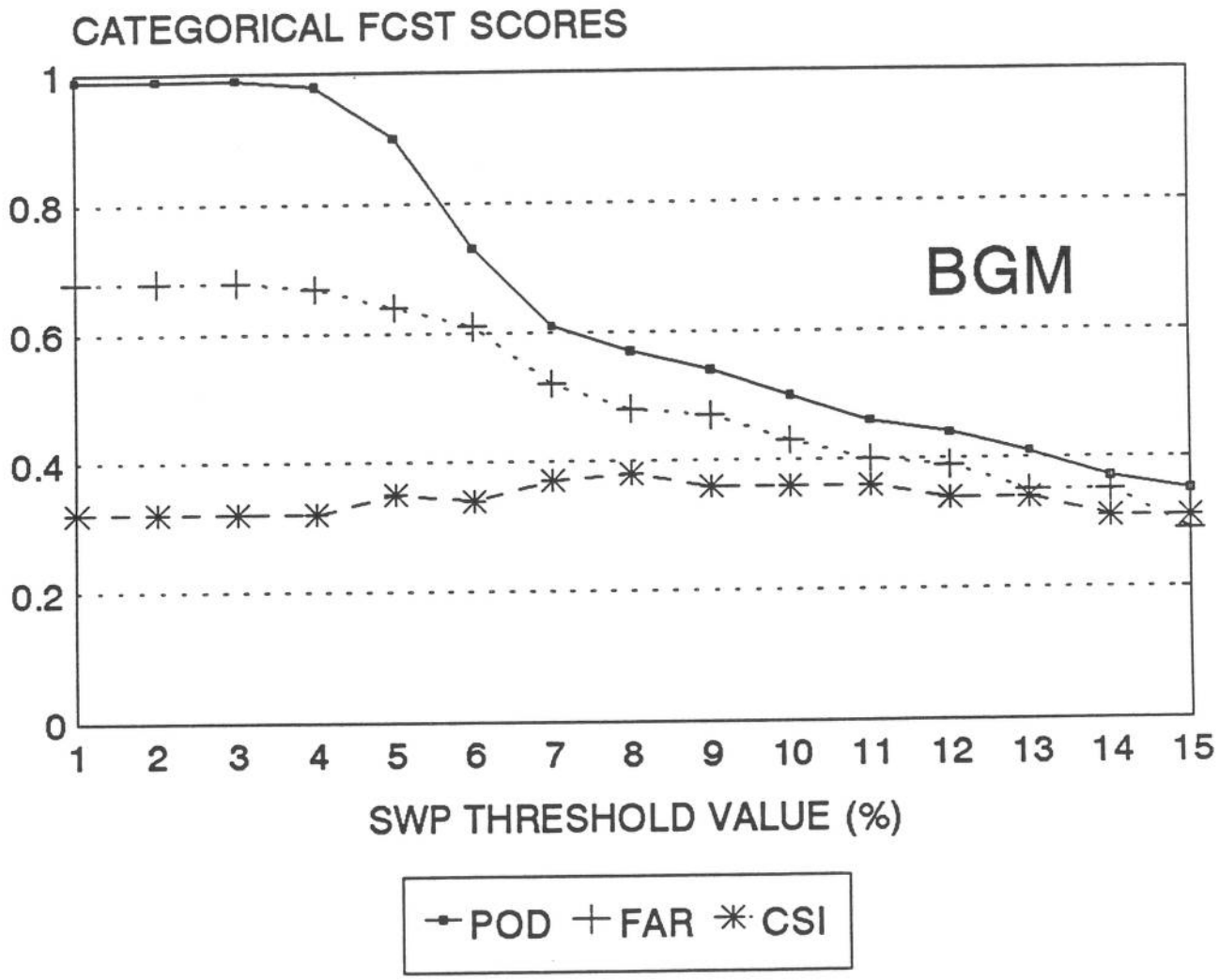

Figure A6. As in Fig. A2, except for BGM, April-September period, 1988-90.

A3. NASHVILLE, TENNESSEE (BNA)

Though thunderstorms are common within the BNA umbrella, a relatively small portion are severe (47, or 8%, of 598 cells observed during the 1986-1988 period). This rather low frequency of severe storm reports is due in part to the rugged and sparsely-populated terrain within much of the umbrella. However, our radar archive included only a few cases from the springtime outbreaks, with most of our observations being of late spring and summer thunderstorms that developed under conditions of weak upper-level winds and only moderate instability.

Our results (Fig. A7) indicate that storms with SWP less than 5, or VIL less than 30 kg m^{-2}, have only about a 6-8% probability of being severe. Even storms with SWP in excess of 30, or VIL in excess of 50 kg m^{-2}, had somewhat less than a 30% probability of being severe. Under these conditions of uncertainty, it is difficult to determine the categorical forecast scores for the SWP algorithm, and the scores shown in Table A4 and Fig. A8 must be accepted with caution.

To improve the utility of the SWP algorithm as applied to storms in this region, more radar observations from the late-winter and spring severe weather season will be necessary. Stratification into separate spring and summer data samples would almost certainly improve the information available from the SWP algorithm.

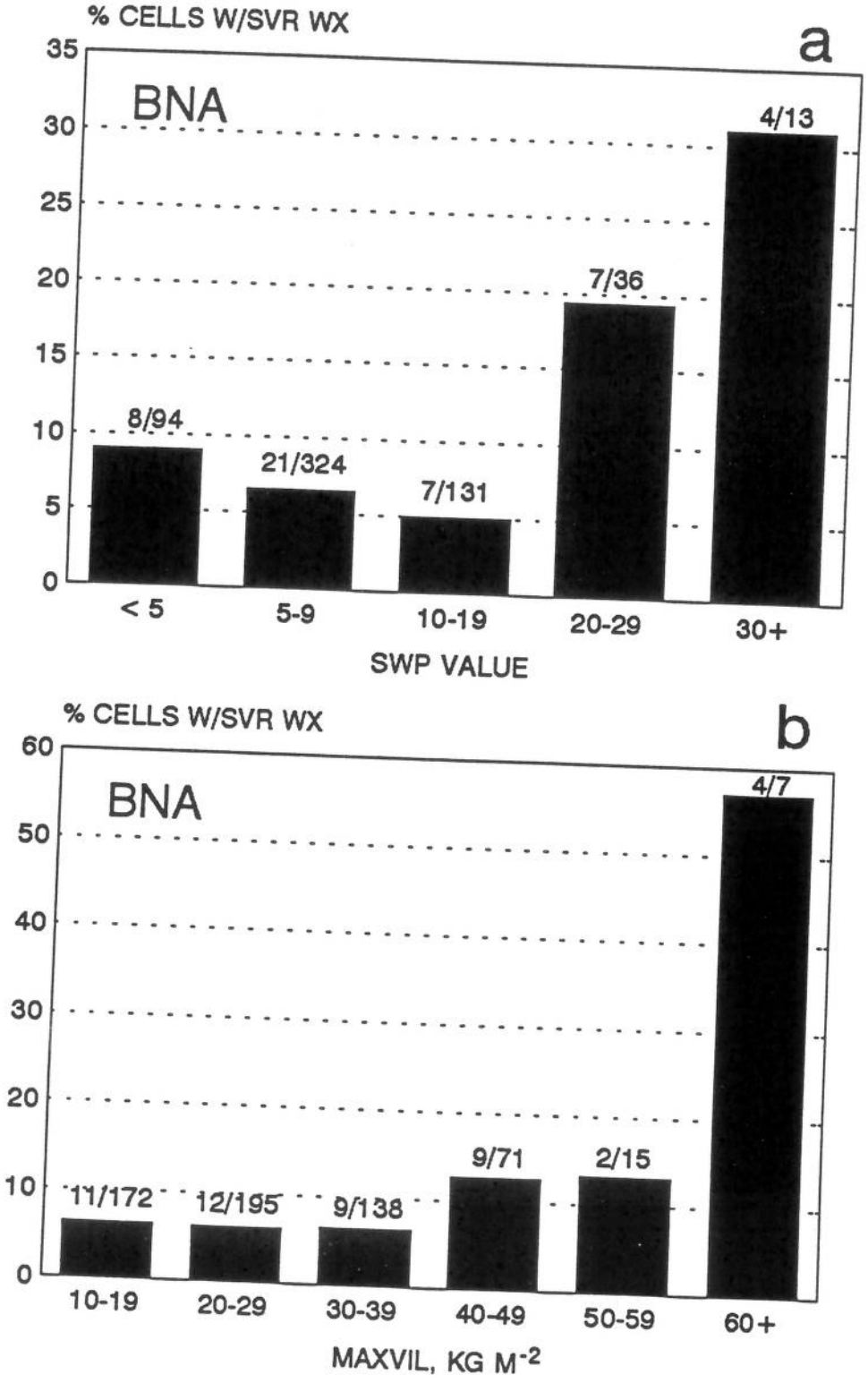

Figure A7. As in Fig. A1, except for BNA, April-September period, 1986-88.

Table A4. As in Table A1, except for BNA, April-September period, 1986-88.

SWP Threshold	POD	FAR	CSI	Bias	X	Y	Z	W
1	1.00	.92	.08	12.72	47	0	551	0
2	1.00	.92	.08	12.68	47	0	549	2
3	.98	.92	.08	12.66	46	1	549	2
4	.96	.92	.08	12.34	45	2	535	16
5	.83	.92	.08	10.77	39	8	467	84
6	.77	.91	.09	8.47	36	11	362	189
7	.64	.91	.09	6.87	30	17	293	258
8	.51	.91	.08	5.53	24	23	236	315
9	.47	.90	.09	4.70	22	25	199	352
10	.38	.90	.09	3.85	18	29	163	388
11	.38	.88	.10	3.23	18	29	134	417
12	.38	.87	.11	2.85	18	29	116	435
13	.36	.85	.12	2.49	17	30	100	451
14	.34	.84	.12	2.13	16	31	84	467
15	.30	.84	.12	1.81	14	33	71	480
16	.28	.83	.12	1.60	13	34	62	489
17	.28	.81	.13	1.47	13	34	56	495
18	.26	.80	.13	1.30	12	35	49	502
19	.26	.79	.13	1.19	12	35	44	507
20	.23	.78	.13	1.04	11	36	38	513
21	.21	.78	.12	.96	10	37	35	516
22	.21	.73	.14	.79	10	37	27	524
23	.21	.71	.14	.74	10	37	25	526
24	.19	.69	.13	.62	9	38	20	531
25	.15	.72	.11	.53	7	40	18	533
26	.13	.70	.10	.43	6	41	14	537
27	.13	.70	.10	.43	6	41	14	537
28	.13	.67	.10	.38	6	41	12	539
29	.13	.63	.11	.34	6	41	10	541
30	.09	.69	.07	.28	4	43	9	542
31	.09	.67	.07	.26	4	43	8	543
32	.09	.67	.07	.26	4	43	8	543
33	.09	.64	.07	.23	4	43	7	544
34	.04	.75	.04	.17	2	45	6	545
35	.04	.75	.04	.17	2	45	6	545
36	.02	.86	.02	.15	1	46	6	545
37	.02	.83	.02	.13	1	46	5	546
38	.00	1.00	.00	.09	0	47	4	547
39	.00	1.00	.00	.06	0	47	3	548
40	.00	1.00	.00	.06	0	47	3	548

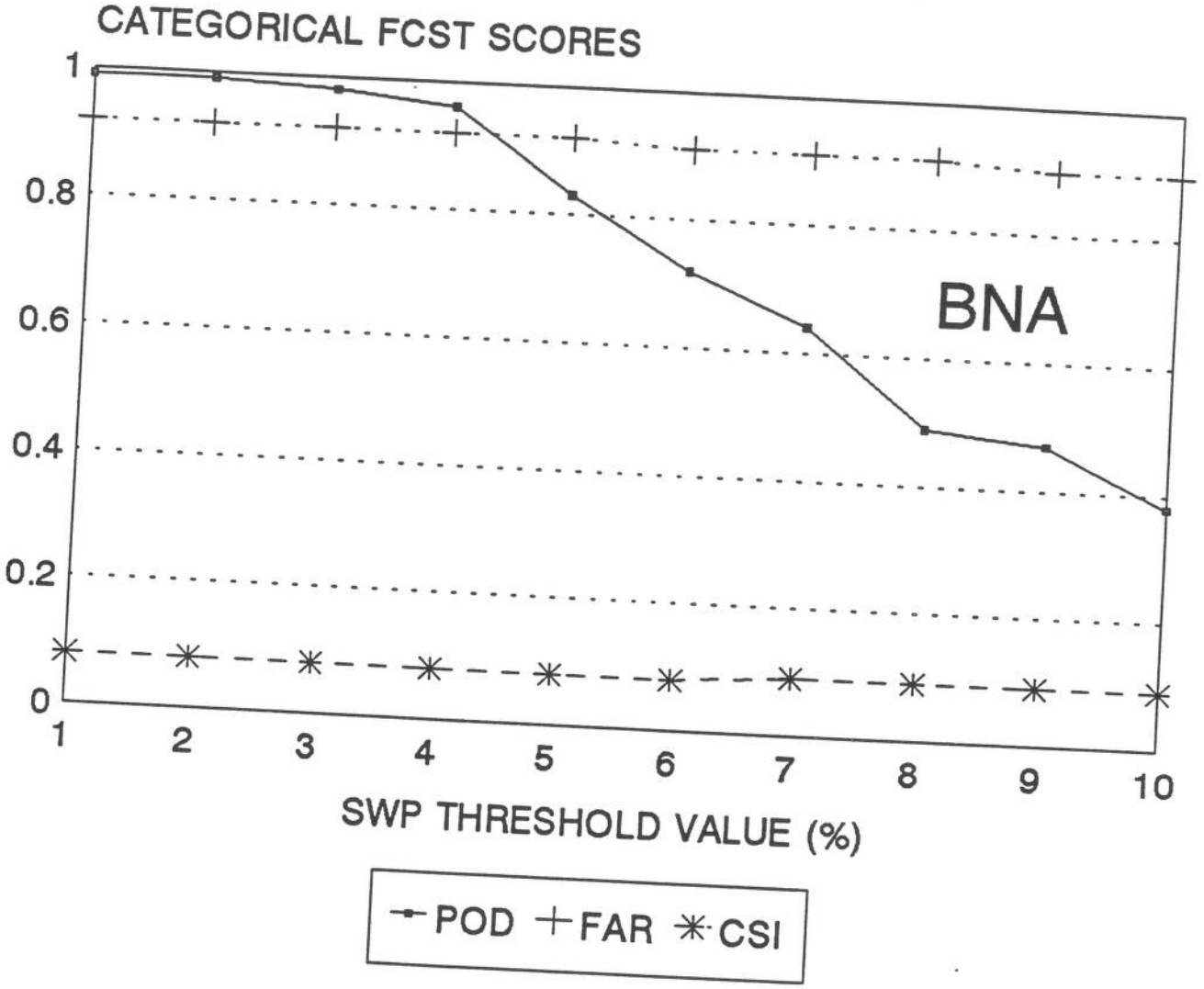

Figure A8. As in Fig. A2, except for BNA, April-September period, 1986-88.

A4. CHARLESTON, WEST VIRGINIA (CRW)

We have thus far processed CRW observations for only 1990, when an intensive severe weather reporting effort was organized within the CRW Weather Service Forecast Office's area of responsibility (Allan Rezek and Robert LaPlante, personal communication). Severe weather observation is quite difficult within this area, much of which is mountainous and sparsely populated. Therefore, caution should be exercised in interpreting our results.

For the 1990 April-September season, the RADAP archive contained observations of 399 storm cells over the reporting network, of which 39 (10%) were severe. Over half of the cells featured maximum VIL of less than 20 kg m^{-2}, and only 3% of these storms were severe (Fig. A9). For SWP values less than 10, approximately 7% of the storms were severe. For VIL in excess of 40 kg m^{-2}, nearly 40% of the cells were severe.

Given the limited sample of data, the SWP verification results (Table A4, Fig. A9), must be considered preliminary. As in the case of BNA, stratification by season or synoptic situation would likely improve the skill of the SWP algorithm.

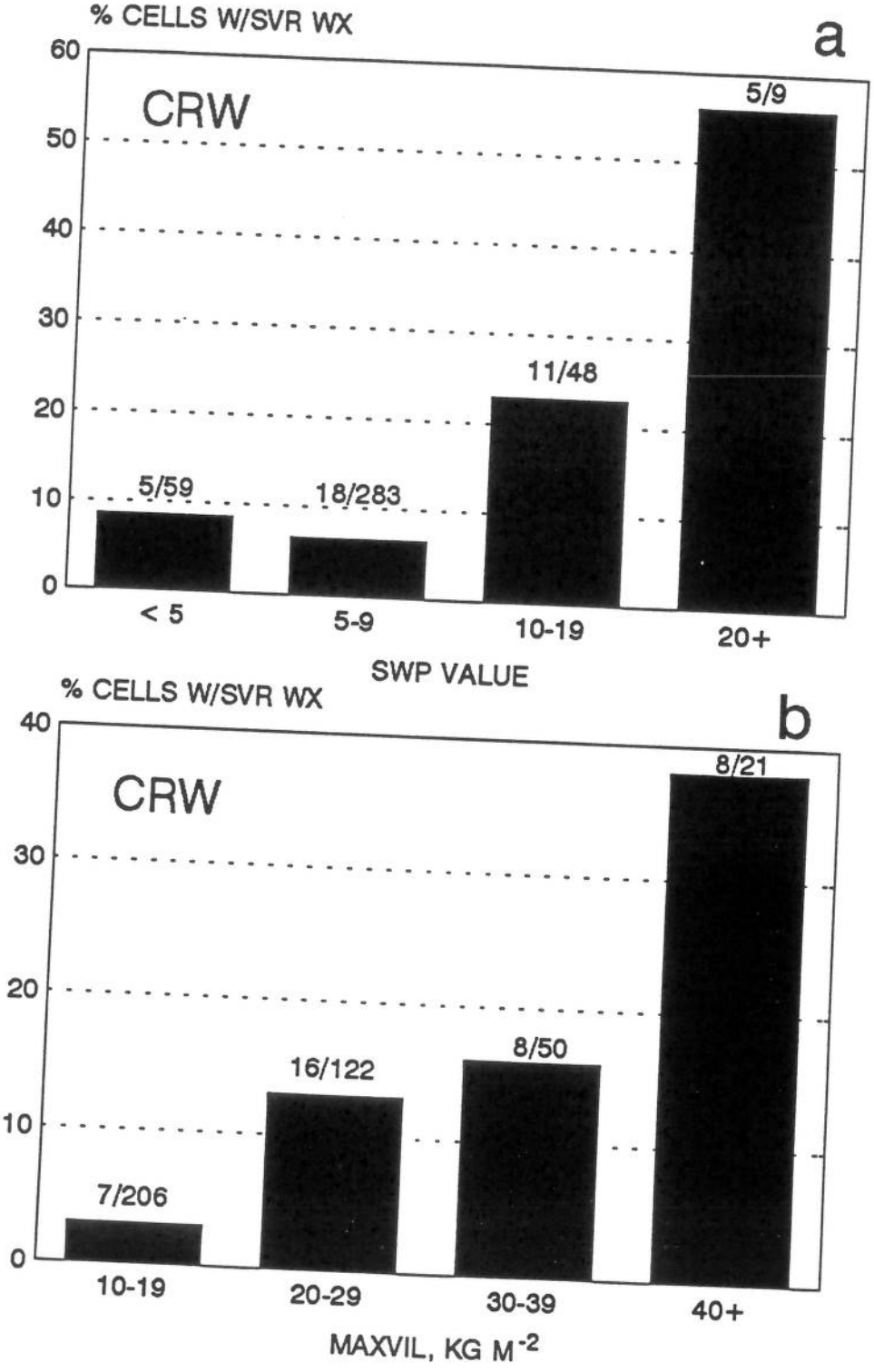

Figure A9. As in Fig. A1, except for CRW, April-September, 1990.

Table A5. As in Table A1, except for CRW, April-September, 1990.

SWP Threshold	POD	FAR	CSI	Bias	X	Y	Z	W
1	1.00	.90	.10	10.23	39	0	360	0
2	1.00	.90	.10	10.23	39	0	360	0
3	1.00	.90	.10	10.21	39	0	359	1
4	1.00	.90	.10	10.03	39	0	352	8
5	.87	.90	.10	8.85	34	5	311	49
6	.69	.87	.12	5.36	27	12	182	178
7	.56	.83	.15	3.33	22	17	108	252
8	.49	.81	.16	2.56	19	20	81	279
9	.46	.76	.19	1.92	18	21	57	303
10	.41	.72	.20	1.49	16	23	42	318
11	.38	.69	.21	1.26	15	24	34	326
12	.28	.71	.17	.97	11	28	27	333
13	.26	.64	.18	.72	10	29	18	342
14	.26	.60	.19	.64	10	29	15	345
15	.23	.59	.17	.56	9	30	13	347
16	.21	.60	.16	.51	8	31	12	348
17	.15	.57	.13	.36	6	33	8	352
18	.15	.54	.13	.33	6	33	7	353
19	.15	.45	.14	.28	6	33	5	355
20	.13	.44	.12	.23	5	34	4	356
21	.13	.38	.12	.21	5	34	3	357
22	.13	.38	.12	.21	5	34	3	357
23	.13	.38	.12	.21	5	34	3	357
24	.13	.38	.12	.21	5	34	3	357
25	.13	.38	.12	.21	5	34	3	357
26	.13	.29	.12	.18	5	34	2	358
27	.10	.33	.10	.15	4	35	2	358
28	.10	.33	.10	.15	4	35	2	358
29	.10	.33	.10	.15	4	35	2	358
30	.10	.33	.10	.15	4	35	2	358
31	.08	.40	.07	.13	3	36	2	358
32	.08	.40	.07	.13	3	36	2	358
33	.08	.40	.07	.13	3	36	2	358
34	.05	.50	.05	.10	2	37	2	358
35	.05	.50	.05	.10	2	37	2	358
36	.05	.50	.05	.10	2	37	2	358
37	.03	.67	.02	.08	1	38	2	358
38	.03	.67	.02	.08	1	38	2	358
39	.03	.67	.02	.08	1	38	2	358
40	.03	.50	.03	.05	1	38	1	359

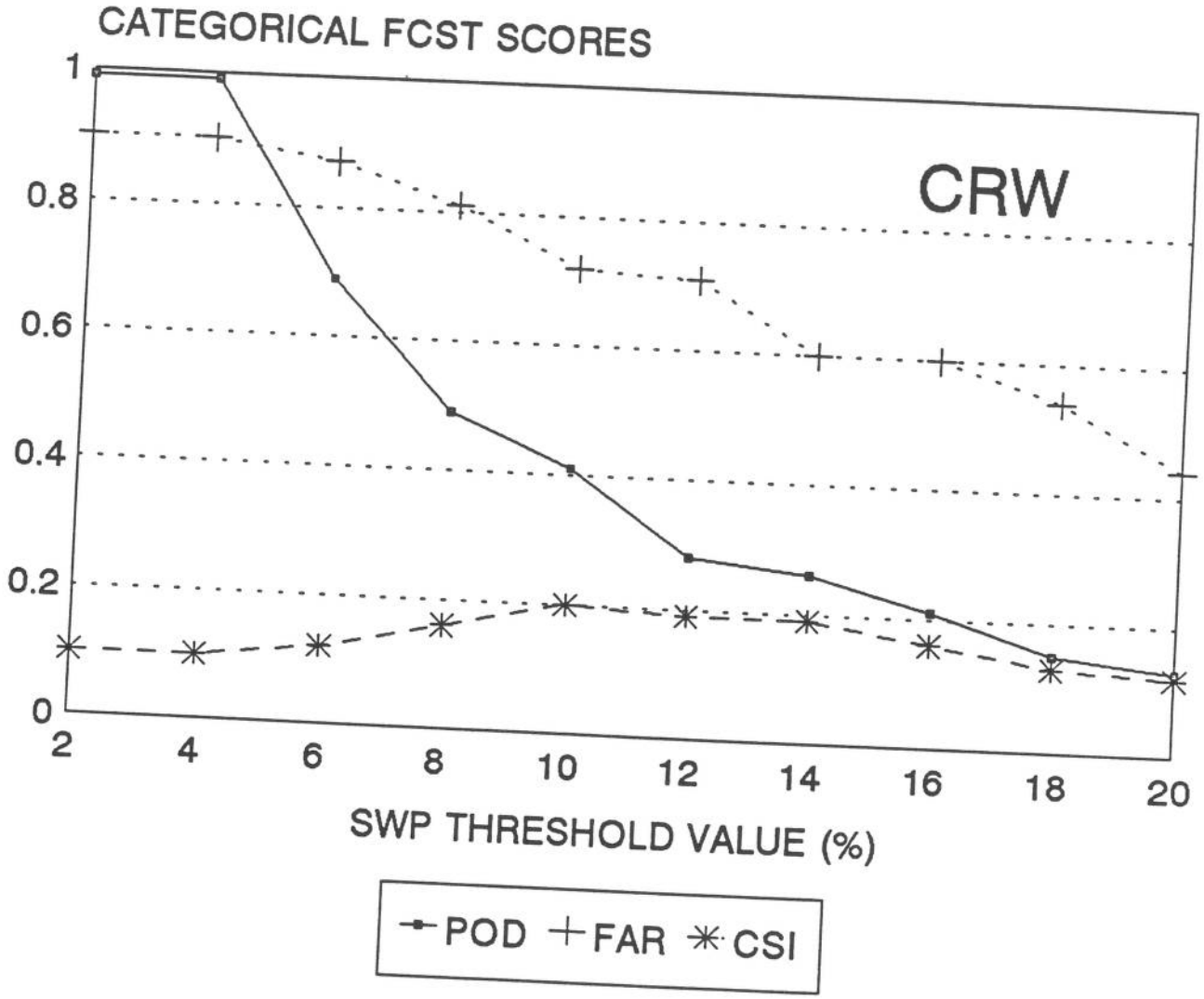

Figure A10. As in Fig. A2, except for CRW, April-September, 1990.

A5. GARDEN CITY, KANSAS (GCK)

The data sample for GCK covers the April-September, 1985-88, and April-May 1989 periods. Observations of 711 cells were available, of which 83, or 12%, were severe.

Our results show that for SWP less than 10, or VIL less than 30 kg m^{-2}, only 3% of the cells in this umbrella were severe; such cells comprise 45% of the total population. The probability of severe phenomena increases sharply for SWP above 25 or VIL above 50, as shown in Fig. A11.

Verification results indicate that an optimal SWP threshold value is between 10 and 15, where the expected POD is 0.7 to 0.8, with similar FAR values. The peak CSI is achieved at higher thresholds (Table A6 and Fig. A12).

Though the data sample for GCK was not extensive enough to obtain reliable results for the spring and summer seasons separately, the results for Amarillo (AMA) and Wichita (ICT) are very likely to be valid here, as well.

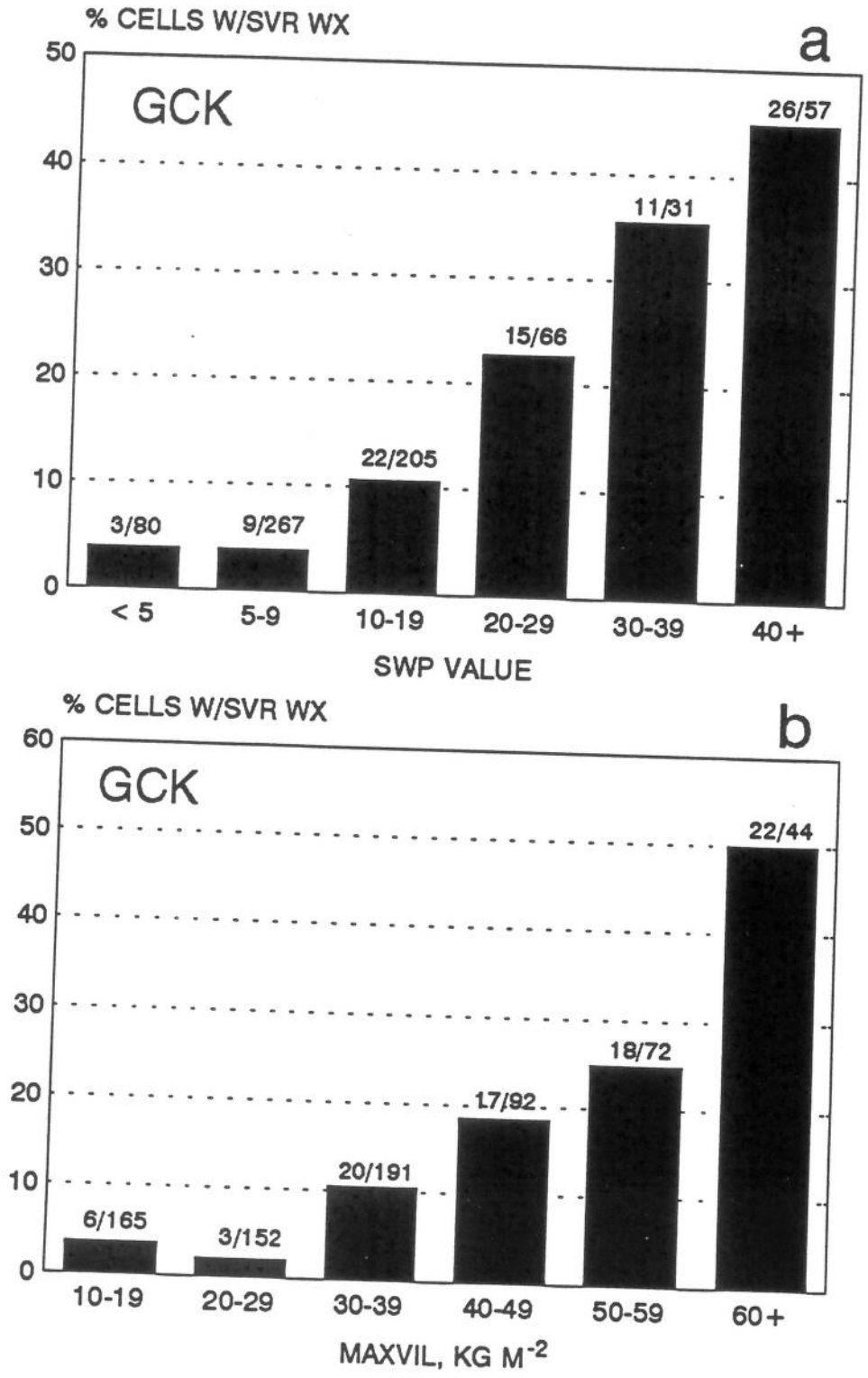

Figure A11. As in Fig. A1, except for GCK, April-September, 1985-88.

Table A6. As in Table A1, except for GCK, April-September, 1985-88.

SWP Threshold	POD	FAR	CSI	Bias	X	Y	Z	W
1	1.00	.88	.12	8.33	86	0	630	0
2	1.00	.88	.12	8.31	86	0	629	1
3	1.00	.88	.12	8.29	86	0	627	3
4	.99	.88	.12	8.05	85	1	607	23
5	.97	.87	.13	7.44	83	3	557	73
6	.94	.85	.15	6.21	81	5	453	177
7	.93	.83	.17	5.41	80	6	385	245
8	.92	.81	.19	4.87	79	7	340	290
9	.90	.80	.19	4.55	77	9	314	316
10	.86	.80	.19	4.29	74	12	295	335
11	.86	.78	.21	3.95	74	12	266	364
12	.84	.77	.22	3.60	72	14	238	392
13	.80	.76	.22	3.37	69	17	221	409
14	.76	.75	.23	3.05	65	21	197	433
15	.73	.74	.23	2.86	63	23	183	447
16	.66	.75	.22	2.63	57	29	169	461
17	.65	.73	.24	2.42	56	30	152	478
18	.63	.71	.25	2.16	54	32	132	498
19	.62	.70	.26	2.02	53	33	121	509
20	.60	.68	.26	1.91	52	34	112	518
21	.59	.67	.27	1.78	51	35	102	528
22	.59	.65	.28	1.71	51	35	96	534
23	.58	.64	.28	1.63	50	36	90	540
24	.55	.64	.28	1.52	47	39	84	546
25	.52	.63	.28	1.42	45	41	77	553
26	.48	.64	.26	1.33	41	45	73	557
27	.48	.63	.26	1.29	41	45	70	560
28	.45	.63	.26	1.22	39	47	66	564
29	.44	.63	.25	1.20	38	48	65	565
30	.43	.62	.25	1.14	37	49	61	569
31	.43	.61	.26	1.12	37	49	59	571
32	.40	.63	.24	1.06	34	52	57	573
33	.40	.62	.24	1.03	34	52	55	575
34	.36	.63	.22	.97	31	55	52	578
35	.35	.62	.22	.91	30	56	48	582
36	.34	.62	.22	.90	29	57	48	582
37	.34	.62	.22	.88	29	57	47	583
38	.31	.63	.21	.84	27	59	45	585
39	.31	.61	.21	.81	27	59	43	587
40	.30	.61	.20	.78	26	60	41	589

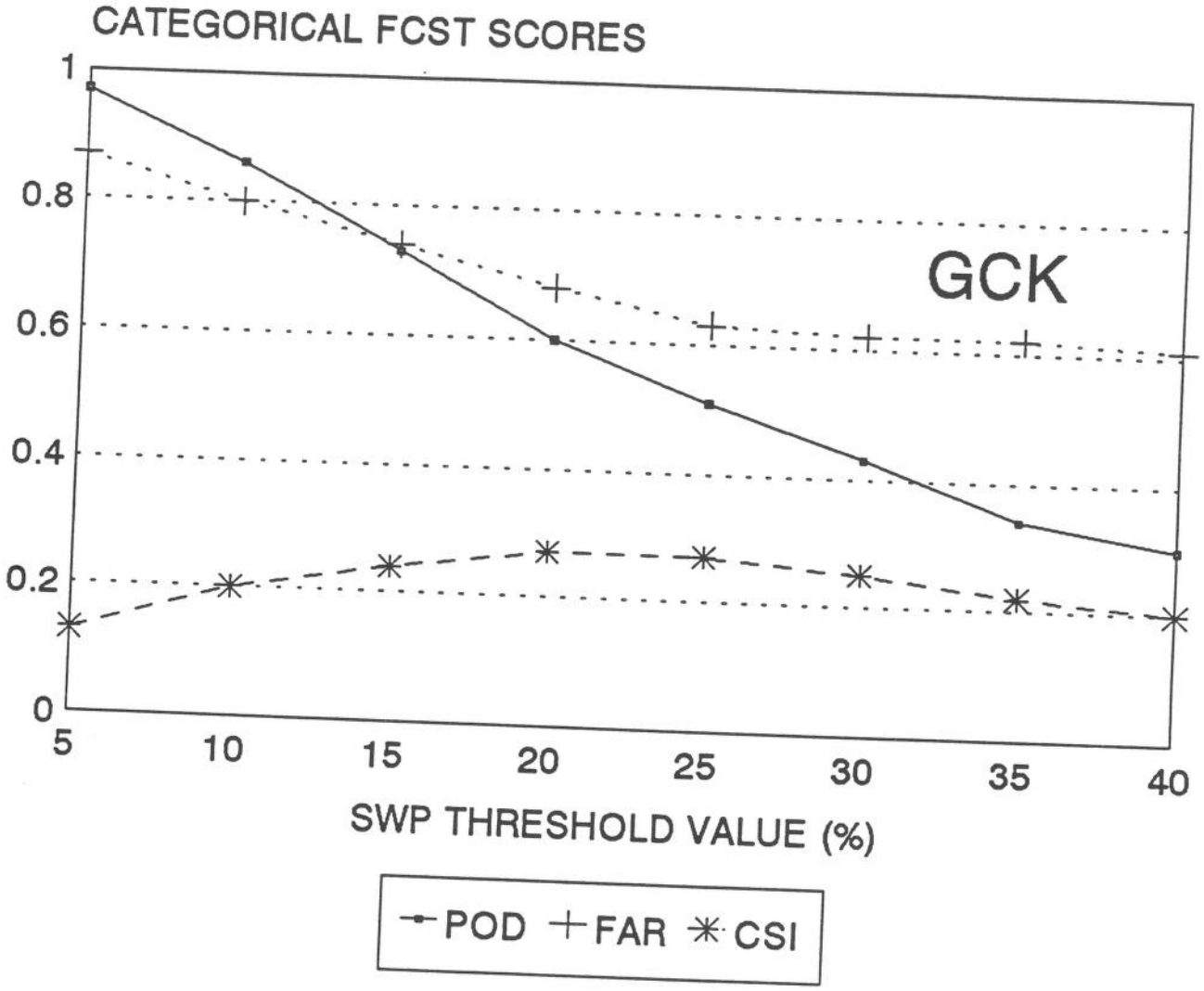

Figure A12. As in Fig. A2, except for GCK, April-September, 1985-88.

A6. WICHITA, KANSAS (ICT)

The sample of data from ICT includes 1621 storm cells from 1985 to 1989, of which 225 (14%) were severe. For the April-May period, there were 232 cells, of which 71 (31%) were severe. During the June-September period, 1389 cells were observed, with 154 (11%) severe.

As noted earlier, the characteristics of the storm population, and of the VIL/severe weather relationship, were very similar at the neighboring AMA and ICT sites. During the spring months, the majority of severe weather is associated with cells having SWP greater than 10, or maximum VIL greater than 30 kg m^{-2}; approximately 10% of the cells weaker than this have severe weather, while nearly half of the rest are severe (Fig. A13). Our verification results (Table A7, Fig. A14) indicate that it should be possible to nowcast with a POD of 0.8 with an FAR of only 0.5, or a bias of less than 2.

The level of forecasting skill is lower in the summer (Figs. A15-A16, Table A8). During this season, severe weather probability increases markedly with SWP values above 20, and VIL's greater than 50. For categorical nowcasts (Table A8), a POD of 0.8 could be achieved with an FAR of about 0.7 and a bias of 2.6.

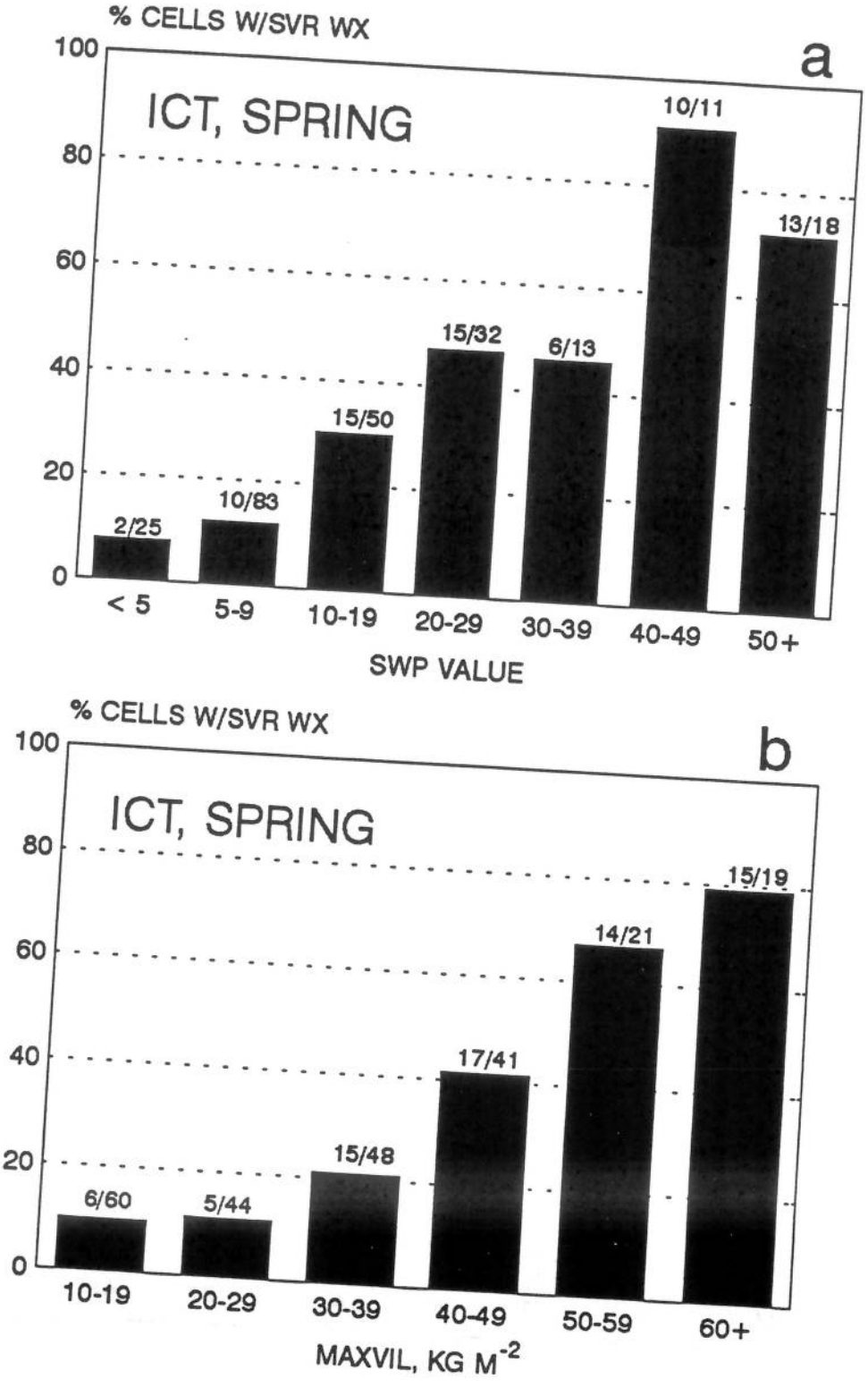

Figure A13. As in Fig. A1, except for ICT, April-May, 1985-89.

Table A7. As in Table A1, except for ICT, April-May, 1985-89.

SWP Threshold	POD	FAR	CSI	Bias	X	Y	Z	W
1	1.00	.69	.31	3.25	71	0	160	1
2	1.00	.69	.31	3.25	71	0	160	1
3	1.00	.69	.31	3.25	71	0	160	1
4	.99	.69	.31	3.21	70	1	158	3
5	.97	.67	.33	2.93	69	2	139	22
6	.89	.65	.34	2.51	63	8	115	46
7	.86	.61	.37	2.18	61	10	94	67
8	.86	.56	.41	1.97	61	10	79	82
9	.85	.53	.43	1.82	60	11	69	92
10	.83	.52	.43	1.75	59	12	65	96
11	.79	.53	.42	1.66	56	15	62	99
12	.76	.51	.43	1.55	54	17	56	105
13	.75	.49	.43	1.46	53	18	51	110
14	.73	.47	.44	1.39	52	19	47	114
15	.72	.46	.44	1.34	51	20	44	117
16	.69	.46	.43	1.28	49	22	42	119
17	.66	.46	.42	1.23	47	24	40	121
18	.66	.43	.44	1.17	47	24	36	125
19	.66	.41	.46	1.11	47	24	32	129
20	.62	.41	.44	1.04	44	27	30	131
21	.62	.39	.44	1.01	44	27	28	133
22	.59	.36	.44	.93	42	29	24	137
23	.51	.38	.39	.82	36	35	22	139
24	.49	.36	.38	.77	35	36	20	141
25	.48	.35	.38	.73	34	37	18	143
26	.45	.33	.37	.68	32	39	16	145
27	.44	.34	.36	.66	31	40	16	145
28	.44	.31	.36	.63	31	40	14	147
29	.42	.30	.36	.61	30	41	13	148
30	.41	.31	.35	.59	29	42	13	148
31	.41	.29	.35	.58	29	42	12	149
32	.38	.31	.33	.55	27	44	12	149
33	.38	.29	.33	.54	27	44	11	150
34	.37	.26	.32	.49	26	45	9	152
35	.34	.27	.30	.46	24	47	9	152
36	.32	.28	.29	.45	23	48	9	152
37	.32	.26	.29	.44	23	48	8	153
38	.32	.26	.29	.44	23	48	8	153
39	.32	.21	.30	.41	23	48	6	155
40	.32	.21	.30	.41	23	48	6	155

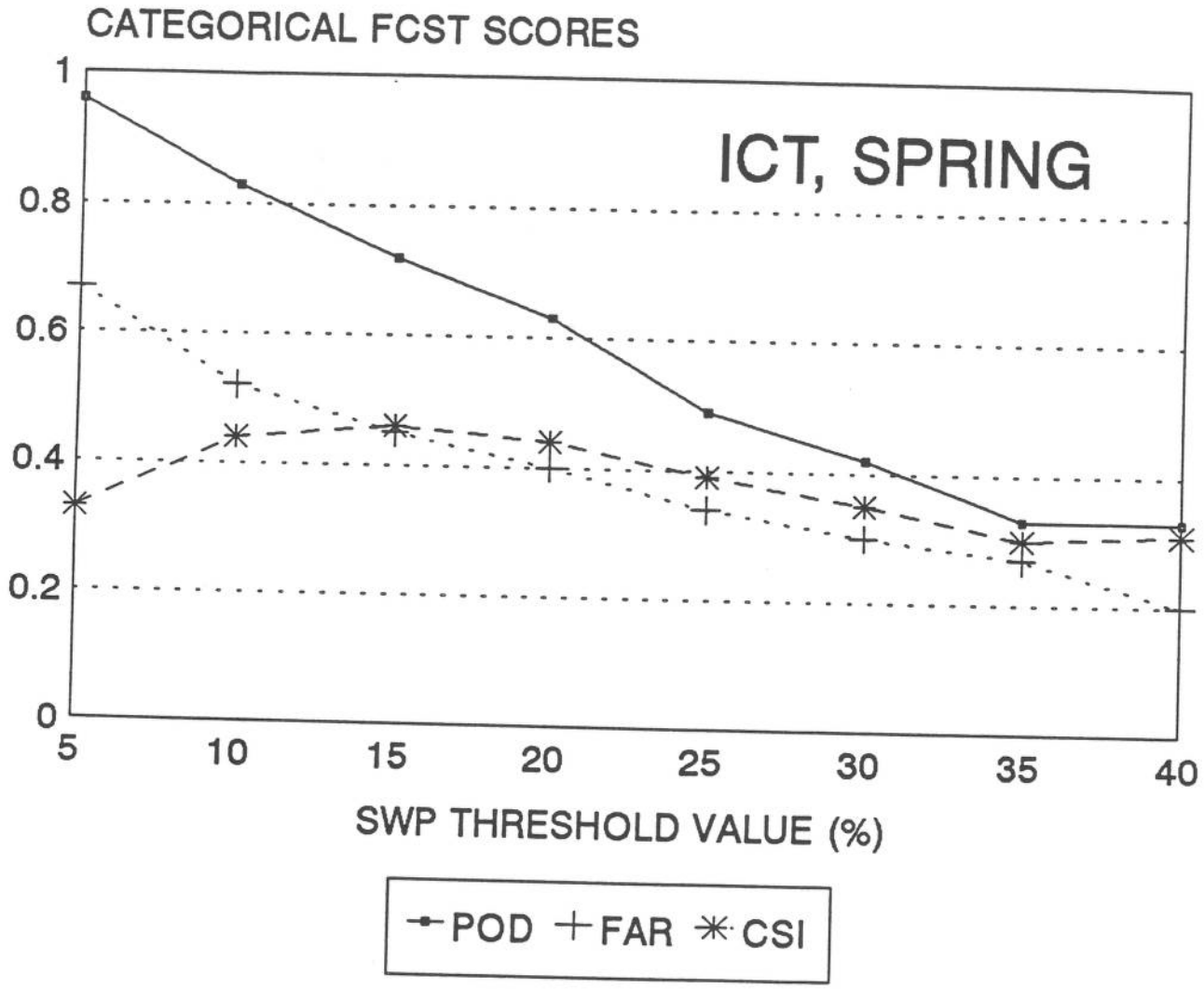

Figure A14. As in Fig. A2, except for ICT, April-May, 1985-89.

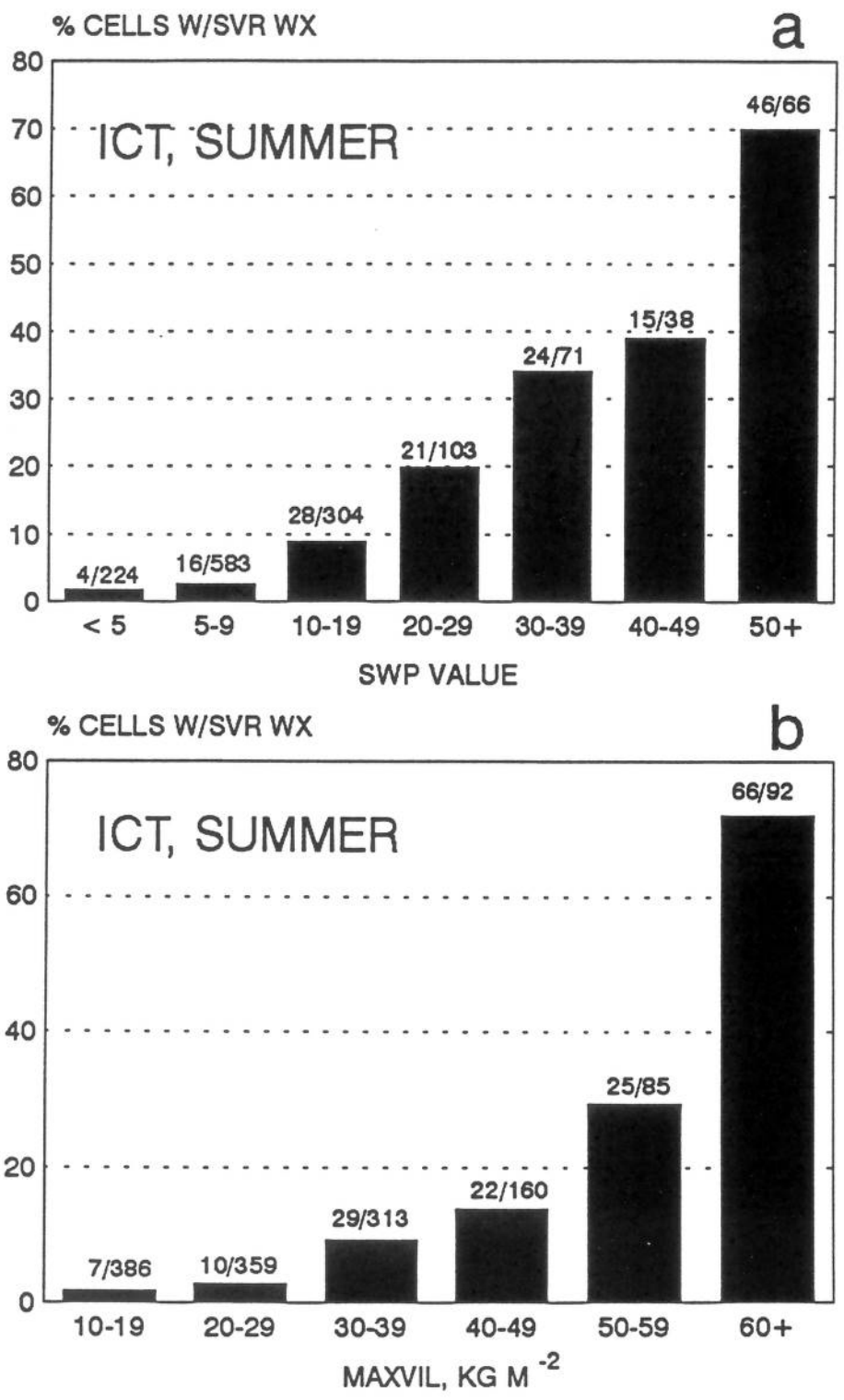

Figure A15. As in Fig. A1, except for ICT, June-September, 1985-89.

Table A8. As in Table A1, except for ICT, June-September, 1985-89.

SWP Threshold	POD	FAR	CSI	Bias	X	Y	Z	W
1	1.00	.89	.11	8.99	154	0	1231	4
2	1.00	.89	.11	8.97	154	0	1227	8
3	1.00	.89	.11	8.93	154	0	1221	14
4	.99	.89	.11	8.60	152	2	1173	62
5	.97	.87	.13	7.62	150	4	1023	212
6	.94	.85	.15	6.12	145	9	797	438
7	.93	.82	.18	5.19	143	11	656	579
8	.92	.80	.20	4.60	141	13	567	668
9	.89	.79	.21	4.14	137	17	501	734
10	.88	.77	.22	3.79	135	19	448	787
11	.86	.75	.24	3.42	133	21	394	841
12	.85	.73	.26	3.15	131	23	354	881
13	.83	.72	.27	2.92	128	26	322	913
14	.81	.70	.28	2.73	125	29	295	940
15	.80	.69	.29	2.58	123	31	275	960
16	.78	.68	.30	2.40	120	34	250	985
17	.75	.66	.30	2.22	115	39	227	1008
18	.73	.65	.31	2.07	113	41	206	1029
19	.73	.63	.33	1.95	112	42	189	1046
20	.69	.62	.33	1.81	106	48	172	1063
21	.68	.60	.34	1.67	104	50	153	1082
22	.66	.59	.34	1.58	101	53	143	1092
23	.63	.59	.33	1.53	97	57	139	1096
24	.63	.58	.34	1.49	97	57	133	1102
25	.62	.57	.34	1.44	95	59	127	1108
26	.60	.56	.34	1.36	93	61	116	1119
27	.60	.55	.35	1.32	92	62	111	1124
28	.59	.54	.35	1.27	91	63	105	1130
29	.57	.53	.35	1.21	88	66	98	1137
30	.55	.51	.35	1.14	85	69	90	1145
31	.53	.50	.34	1.06	81	73	82	1153
32	.51	.50	.34	1.03	79	75	79	1156
33	.49	.49	.34	.96	76	78	72	1163
34	.49	.47	.34	.93	76	78	67	1168
35	.47	.47	.33	.88	72	82	63	1172
36	.45	.47	.32	.85	69	85	62	1173
37	.44	.45	.32	.79	67	87	54	1181
38	.42	.44	.31	.75	64	90	51	1184
39	.42	.42	.32	.72	64	90	47	1188
40	.40	.41	.31	.68	61	93	43	1192

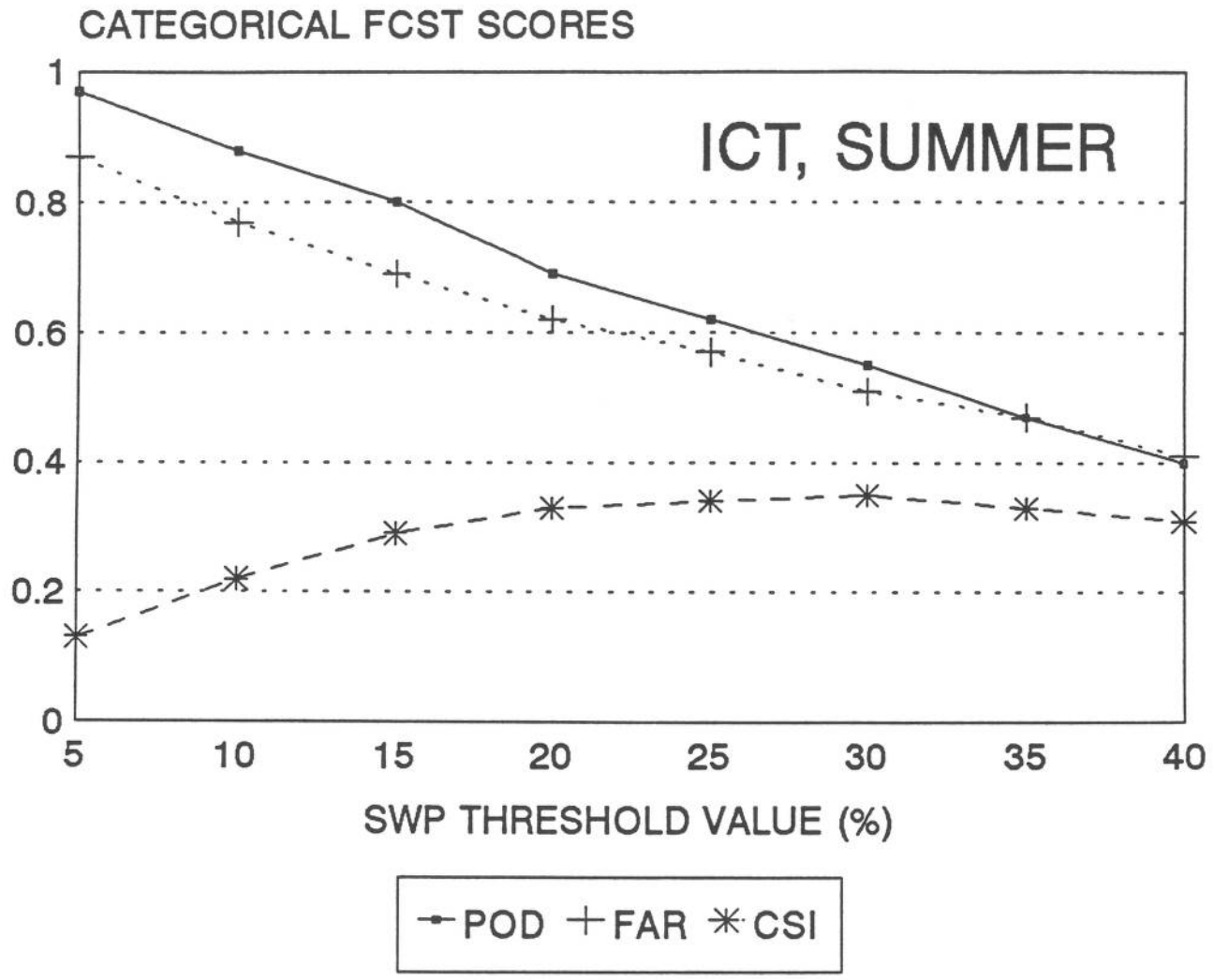

Figure A16. As in Fig. A2, except for ICT, June-September, 1985-89.

A7. LIMON, COLORADO (LIC)

The LIC umbrella includes the Colorado Front Range and much of northeastern Colorado, an area often visited by intense hailstorms. During the period of our study (1985-89), a fairly high percentage of the storm cells over populated regions of the umbrella were indeed severe (120 of 756, or 16%). Most of the radar observations were taken between May and August.

As shown in Fig. A17, the probability of severe weather increases from 10% or less to above 20% around an SWP value of 10, or a VIL of 40 kg m^{-2}. However, a majority of cells are severe only when the SWP exceeds 40. The verification scores (Table A9, Fig. A18), indicate a level of information approximately equal to that of AMA and ICT during the summer months. For an SWP threshold value of 15, a POD of 0.8, FAR of 0.7, and bias of 2.6 would be achieved.

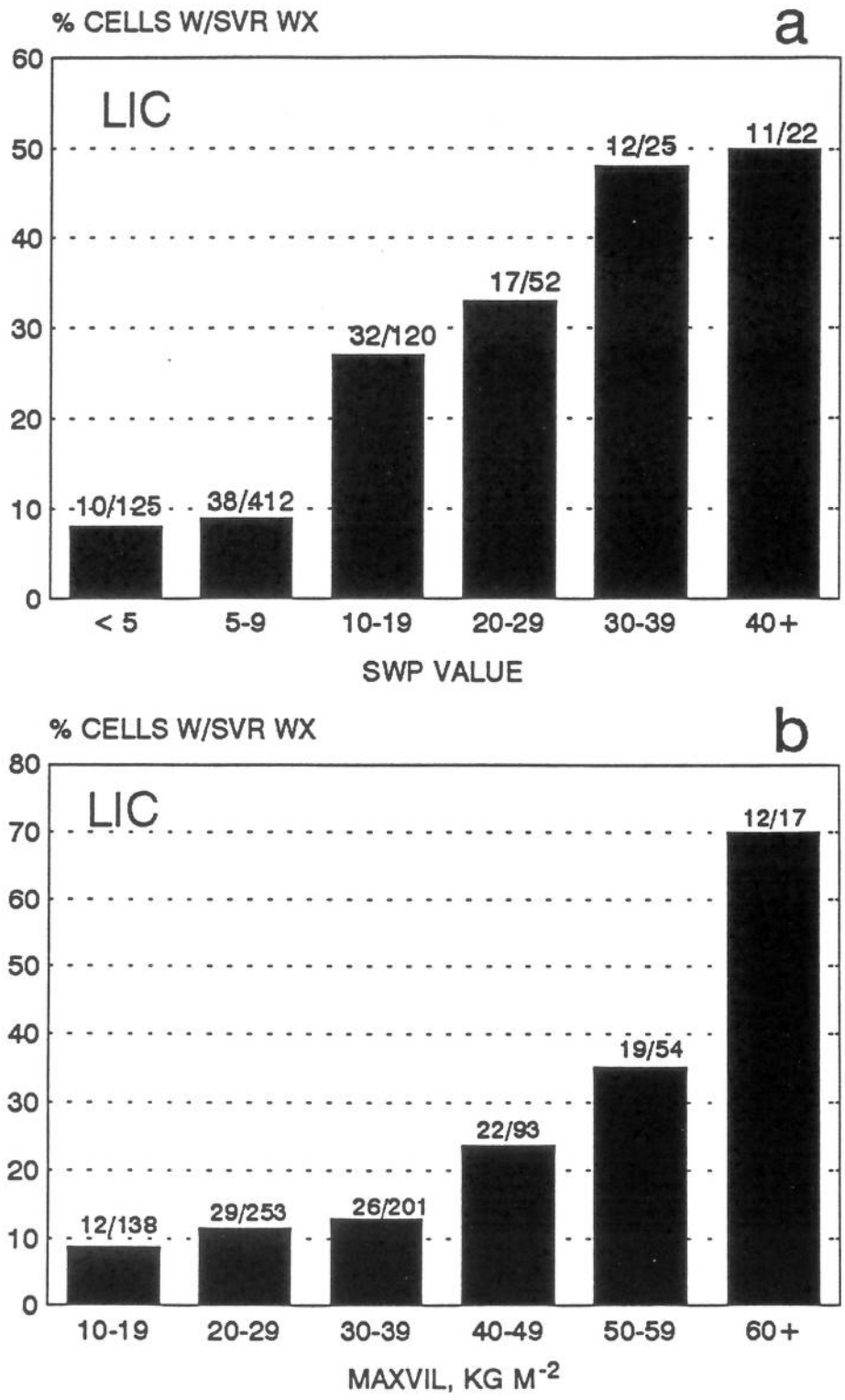

Figure A17. As in Fig. A1, except for LIC, April-September, 1985-89.

Table A9. As in Table A1, except for LIC, April-May, 1985-89.

SWP Threshold	POD	FAR	CSI	Bias	X	Y	Z	W
1	1.00	.84	.16	6.30	120	0	636	0
2	1.00	.84	.16	6.30	120	0	636	0
3	1.00	.84	.16	6.26	120	0	631	5
4	.97	.84	.16	5.97	116	4	601	35
5	.92	.83	.17	5.30	110	10	526	110
6	.84	.78	.21	3.82	101	19	357	279
7	.77	.73	.25	2.85	92	28	250	386
8	.72	.70	.26	2.42	86	34	205	431
9	.63	.70	.26	2.06	75	45	172	464
10	.60	.67	.27	1.83	72	48	147	489
11	.55	.67	.26	1.66	66	54	133	503
12	.52	.66	.26	1.51	62	58	119	517
13	.51	.64	.27	1.40	61	59	107	529
14	.46	.62	.26	1.22	55	65	91	545
15	.41	.63	.24	1.09	49	71	82	554
16	.40	.62	.24	1.05	48	72	78	558
17	.38	.62	.23	.99	45	75	74	562
18	.35	.60	.23	.88	42	78	63	573
19	.35	.59	.23	.86	42	78	61	575
20	.33	.60	.22	.82	40	80	59	577
21	.30	.60	.21	.75	36	84	54	582
22	.30	.57	.22	.69	36	84	47	589
23	.28	.57	.20	.63	33	87	43	593
24	.28	.55	.20	.62	33	87	41	595
25	.27	.53	.21	.57	32	88	36	600
26	.23	.53	.18	.50	28	92	32	604
27	.21	.55	.17	.46	25	95	30	606
28	.19	.56	.15	.43	23	97	29	607
29	.19	.56	.15	.43	23	97	29	607
30	.19	.51	.16	.39	23	97	24	612
31	.19	.51	.16	.39	23	97	24	612
32	.17	.49	.15	.34	21	99	20	616
33	.17	.47	.14	.32	20	100	18	618
34	.16	.46	.14	.29	19	101	16	620
35	.14	.47	.13	.27	17	103	15	621
36	.13	.47	.12	.25	16	104	14	622
37	.13	.48	.11	.24	15	105	14	622
38	.12	.50	.10	.23	14	106	14	622
39	.09	.52	.08	.19	11	109	12	624
40	.09	.50	.08	.18	11	109	11	625

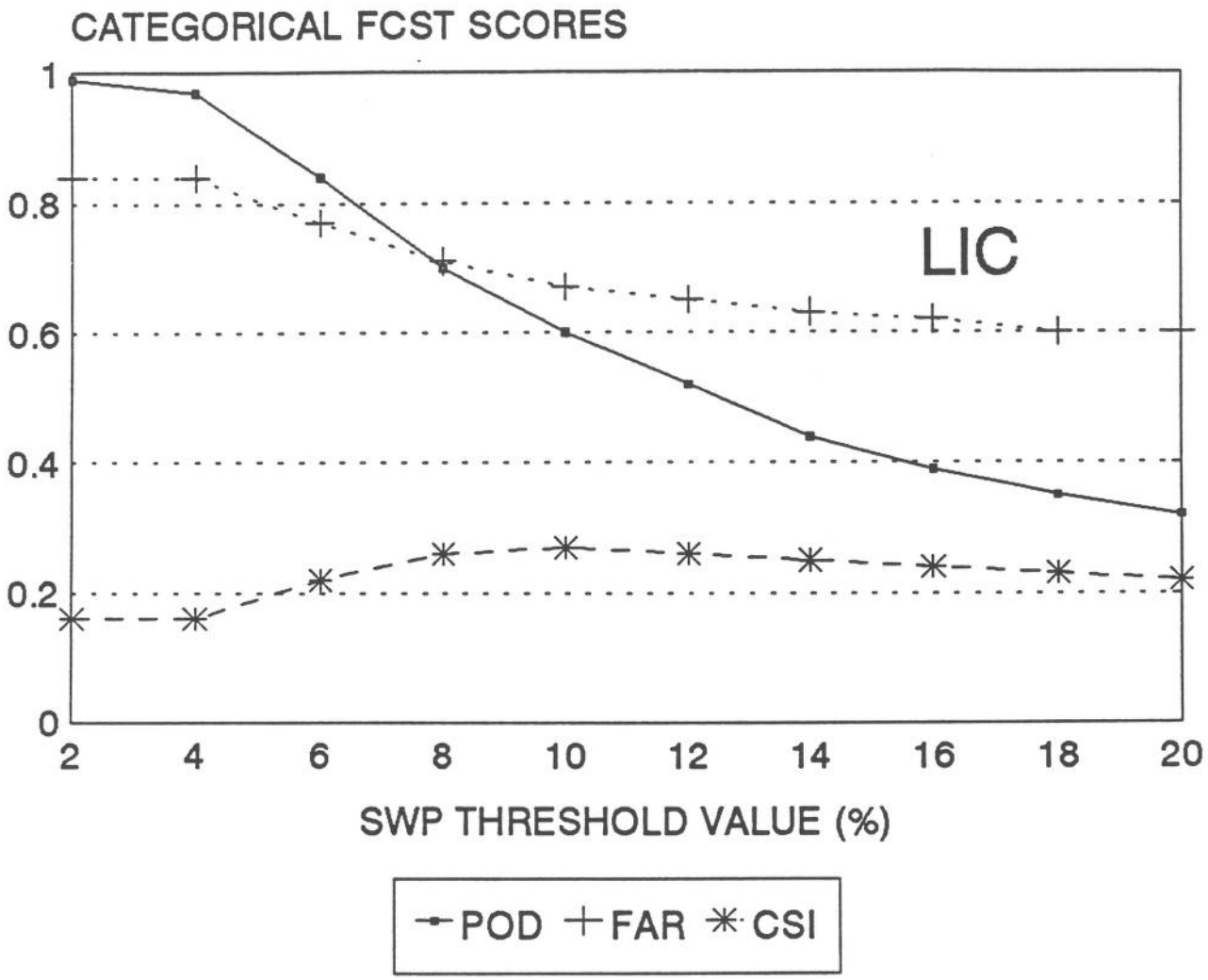

Figure A18. As in Fig. A2, except for LIC, April-May, 1985-89.

A8. OKLAHOMA CITY, OKLAHOMA (OKC)

Because of the intensive verification program implemented within this umbrella, we have been able to document the characteristics of the SWP algorithm not only during the warm season, but during the autumn and early winter (October to December). For this site, we have also included March observations in the spring sample. A total of 1985 cells were included in this site's sample.

For the spring season, approximately 24% of the cells were severe (118 of 487, Fig. A19). The potential for severe weather increases sharply, from about 20% to over 50%, near an SWP of 20 or a VIL of 40 kg m^{-2}. The verification results for categorical forecasts (Table A10, Fig. A20), show that an SWP threshold of 8 yields a POD of 0.8, with an FAR of 0.6 and a bias of 2.1.

As might be expected, the skill level drops somewhat in the summer, as the portion of cells with severe weather drops to around 13% (148 of 1135). The probability of severe weather is greatest in cells with SWP above 30 or VIL above 50, though the majority of severe events actually occur in cells weaker than these values (Fig. A21). An SWP threshold of 9 yields a POD of 0.8, though the FAR increases to 0.7 and the bias to 2.9. However, a threshold of 11 still yields a POD of 0.75, while decreasing the bias to 2.3.

The relative frequency of severe weather increases slightly from summer to autumn (Figs. A22-A23 and Table A12) and the forecasting skill appears roughly the same. This sample includes 362 cells, of which 50, or 14%, were severe. Though severe outbreaks have occurred over this portion of the southern Plains in January and February, our archive includes only a few cells from these months; they were incorporated into the October-December sample. The majority of the severe weather develops in cells with SWP greater than 20, or VIL greater than 40. For categorical forecasts, an SWP threshold of 10 yields a POD of nearly 0.8, with an FAR of 0.7 and a bias of 2.4 (Table A12, Fig. A23).

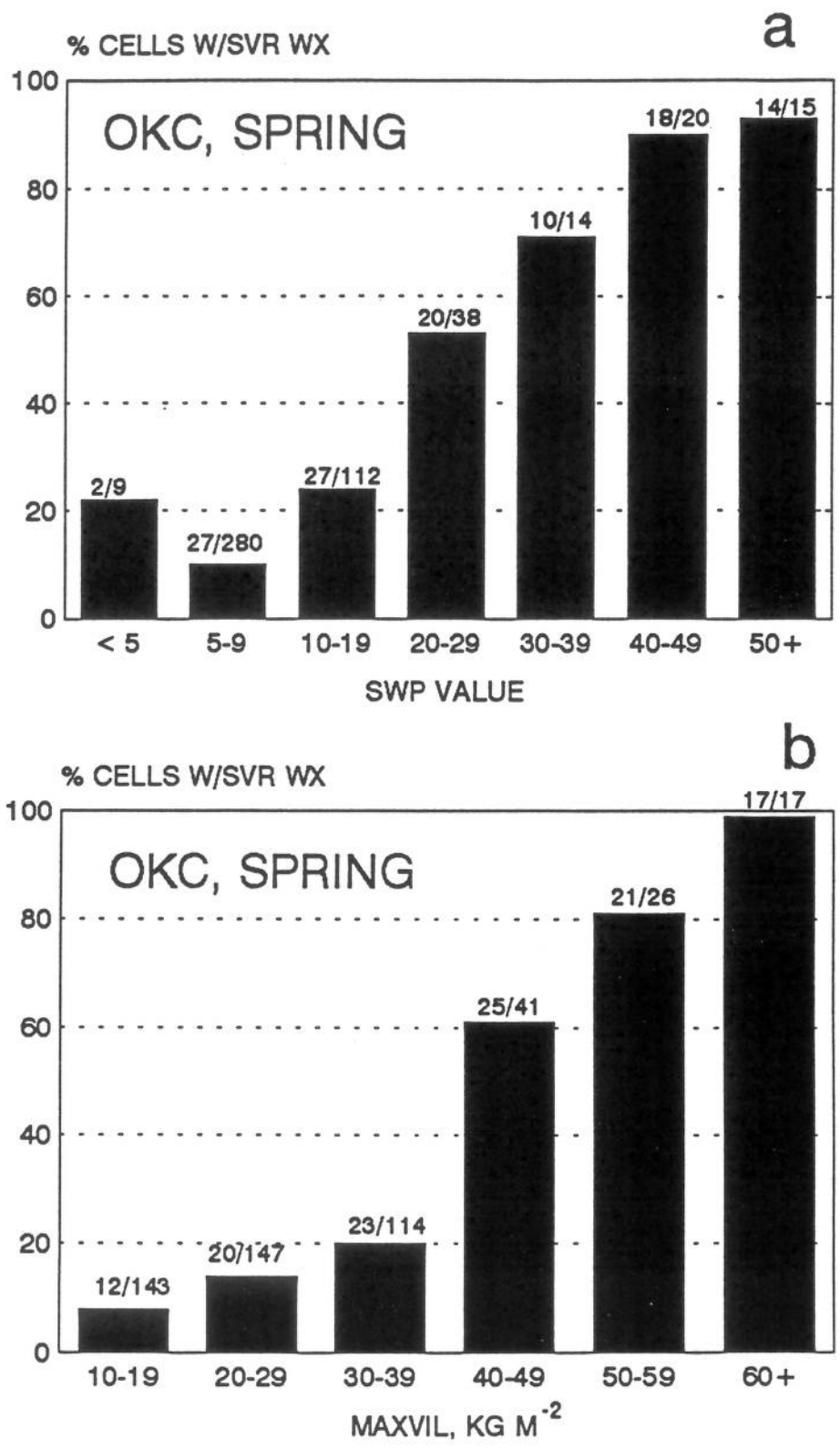

Figure A19. As in Fig. A1, except for OKC, March-May, 1983, 1985, 1987-1989.

Table A10. As in Table A1, except for OKC, March-May, 1983, 1985, 1987-1989.

SWP Threshold	POD	FAR	CSI	Bias	X	Y	Z	W
1	1.00	.76	.24	4.13	118	0	369	0
2	1.00	.76	.24	4.13	118	0	369	0
3	.98	.76	.24	4.11	116	2	369	0
4	.98	.76	.24	4.10	116	2	368	1
5	.95	.75	.24	3.86	112	6	344	25
6	.90	.70	.29	3.03	106	12	251	118
7	.81	.66	.32	2.34	95	23	181	188
8	.80	.61	.35	2.06	94	24	149	220
9	.75	.57	.38	1.75	89	29	118	251
10	.75	.53	.40	1.59	88	30	100	269
11	.71	.49	.42	1.40	84	34	81	288
12	.69	.46	.44	1.26	81	37	68	301
13	.66	.43	.44	1.17	78	40	60	309
14	.62	.40	.44	1.03	73	45	48	321
15	.62	.37	.45	.98	73	45	43	326
16	.59	.36	.45	.92	70	48	39	330
17	.59	.33	.46	.88	70	48	34	335
18	.56	.30	.45	.80	66	52	28	341
19	.54	.30	.44	.77	64	54	27	342
20	.52	.29	.43	.73	61	57	25	344
21	.49	.25	.42	.65	58	60	19	350
22	.48	.23	.42	.63	57	61	17	352
23	.47	.23	.41	.60	55	63	16	353
24	.46	.19	.41	.57	54	64	13	356
25	.42	.20	.38	.52	49	69	12	357
26	.39	.19	.36	.48	46	72	11	358
27	.38	.15	.36	.45	45	73	8	361
28	.37	.15	.35	.44	44	74	8	361
29	.36	.14	.34	.42	43	75	7	362
30	.36	.14	.34	.42	42	76	7	362
31	.36	.13	.34	.41	42	76	6	363
32	.32	.14	.31	.37	38	80	6	363
33	.31	.14	.29	.36	36	82	6	363
34	.31	.12	.29	.35	36	82	5	364
35	.29	.13	.28	.33	34	84	5	364
36	.29	.11	.28	.32	34	84	4	365
37	.29	.11	.28	.32	34	84	4	365
38	.29	.11	.28	.32	34	84	4	365
39	.27	.09	.26	.30	32	86	3	366
40	.25	.09	.25	.28	30	88	3	366

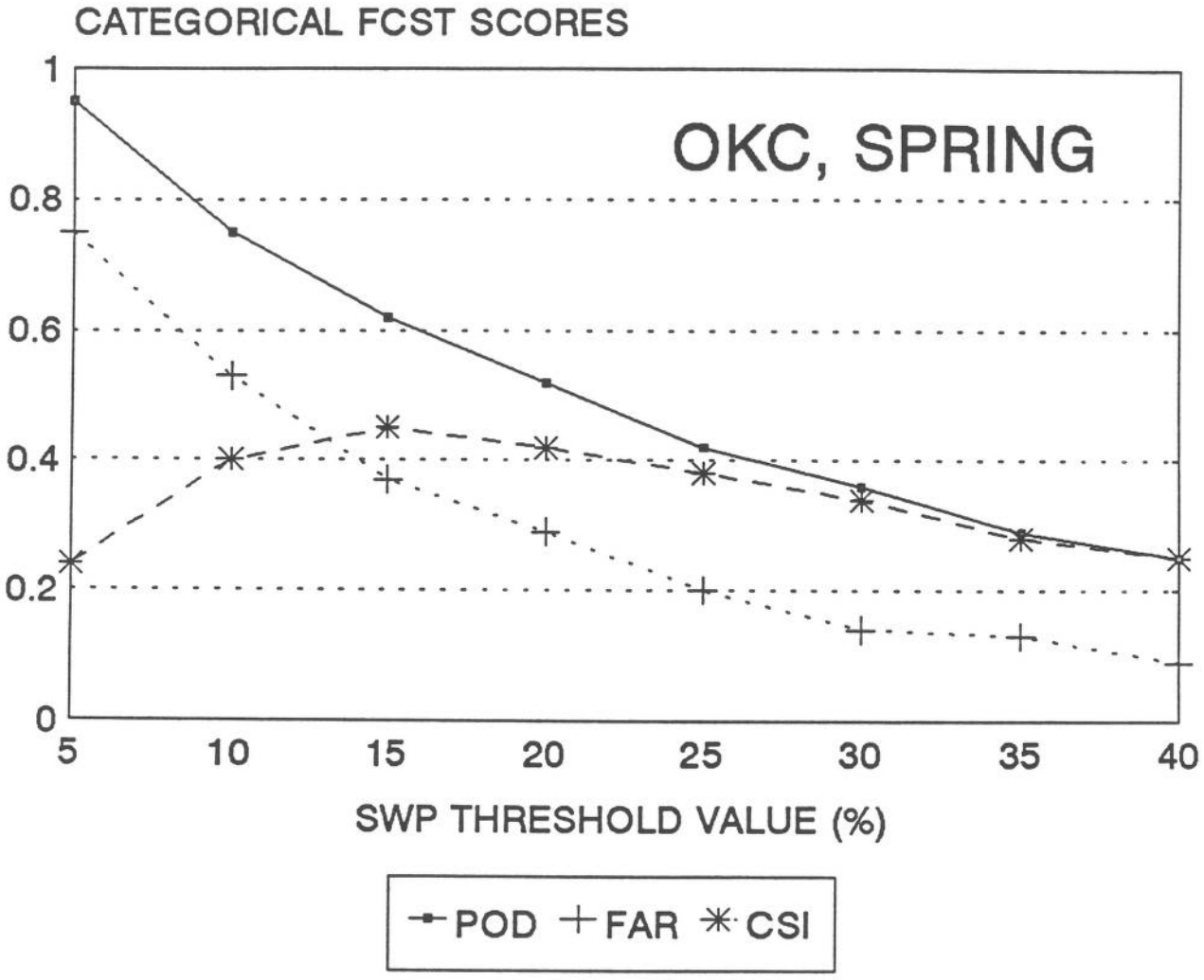

Figure A20. As in Fig. A2, except for OKC, March-May, 1983, 1985, 1987-89.

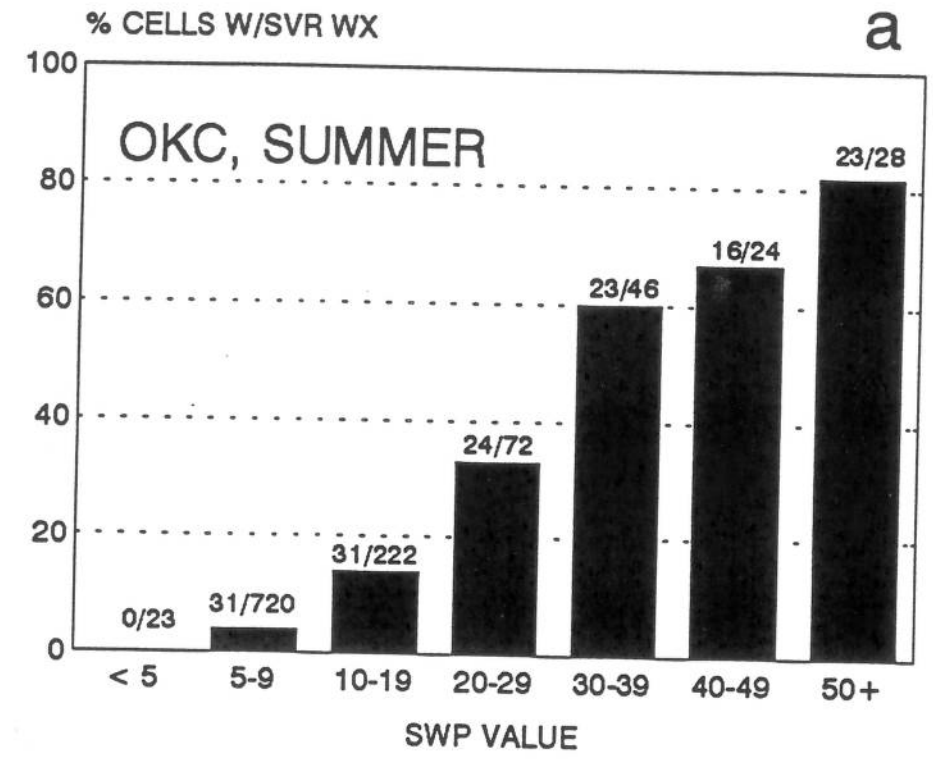

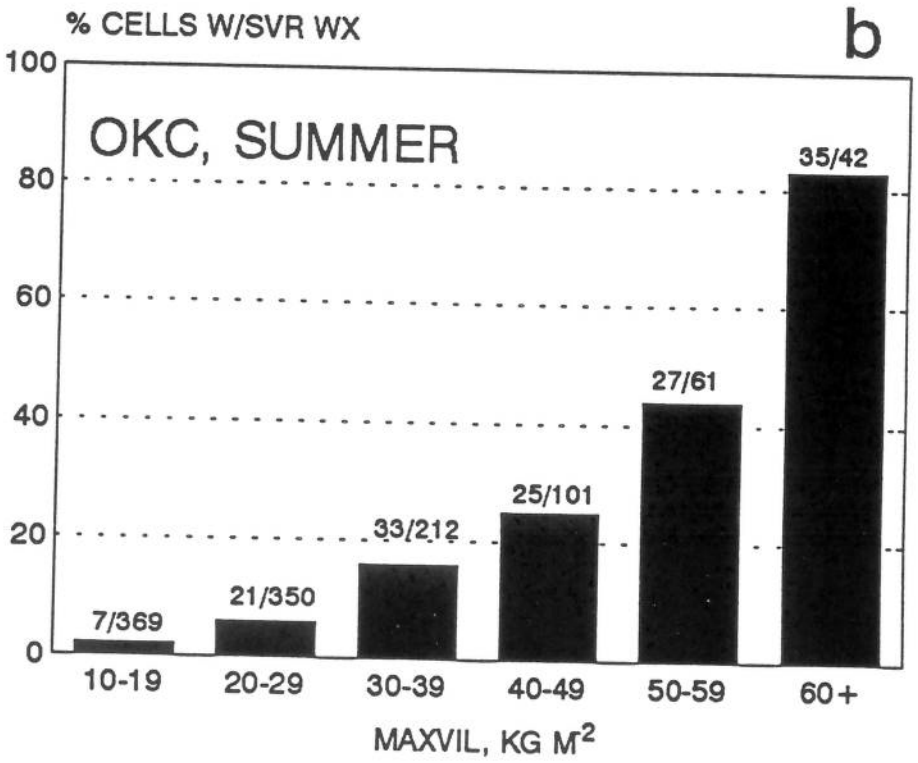

Figure A21. As in Fig. A1, except for OKC, June-September, 1983, 1985, 1987-1989.

Table A11. As in Table A1, except for OKC, June-September, 1983, 1985, 1987-1989.

SWP Threshold	POD	FAR	CSI	Bias	X	Y	Z	W
1	1.00	.87	.13	7.67	148	0	987	0
2	1.00	.87	.13	7.67	148	0	987	0
3	1.00	.87	.13	7.66	148	0	985	2
4	1.00	.87	.13	7.61	148	0	979	8
5	.98	.86	.14	7.14	145	3	911	76
6	.95	.82	.18	5.21	140	8	631	356
7	.91	.78	.22	4.08	134	14	470	517
8	.85	.74	.25	3.32	126	22	365	622
9	.80	.72	.26	2.89	119	29	308	679
10	.78	.69	.28	2.54	116	32	260	727
11	.76	.67	.30	2.30	112	36	229	758
12	.73	.65	.31	2.09	108	40	201	786
13	.67	.64	.30	1.87	99	49	178	809
14	.64	.62	.31	1.70	95	53	156	831
15	.63	.59	.33	1.53	93	55	134	853
16	.63	.56	.35	1.43	93	55	118	869
17	.61	.54	.36	1.32	90	58	105	882
18	.59	.52	.36	1.22	87	61	94	893
19	.58	.51	.36	1.18	86	62	89	898
20	.57	.48	.37	1.11	85	63	80	907
21	.55	.46	.38	1.02	82	66	69	918
22	.53	.45	.37	.97	79	69	64	923
23	.52	.44	.37	.93	77	71	61	926
24	.51	.43	.37	.89	75	73	57	930
25	.48	.41	.36	.82	71	77	50	937
26	.46	.41	.35	.78	68	80	47	940
27	.44	.41	.34	.75	65	83	46	941
28	.44	.39	.34	.72	65	83	41	946
29	.42	.38	.33	.68	62	86	38	949
30	.42	.36	.34	.66	62	86	35	952
31	.40	.36	.33	.62	59	89	33	954
32	.38	.36	.31	.59	56	92	32	955
33	.36	.36	.30	.57	54	94	31	956
34	.36	.35	.30	.55	53	95	29	958
35	.34	.34	.29	.52	51	97	26	961
36	.30	.37	.25	.47	44	104	26	961
37	.28	.36	.24	.43	41	107	23	964
38	.27	.30	.24	.39	40	108	17	970
39	.26	.26	.24	.36	39	109	14	973
40	.23	.26	.21	.31	34	114	12	975

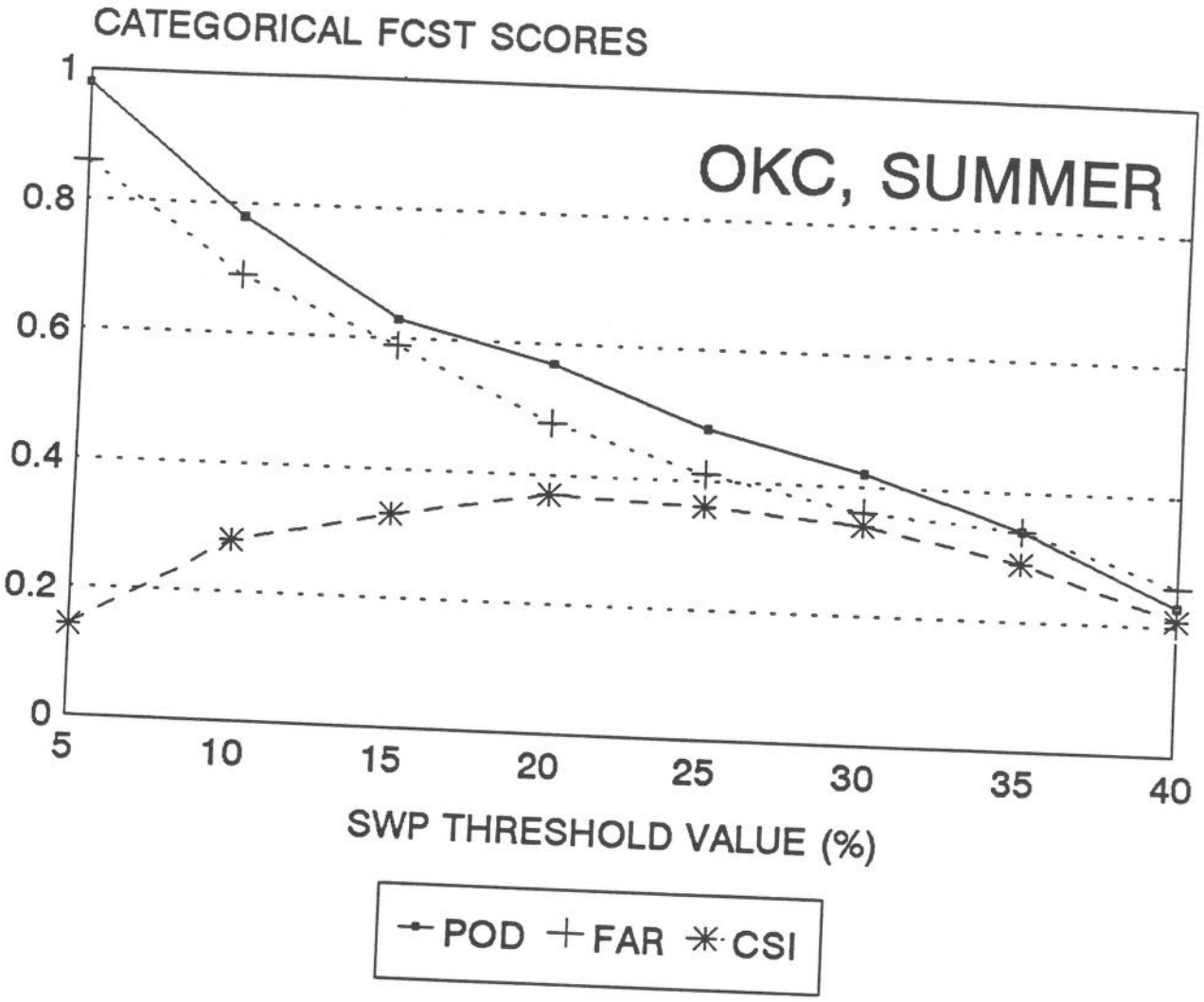

Figure A22. As in Fig. A2, except for OCK, June-September, 1983, 1985, 1987-1989.

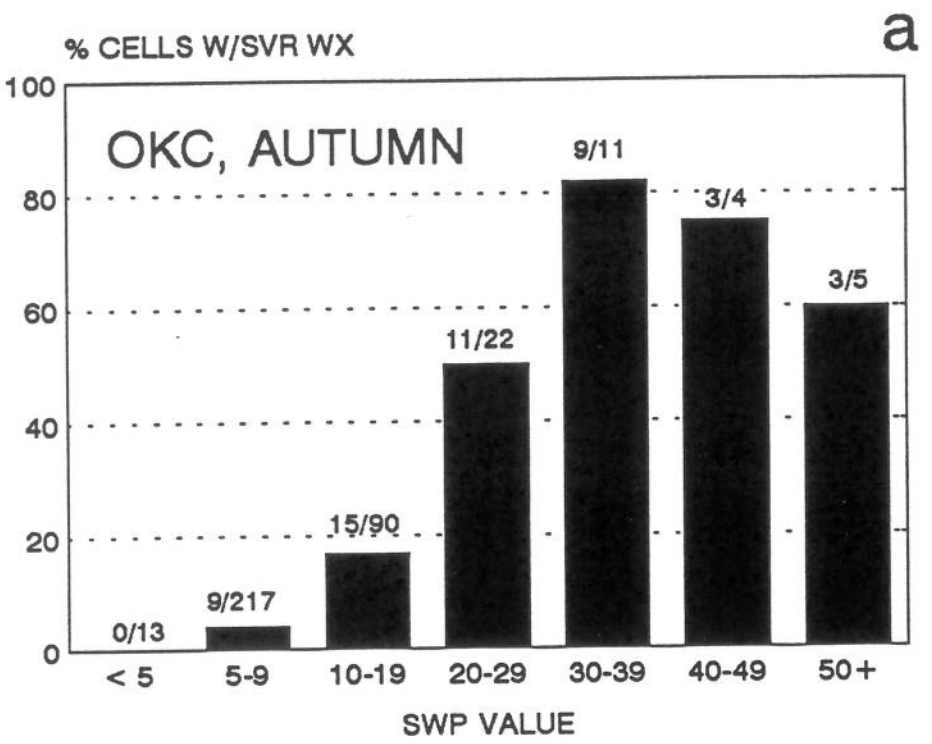

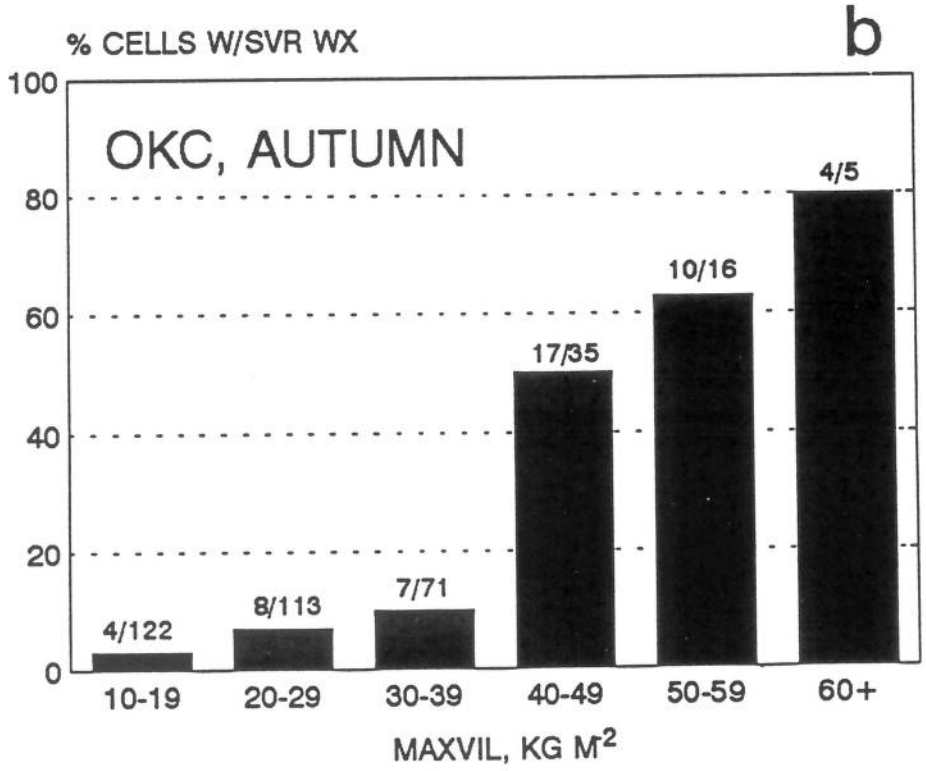

Figure A23. As in Fig. A1, except for OKC, October-December, 1983, 1985, 1987-1989.

Table A12. As in Table A1, except for OKC, October-December, 1983, 1985, 1987-1989.

SWP Threshold	POD	FAR	CSI	Bias	X	Y	Z	W
1	1.00	.86	.14	7.24	50	0	312	0
2	1.00	.86	.14	7.24	50	0	312	0
3	1.00	.86	.14	7.24	50	0	312	0
4	1.00	.86	.14	7.10	50	0	305	7
5	1.00	.85	.15	6.68	50	0	284	28
6	.96	.81	.19	5.12	48	2	208	104
7	.88	.78	.21	4.08	44	6	160	152
8	.84	.75	.24	3.40	42	8	128	184
9	.82	.71	.28	2.80	41	9	99	213
10	.78	.68	.29	2.44	39	11	83	229
11	.76	.65	.31	2.20	38	12	72	240
12	.70	.61	.33	1.80	35	15	55	257
13	.68	.59	.35	1.64	34	16	48	264
14	.66	.55	.36	1.48	33	17	41	271
15	.64	.54	.37	1.38	32	18	37	275
16	.62	.48	.39	1.20	31	19	29	283
17	.62	.45	.41	1.12	31	19	25	287
18	.60	.40	.43	1.00	30	20	20	292
19	.56	.38	.42	.90	28	22	17	295
20	.52	.37	.40	.82	26	24	15	297
21	.50	.32	.40	.74	25	25	12	300
22	.46	.32	.38	.68	23	27	11	301
23	.46	.32	.38	.68	23	27	11	301
24	.44	.33	.36	.66	22	28	11	301
25	.40	.33	.33	.60	20	30	10	302
26	.40	.33	.33	.60	20	30	10	302
27	.36	.33	.31	.54	18	32	9	303
28	.34	.32	.29	.50	17	33	8	304
29	.32	.27	.29	.44	16	34	6	306
30	.28	.26	.25	.38	14	36	5	307
31	.26	.28	.24	.36	13	37	5	307
32	.24	.29	.22	.34	12	38	5	307
33	.24	.29	.22	.34	12	38	5	307
34	.24	.29	.22	.34	12	38	5	307
35	.22	.31	.20	.32	11	39	5	307
36	.18	.31	.17	.26	9	41	4	308
37	.14	.36	.13	.22	7	43	4	308
38	.14	.36	.13	.22	7	43	4	308
39	.12	.33	.11	.18	6	44	3	309
40	.12	.33	.11	.18	6	44	3	309

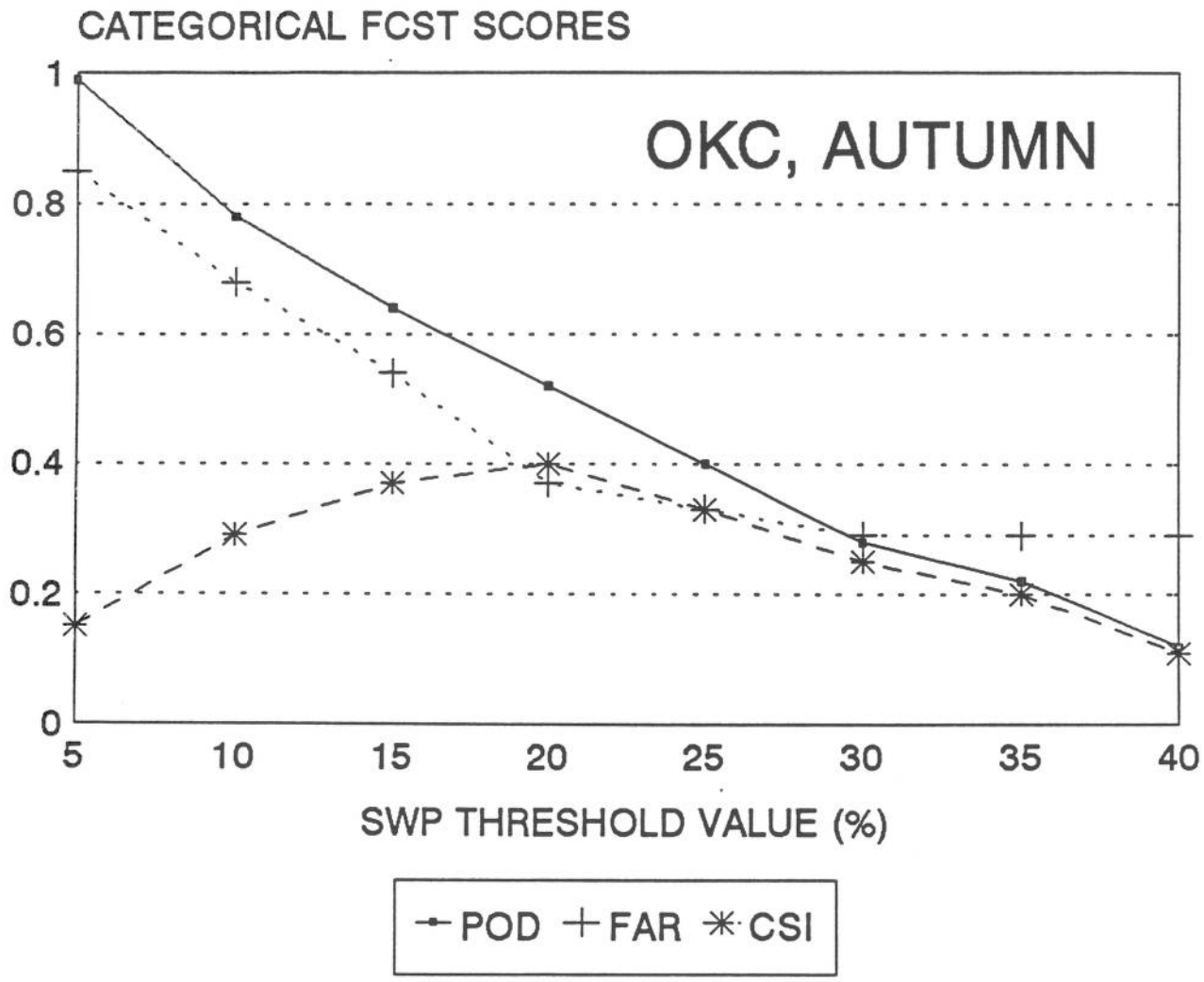

Figure A24. As in Fig. A2, except for OKC, October-December, 1983, 1987-1989.

A9. TAMPA BAY, FLORIDA (TBW)

As noted earlier, the severe/nonsevere discriminating skill of VIL is much lower in the subtropical regime of Florida than over the Central Plains and the northeastern United States. The most concentrated outbreaks of severe weather in Florida occur during the winter and early spring, a period for which we had very few radar observations. Still, the SWP algorithm has statistically significant skill for Florida storms during the warm season, and it may be applied to screen innocuous cells from those that have some potential for producing severe weather.

The sample of warm-season data for TBW does not include cells with maximum VIL less than 20 kg m^{-2}, since cell tracking became extremely complicated when weaker cells were taken into account. Only 5% (50 of 1068) of the cells were severe, and the majority of these events were from high winds and small tornadoes. The majority of the severe cells (34) had an SWP of at least 20; 31 of the severe cells had a VIL of 55 or greater (Fig. A25). The threat of severe phenomena is very low, about 2.4%, for storms with SWP less than 20, and these storms make up over 60% of the total.

Because they appeared to have such radically different characteristics from the remainder of the observations, the TBW data were not used in the SWP algorithm development sample. Thus the verification statistics presented here (Table A13, Fig. A26) are for a statistically independent sample. It is evident that nowcasting based purely on the SWP algorithm will produce very low skill. Obtaining even a POD of 0.5 requires overforecasting with a bias of 5.8.

The use of other information, especially real-time spotter reports and consideration of cell translation speed, could aid in determining which of the larger cells might cause severe weather. Doppler information from WSR-88D might provide clues on the existence and propagation of strong surface gust fronts. We are also currently assessing a variety of other reflectivity predictors, such as partial VIL and echo strength aloft, that may be derived from current WSR-88D displays or which may be incorporated in later versions of the SWP algorithm.

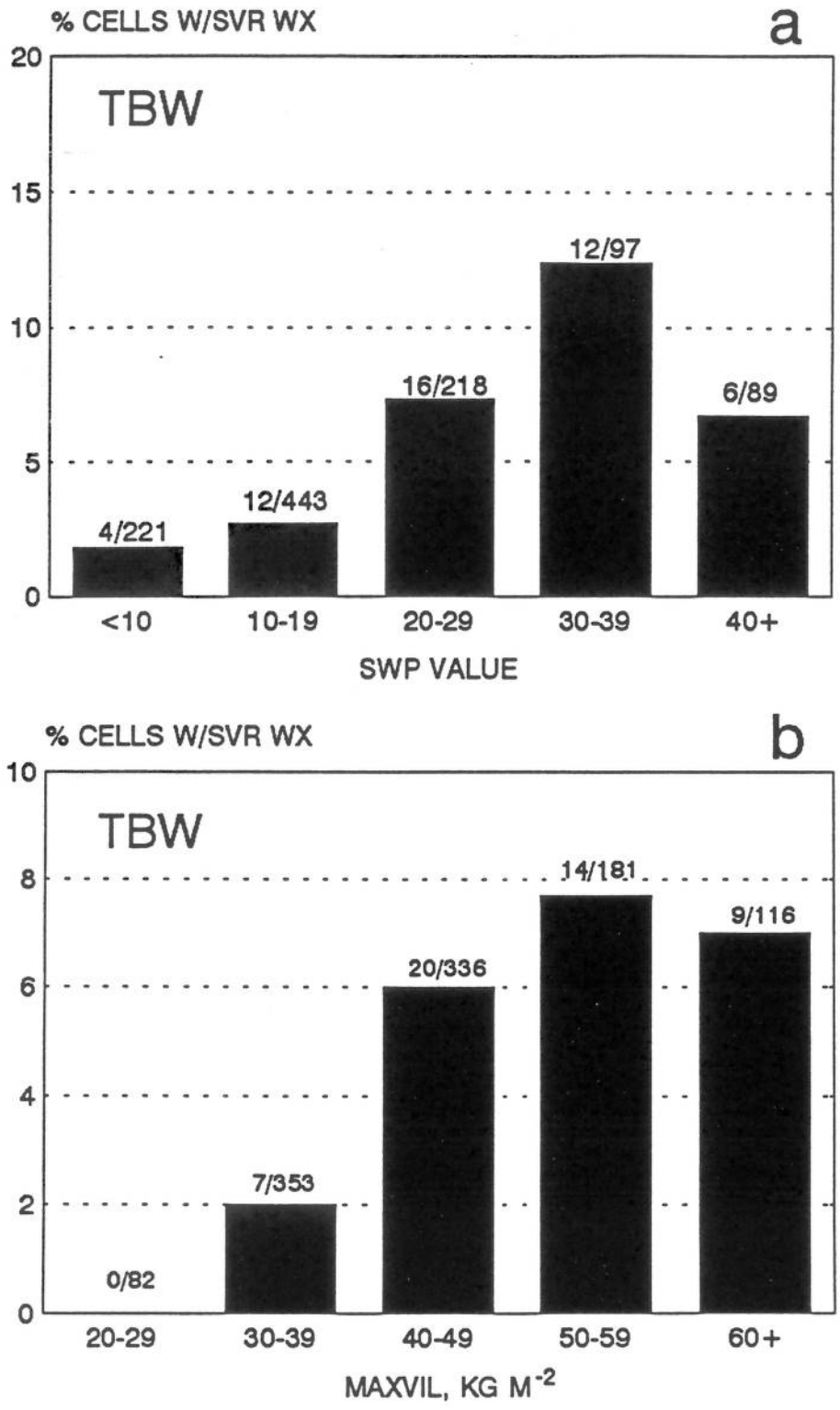

Figure A25. As in Fig. A1, except for TBW, April-September, 1985-1989.

Table A13. As in Table A1, except for TBW, April-September, 1985-1989.

SWP Threshold	POD	FAR	CSI	Bias	X	Y	Z	W
1	1.00	.95	.05	21.28	50	0	1014	4
2	1.00	.95	.05	21.24	50	0	1012	6
3	1.00	.95	.05	21.18	50	0	1009	9
4	1.00	.95	.05	21.02	50	0	1001	17
5	1.00	.95	.05	20.82	50	0	991	27
6	1.00	.95	.05	20.38	50	0	969	49
7	1.00	.95	.05	19.74	50	0	937	81
8	1.00	.95	.05	18.96	50	0	898	120
9	.98	.95	.05	18.20	49	1	861	157
10	.92	.95	.05	16.96	46	4	802	216
11	.90	.94	.06	15.72	45	5	741	277
12	.86	.94	.06	14.48	43	7	681	337
13	.86	.94	.06	13.62	43	7	638	380
14	.84	.93	.07	12.64	42	8	590	428
15	.82	.93	.07	11.66	41	9	542	476
16	.78	.93	.07	10.56	39	11	489	529
17	.78	.92	.08	10.04	39	11	463	555
18	.76	.92	.08	9.26	38	12	425	593
19	.74	.91	.08	8.70	37	13	398	620
20	.68	.92	.08	8.08	34	16	370	648
21	.66	.91	.08	7.58	33	17	346	672
22	.62	.91	.08	6.92	31	19	315	703
23	.60	.91	.09	6.44	30	20	292	726
24	.56	.91	.09	6.08	28	22	276	742
25	.50	.91	.09	5.38	25	25	244	774
26	.48	.90	.09	4.94	24	26	223	795
27	.46	.90	.09	4.66	23	27	210	808
28	.42	.90	.09	4.26	21	29	192	826
29	.42	.89	.09	3.96	21	29	177	841
30	.36	.90	.08	3.72	18	32	168	850
31	.30	.91	.07	3.38	15	35	154	864
32	.28	.91	.07	3.18	14	36	145	873
33	.24	.92	.06	3.00	12	38	138	880
34	.20	.93	.06	2.82	10	40	131	887
35	.20	.92	.06	2.54	10	40	117	901
36	.14	.94	.04	2.30	7	43	108	910
37	.12	.95	.04	2.20	6	44	104	914
38	.12	.94	.04	2.08	6	44	98	920
39	.12	.94	.04	1.94	6	44	91	927
40	.12	.93	.05	1.78	6	44	83	935

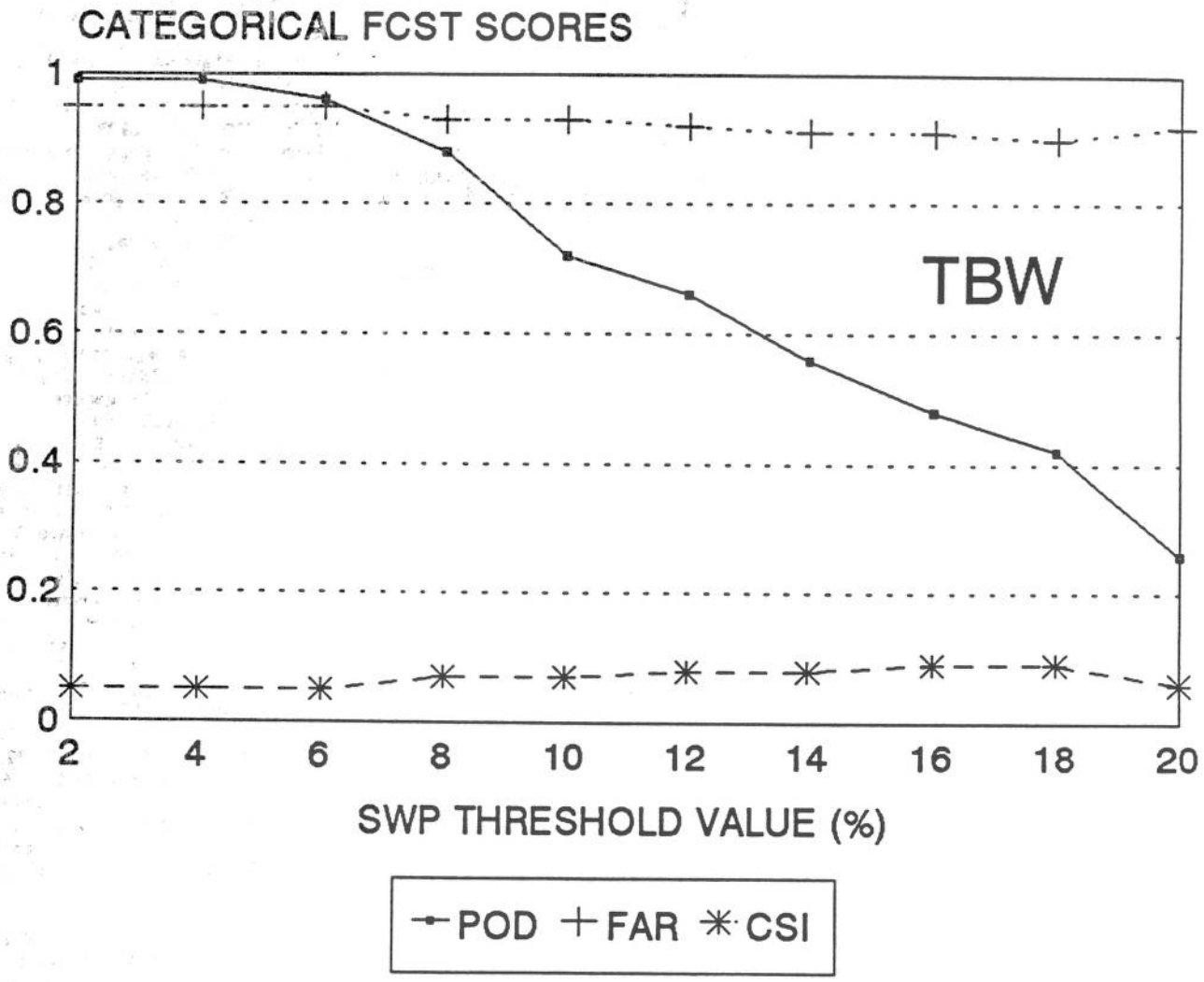

Figure A26. As in Fig. A2, except for TBW, April-September, 1985-1989.

(Continued from inside front cover)

NOAA Technical Memorandums

NWS TDL 46 SPLASH (Special Program to List Amplitudes of Surges From Hurricanes): I. Landfall Storms. Chester P. Jelesnianski, April 1972, 52 pp. (COM-72-10807)

NWS TDL 47 Mean Diurnal and Monthly Height Changes in the Troposphere Over North America and Vicinity. August F. Korte and DeVer Colson, August 1972, 30 pp. (COM-72-11132)

NWS TDL 48 Synoptic Climatological Studies of Precipitation in the Plateau States From 850-, 700-, and 500-Millibar Lows During Spring. August F. Korte, Donald L. Jorgensen, and William H. Klein, August 1972, 130 pp. (COM-73-10069)

NWS TDL 49 Synoptic Climatological Studies of Precipitation in the Plateau States From 850-Millibar Lows During Fall. August F. Korte and DeVer Colson, August 1972, 56 pp. (COM-74-10464)

NWS TDL 50 Forecasting Extratropical Storm Surges for the Northeast Coast of the United States. N. Arthur Pore, William S. Richardson, and Herman P. Perrotti, January 1974, 70 pp. (COM-74-10719)

NWS TDL 51 Predicting the Conditional Probability of Frozen Precipitation. Harry R. Glahn and Joseph R. Bocchieri, March 1974, 33 pp. (COM-74-10909)

NWS TDL 52 SPLASH (Special Program to List Amplitudes of Surges From Hurricanes): Part Two. General Track and Variant Storm Conditions. Chester P. Jelesnianski, March 1974, 55 pp. (COM-74-10925)

NWS TDL 53 A Comparison Between the Single Station and Generalized Operator Techniques for Automated Prediction of Precipitation Probability. Joseph R. Bocchieri, September 1974, 20 pp. (COM-74-11763)

NWS TDL 54 Climatology of Lake Erie Storm Surges at Buffalo and Toledo. N. Arthur Pore, Herman P. Perrotti, and William S. Richardson, March 1975, 27 pp. (COM-75-10587)

NWS TDL 55 Dissipation, Dispersion and Difference Schemes. Paul E. Long, Jr., May 1975, 33 pp. (COM-75-10972)

NWS TDL 56 Some Physical and Numerical Aspects of Boundary Layer Modeling. Paul E. Long, Jr. and Wilson A. Shaffer, May 1975, 37 pp. (COM-75-10980)

NWS TDL 57 A Predictive Boundary Layer Model. Wilson A. Shaffer and Paul E. Long, Jr., May 1975, 44 pp. (PB-265-412)

NWS TDL 58 A Preliminary View of Storm Surges Before and after Storm Modifications for Alongshore-Moving Storms. Chester P. Jelesnianski and Celso S. Barrientos, October 1975, 16 pp. (PB-247-362)

NWS TDL 59 Assimilation of Surface, Upper Air, and Grid-Point Data in the Objective Analysis Procedure for a Three-Dimensional Trajectory Model. Ronald M. Reap, February 1976, 17 pp. (PB-256-082)

NWS TDL 60 Verification of Severe Local Storms Warnings Based on Radar Echo Characteristics. Donald S. Foster, June 1976, 9 pp. plus supplement. (PB-262-417)

NWS TDL 61 A Sheared Coordinate System for Storm Surge Equations of Motion With a Mildly Curved Coast. Chester P. Jelesnianski, July 1976, 52 pp. (PB-261-956)

NWS TDL 62 Automated Prediction of Thunderstorms and Severe Local Storms. Ronald M. Reap and Donald S. Foster, April 1977, 20 pp. (PB-268-035)

NWS TDL 63 Automated Great Lakes Wave Forecasts. N. Arthur Pore, February 1977, 13 pp. (PB-265-854)

NWS TDL 64 Operational System for Predicting Thunderstorms Two to Six Hours in Advance. Jerome P. Charba, March 1977, 24 pp. (PB-266-969)

NWS TDL 65 Operational System for Predicting Severe Local Storms Two to Six Hours in Advance. Jerome P. Charba, May 1977, 36 pp. (PB-271-147)

NWS TDL 66 The State of the Techniques Development Laboratory's Boundary Layer Model: May 24, 1977. P. E. Long, W. A. Shaffer, J. E. Kemper, and F. J. Hicks, April 1978, 58 pp. (PB-287-821)

NWS TDL 67 Computer Worded Public Weather Forecasts. Harry R. Glahn, November 1978, 25 pp. (PB-291-517)

NWS TDL 68 A Simple Soil Heat Flux Calculation for Numerical Models. Wilson A. Shaffer, May 1979, 16 pp. (PB-297-350)

NWS TDL 69 Comparison and Verification of Dynamical and Statistical Lake Erie Storm Surge Forecasts. Wil- liam S. Richardson and David J. Schwab, November 1979, 20 pp. (PB80 137797)

NWS TDL 70 The Sea Level Pressure Prediction Model of the Local AFOS MOS Program. David A. Unger, April 1982, 33 pp. (PB82 215492)

NWS TDL 71 A Tide Climatology for Boston, Massachusetts. William S. Richardson, N. Arthur Pore, and David M. Feit, November 1982, 67 pp. (PB83 144196)

NWS TDL 72 Experimental Wind Forecasts From the Local AFOS MOS Program. Harry R. Glahn, January 1984, 60 pp. (PB84-155514)

NWS TDL 73 Trends in Skill and Accuracy of National Weather Service POP Forecasts. Harry R. Glahn, July 1984, 34 pp. (PB84 229053)

NWS TDL 74 Great Lakes Nearshore Wind Predictions from Great Lakes MOS Wind Guidance. Lawrence D. Burroughs, July 1984, 21 pp. (PB85 212876/AS)

NWS TDL 75 Objective Map Analysis for the Local AFOS MOS Program. Harry R. Glahn, Timothy L. Chambers, William S. Richardson, and Herman P. Perrotti, March 1985, 35 pp. (PB85 212884/AS)

NWS TDL 76 The Application of Cumulus Models to MOS Forecasts of Convective Weather. David H. Kitzmiller, June 1985, 50 pp. (PB86 136686)

NWS TDL 77 The Moisture Model for the Local AFOS MOS Program. David A. Unger, December 1985, 41 pp. (PB86 151305)

NWS TDL 78 Objective Assessment of 1984-85 VAS Products as Indices of Thunderstorm and Severe Local Storm Potential. David H. Kitzmiller and Wayne E. McGovern, March 1988, 38 pp. (PB89-107668)

NWS TDL 79 Performance of Operational Objective 0-6 H Quantitative Precipitation Forecasts Relative to Manual and Model Generated Forecasts: A preliminary Assessment. Jerome P. Charba, Joel T. Moeller, and Paul D. Yamamoto, October 1988, 31 pp. (PB89 162028)

NWS TDL 80 Use of Operational 0-6 and 3-9 H Quantitative Precipitation Forecasts for Predicting Heavy Rain Events. Jerome P. Charba and Joel T. Moeller, June 1989, 34 pp. (PB90 103946)